UNIVERSITY OF VERONA

Department of

NEUROSCIENCE, BIOMEDICINE AND MOVEMENT

Graduate School of

LIFE AND HEALTH SCIENCES

Doctoral Program in

BIOMOLECULAR MEDICINE

Cycle XXXII

STRUCTURAL DETERMINANTS AFFECTING THE OLIGOMERIZATION TENDENCY OF SOME PANCREATIC RIBONUCLEASES

S.S.D. BIO/10 Biochemistry

Coordinator: Prof. Lucia De Franceschi

Signature _____

Tutor: Prof. Giovanni Gotte

Signature _____

Doctoral Student: Dott.ssa Sabrina Fasoli

Signature _____

University of Verona
Research Office – National and International PhD programmes
ph: 045.802.8608 – fax 045.802.8411 – Via Giardino Giusti 2 – 37129 Verona

Structural Determinants affecting the Oligomerization Tendency of some Pancreatic Ribonucleases
Sabrina Fasoli
PhD Thesis
Verona, December 2019

University of Verona
Research Office – National and International PhD programmes
ph: 045.802.8608 – fax 045.802.8411 – Via Giardino Giusti 2 – 37129 Verona

Abstract

The three dimensional domain swapping (3D-DS) mechanism represents a useful strategy that proteins can follow to self-associate. This mechanism requires the presence of a flexible portion that generally links the N- and/or C-terminus of the protein to its core. This portion, called hinge loop, can adopt different conformations as a function of the environmental conditions and allows the mentioned N- and/or C-terminal domains to be detached from the protein core and to be swapped with an identical domain of another protomer. This induces the formation of dimer(s) or larger oligomer(s) that often display, or enforce, biological properties that are absent, or attenuated, in the native monomer.

The 3D-DS mechanism is shared by some proteins involved in amyloidosis, such as the human prion protein, β_2-microglobulin, or some cystatins. Although not being amyloidogenic, the "pancreatic-type" RNases, i.e. resembling the features of the well-known pancreatic bovine RNase A, have become milestones to comprehend the determinants ruling out the 3D-DS mechanism. This is true especially for RNase A and for its natively dimeric homolog bovine seminal (BS)-RNase, whose structural determinants characterizing their self-association through 3D-DS have been deeply studied in the recent past. Moreover, also other ribonucleases included in the same RNase A super-family can oligomerize through this mechanism, as for example onconase (ONC), that can be induced to dimerize through the 3D-DS of its N-terminal domain.

In this thesis, my aim was to elucidate some structural determinants that settle the tendency of some pancreatic-type RNases to self-associate, keeping the known features of RNase A as a reference.

Therefore, we firstly investigated if the different methods that can be used to obtain the oligomers of RNase A might influence their properties. We treated RNase A with two different protocols: in particular, *i.* lyophilization of acetic acid solutions of the protein, or, *ii.* thermal incubations performed at 60°C in 20 or 40% aqueous ethanol. We observed that the enzymatic activity of the monomers

and of the N- and C-swapped dimers (N_D and C_D, respectively) are slightly affected by the particular method used to induce their self-association.

Then, I focused my attention to onconase (ONC), an amphibian member of the "pancreatic-type" RNase super-family lead by RNase A. In particular my aim was to unlock its C-terminal domain, that in the wild-type is blocked by a disulfide bond involving its C-terminal Cys104 residue, in order to investigate if this RNase variant may dimerize also through the C-terminal-end swapping. Unfortunately, none of numerous ONC mutant that I produced could form either the C-dimer, or also larger oligomers. In addition, all these variants formed less N-dimer than the wild type, confirming the actual mutual influence existing between the N- and C-termini of the protein, as it occurs for other RNases. We also supposed that the impossibility for ONC to form a C-dimer could be ascribable to the elongation of its C-terminal domain, with respect to RNase A. Therefore, we analyzed also the aggregation propensity of human pancreatic RNase, a variant that displays a C-terminus elongation of four AA residues in comparison with RNase A, similarly to ONC. Both the wt and a mutant obtained by the deleting the four mentioned residues displayed SEC profiles qualitatively very similar to the one of RNase A. Therefore, the human variant actually displayed that it can extensively oligomerize, but we could also deduce that the C-terminal elongation influences only marginally this process.

The last project I developed was focused on the analysis of the oligomerization tendency of human angiogenin (ANG), a 14 kDa RNase variant characterized by a low ribonucleolytic activity ($10^{-5}/10^{-6}$ fold less than of RNase A), however necessary for its crucial angiogenic effects. ANG is involved in tumorigenesis but it exerts also a survival-promoting effect on the central nervous system (CNS) neuronal progenitors. However, some ANG variants are involved in neurodegenerative diseases, such as Amyotrophic Lateral Sclerosis (ALS) and Parkinson Disease (PD). ALS is a multifactor disease, but one hypothesis to explain the pathogenic effect could be related to a possible oligomerization and precipitation of the mutants in the CNS. Among the numerous pathogenic ANG variants existing, one candidate retained by some scientists prone to undergo self-association is the S28N mutant. In our hands, this variant showed to dimerize at a

slightly higher extent than the wild type, that in turn dimerized as well. Then, other ANG pathogenic mutants, in particular H13A and Q117G, also showed to dimerize, but with less reproducible results. Anyway, we detected for the first time that also ANG can dimerize through the 3D-DS mechanism, as many other RNases do.

In conclusion, all the results of this thesis can be considered a step forward to comprehend the determinants settling the 3D-DS dimerization, or oligomerization tendency of many pancreatic-type RNases, and to compare the determinants that induce the differences emerging within them.

ABBREVIATIONS

3D-DS: three dimensional domain swapping
AA: aminoacid
ANG: angiogenin
AD: Alzheimer's Disease
ALS: Amyotrophic Lateral Sclerosis
BS-RNase: bovine seminal ribonuclease
C>p: 2',3'-cyclic cytidilate
CD: circular dichroism
C_D: C-dimer
CNS: central nervous system
DNA: deoxyribonucleic acid
ds-RNA: double stranded RNA
DT: diphtheria toxin
DVS: divinyl sulfone
EDC: ethylene carbodiimide
EDN: eosinophil-derivered neurotoxin
EtOH: ethanol
HAc: acetic acid
HL-60: human promyelocytic leukemia cells
HP-RNase: human pancreatic ribonuclease
IL-5: interleukin 5
M: monomer
MS: mass spectrometry
MW: molecular weight
NaAc: sodium acetate
NaPi: sodium phosphate
N_D: N-dimer
ONC: onconase
PCR: polymerase chain reaction
PD: Parkinson's Disease
PEG: polyethylene glycol
Poly(A): polyadenylic acid
poly(A):poly(U): polyadenylic acid-polyuridylic acid
Poly(C): polycytidylic acid
Poly(U): polyuridylic acid
RI: ribonuclease inhibitor
RNA: ribonucleic acid
RNase: ribonuclease
SEC: size exclusion chromatography
ss-RNA: single stranded RNA

Index

Chapter 1

INTRODUCTION

1.1 Ribonucleases

The flow of genetic information is encoded by DNA, while both transcription and translation to proteins involve ribonucleic acid (RNA).

The metabolism of RNA, therefore crucial for life processes, is under the control of two classes of enzymes: RNA polymerases and RNA depolymerases or ribonucleases (RNases). RNA polymerases take part in the synthesis of RNA molecules, while their degradation is catalyzed by RNases. These events represent the intermediate steps in the genetic information transfer from DNA to proteins.

RNA turnover is regulated by more than 20 exo- and endoribolucleases, whose function is to process RNA into mature forms. Ribonucleases are small basic proteins with a molecular weight ranging from 11.8 to 27.2 kDa. Numerous variants are known, forming a large family of enzymes whose activity drives to the hydrolysis of the phosphodiester bonds present in mRNAs, rRNAs or also tRNAs. Therefore, the main functions of RNases are devoted to the degradation of several types of RNAs or also to process RNAs toward mature forms.

In non-herbivorous species, an important classification addresses the different secretory RNases into two super-families named pancreatic and non-pancreatic type RNases. The first ones are present at a very low levels in secretory organs and body fluids, such as pancreas, prostate, seminal fluid, milk and saliva[1–8], with respect to the high quantity of bovine pancreatic ribonuclease A (RNase A) secreted by the bovine pancreas. All the proteins referring to RNase A are characterized by sequence, structure and catalytic properties similar to those of both bovine and human pancreatic RNases, and their positive amino acid residues are localized in the vicinity of the active site[8,9].

Furthermore, many pancreatic-type RNases are not involved only in RNA metabolism, but also in other pathways, such as cell maturation, apoptosis, angiogenesis and defense against exogenous RNA viruses[10,11]. Some RNases, including the microbial binase from *Bacillus intermedius*[12], RNase Sa from *Streptomyces aureofaciens*[13], α-sarcin from *Aspergillus giganteus*[14], or amphibian ranpirnase (also called onconase) and amphinase from *Rana pipiens*[15], and mammalian bovine seminal RNase (BS-RNase) from *Bos Taurus*[11,16,17] are also

cytotoxic. Also natural mutants[18–22], as well as chemically modified[23,24] or engineered variants[25,26] of human and bovine pancreatic RNases can become cytotoxic at an extent comparable to, or sometimes higher than the wild-type species.

Instead, the "non pancreatic-type" RNases display sequence and catalytic properties similar to bovine kidney RNase K2 or human EDN/liver RNase, and their basic amino acid residues are randomly located in their structure, often far from the active site[9,27]. Some variants belonging to this latter group are present in human spleen, liver, kidney, urine and serum[3,4,7,28–32].

1.2 Ribonuclease A

Bovine pancreatic ribonuclease (RNase A) has become the proto-type of the vast super-family of secretory RNases that are called “pancreatic-type”. All the members of this super-family display a structure and a basic charge distribution similar to RNase A. Although many members are not secreted by the pancreas, they belong to the mentioned superfamily at the same time.

RNase A from *Bos taurus* (13686 Da) is secreted in large quantities by the bovine pancreas, possibly because of the large RNA amount produced by the bacteria present in the rumen. The “A” refers to the most abundant isoform of the protein. In fact, other glycosylated isoforms accompany RNase A, such as RNase B[33–35], which is a mixture of glycoforms in which $Man_{5-9}GlcNAc_2$ are bound to the side-chain nitrogen of Asn34, or the less abundant RNase C and D[36,37], that are even more heterogeneous in their glycosylation profiles.

RNase A was the first enzyme and the third protein whose amino acid sequence was determined[38,39], and the fourth protein, but the third enzyme whose 3D crystallographic structure was solved by X ray diffraction[40]. Therefore, RNase A has represented a reference for the study of protein structure and function, and more recently has become a model also for the studies of protein aggregation in general. However, above all, it displays two remarkable functions: a high catalytic activity against ss-RNA substrates and a high conformational stability[41].

Monomeric RNase A (13.7kDa) is able to oligomerize under controlled conditions, such as lyophilisation from 40% acetic acid or thermal incubation of highly concentrated solution in various solvents[42–44]. The protein oligomerizes through a three dimensional domain swapping (3D-DS) mechanism that involves the N- or C-terminus of the protein, or both[45–48].

1.2.1 RNase A structure

RNase A is a single-domain, monomeric protein, composed by 124 aminoacid residues that originate a “V-like” or “kidney-like” shaped 3D structure comprising three α-helices and six β-strands: in particular, helix I (residues 3-13), helix II (24-34) and helix III (50-60), and an antiparallel β-sheet comprising six β-strands, in particular β-strand I (residues 43-49), II (61-63), III (72-74), IV (79-87), V (96-111) and VI (116-124).

The RNase A structure is stabilized by four disulfide bonds that link the eight Cys residues located at the positions 26-84, 40-95, 58-110 and 65-72. These disulfide bonds are crucial for the stability of the protein, since the mutation of any cysteine into alanine, or serine, residues definitely decreases the protein melting temperature[49–51]. The prevalence of basic residues (four Arg, four His and ten Lys) over acidic ones (five Asp and five Glu) confers to the protein a positive net charge with a resulting pI of 9.3[52]. The N-terminal domain (residues 1-15) is connected to the protein core through a flexible loop (residues 16-22). On the contrary, the C-terminal β-hairpin involves by two β-strands (105-124), in which a higher number of hydrophobic residues are present with respect to the N-terminus of the protein[44].

Figure 1.1. Crystal structure of bovine pancreatic ribonuclease A (5RSA.pdb).

1.2.2 Catalytic activity of RNase A

RNase A exerts its catalytic activity against single-stranded RNA (ss-RNA), but, like other RNases, is active on di-trinucleotides, on short oligonucleotides, or on long RNA substrates as well.

Moreover, some experiments demonstrated that it is also able to bind one of the two strands of the double-stranded DNA (ds-DNA) molecule, leading to its destabilization[53–55]. RNase A displays several catalytic subsites (B1, B2 and B3) that interact with the bases of the RNA substrate. Subsite B1 (Thr45, Asp83) interacts only with pyrimidine residues[56,57], with a higher preference for cytosine with respect to uracil. In contrast, the B2 (Asn71, Glu111) and B3 (unknown) subsites are less specific, with B2 preferring adenine[58] while, instead, B3 purine bases[59,60]. Then, also other subsites are present to interact with the phosphoryl group of the substrate in order to stabilize the interaction are present in RNase A. These sites are P0 (Lys66), P1 (Gln11, His12, Lys41, His119 and Asp121) and P2 (Lys7, Arg10)[55].

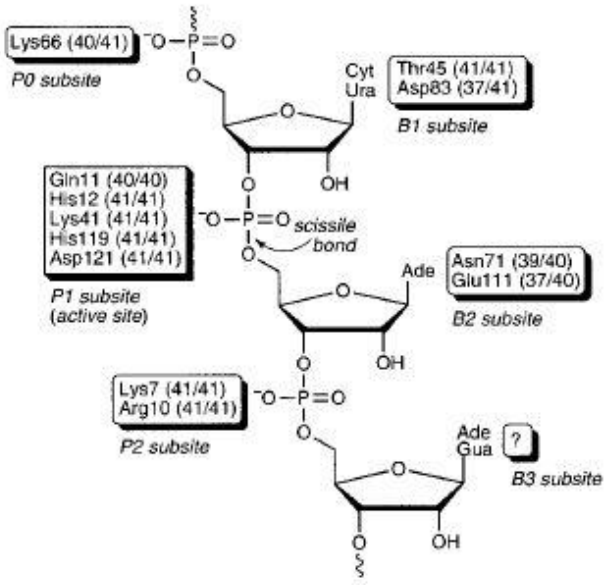

Figure 1.2. RNase A residues involved in the interaction with a RNA molecule. Numbers in parentheses refer to the aminoacid conservation in the pancreatic ribonuclease family. (from Raines, 1998[61])

P1 is the active site triad that directly catalyzes the cleavage of the P-O$^{5'}$ bond[62–67], and is composed by Gln11 and His12 located in the N-terminal domain, by His119 and Asp121 in the C-terminus and by Lys41 situated in protein core. It has to be underlined, however, that the actual catalytic triad is made by His12, Lys41 and His119. In the initial transphosphorylation step, His12 acts as a general base, removing a proton from the 2' oxygen of the substrate[68,69], while His119 acts as the electrophile that allows the protonation of the 5' oxygen and favors the cleavage of the P-O bond located between two RNA bases. This event leads to the formation of a nucleoside 2',3'-cyclic phosphodiester. In the second reaction step, the hydrolysis of the 2'-3'-cyclic phopshodiester is induced by a nucleophilic attack of a water molecule to the 3' phosphate, facilitated by the action of His119 that behaves as a general base, with the consequent protonation of the 2' oxygen and deprotonation of His12. Instead, Lys41 electrostatically stabilizes the transition state, when the phosphorous is covalently bound to 5 oxygen atoms, surrounded in this way by a high negative charge density. This transient interaction is not possible with ds-RNA, because the 2' hydroxide group sterically prevents the formation of the transition state.

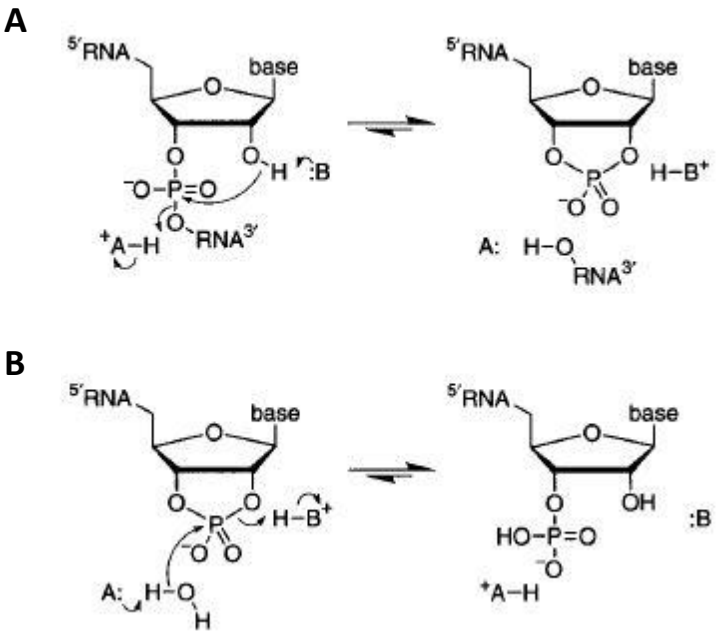

Figure 1.3. Mechanisms of (A) transphosphorylation and (B) hydrolysis reactions catalyzed by RNase A. "A:" represent the His12 residue, while "B:" His119 (from Raines, 1998[61]).

RNase A cleaves CpX substrates and hydrolyzes 2',3'-cyclic cytidilate (C>p) 2-fold faster than the corresponding uridylyl substrates[61]. Poly(C) is cleaved about 20-fold faster than poly(U), while poly(A) is hydrolyzed 10^3-10^4-folds lower than poly(U)[27,70].

In vivo, the activity of RNase A is strongly reduced, or lost, for the presence of cellular inhibitors that inglobate the protein in their structure[19,71–73]. The most potent is the "ribonuclease inhibitor" (RI), a ≈50 kDa horse-shoe structured and leucine+cysteine-rich protein present in almost all mammalian cells[74]. The main role of RI is to protect the cytosolic RNA from the invasion of external ribonucleases. Moreover, being rich of Cys residues, RI is known to be active in maintaining the cellular redox equilibrium[75]. The RNase A-RI complex formation is possible for the presence in the RNase moiety of specific residues, like K7 and G88, that allow the accommodation and productive interaction with the RI counterpart. There are, instead, other cytotoxic pancreatic-type ribonucleases that are able to escape RI, such as onconase, that lacks the mentioned key-residues, or bovine seminal (BS)-RNase, whose natively dimeric structures induces a steric hindrance that makes its interaction with RI impossible[76].

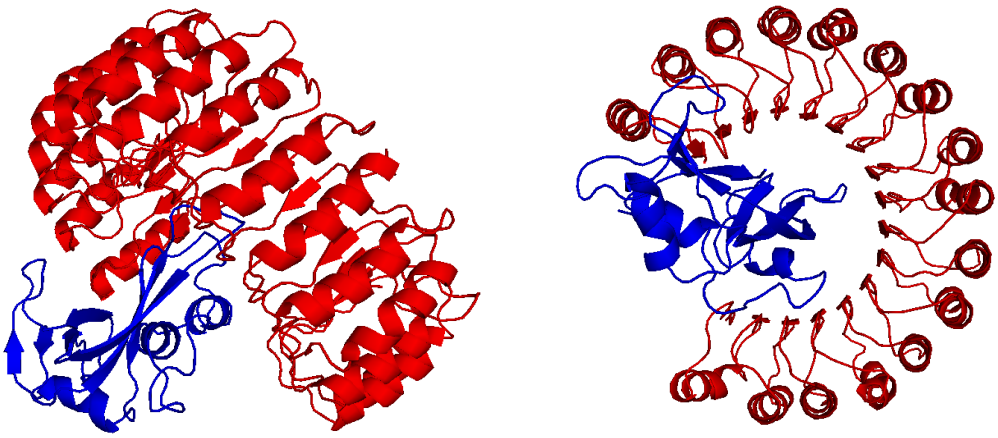

Figure 1.4. Crystal structure of RNase A (blue) in complex with ribonuclease inhibitor (red) (1DFJ.pdb), shown in two different orientations.

1.2.3 RNase A oligomerization

It is known that RNase A is able to covalently dimerize around neutral pH. This is possible in two different ways: the first requires the introduction of the two Cys residues present in BS-RNase at the positions 31 and 32: the resulting RNase A K31C/S32C mutant forms a dimer displaying a conformation similar to one of the two BS-RNase dimeric conformers in which the two monomers are crosslinked with two intermolecular antiparallel 31-32 + 32-31 disulfide bonds (M=M). Incidentally, another dimeric isoform covalently stabilized by the two mentioned disulfide bonds exists in equilibrium with M=M, and is called MxM because it displays also the swapping of the two N-terminal domains[77–79].

Another way to create covalent RNase A dimers, trimers or larger oligomers foresees the use of chemical cross-linkers that bind specific AA residues of the enzyme. For example, molecules characterized by multiple maleimide ends are used to create oligomers upon reacting with the SH group of free cysteines[80]. These oligomers have some new biological and enzymatic activity, such as a reduction of the affinity with RI, due to the bulky structure of dimers trimers, and so on. Furthermore, the increase of the basic charge density could induce an increase in the citotoxicity[80]. Another class of cross-linkers are homo-bifunctional molecules containing amine-reactive diimidoesters that can react with the ε-amine N-terminal group of the lysine residues. In this way, oligomeric derivatives can be produced without losing positive charges, as instead can be provoked by a reaction with dialdehydes such as glutaraldehyde. In particular, RNase A trimers obtained upon reacting with dimethyl-suberimidate display remarkable cytotoxic/cytostatic actions against a human cell line derived from squamous carcinoma of uterus cervix, while cross-linked dimers are almost ineffective[81].

Thanks to its structural and functional versatility, RNase A has become also a model for many experimental investigations devoted to elucidate the mechanisms leading to non covalent proteins to self-association, and form different aggregation products[42].The mechanism followed by RNase A, and that continues to be found to involve an increasing number of proteins is called three dimensional domain swapping (3D-DS), as it will be described below.

1.2.4 RNase A self-association: the 3D-DS mechanism

Under specific conditions, such as lyophilization from 40% acetic acid or incubation of highly concentrated protein solutions in various solvents at high temperature[42–44], RNase A forms oligomeric aggregates, some of which have been characterized[45–47]. These aggregates are metastable species, ranging from dimers to trimers, tetramers and larger oligomers, up to tetradecamers[82,83]. RNase A oligomerizes through the 3D-DS mechanism[84]. The term 3D-DS was used for the first time by Eisenberg and co-workers[85] to describe the structure of the diphtheria toxin dimer (DT), but the mechanism was previously hypothized and proposed in 1962 by Crestfield et al.[42] for RNase A. Indeed, the structure of more than sixty domain-swapped protein dimers or oligomers had been solved up to the beginning of this last decade[86].

The 3D-DS mechanism takes place when one, or more, domain(s) of a monomeric protein are reciprocally exchanged to form a dimer or large oligomers. This is possible thanks to the presence of one, or more, flexible loop(s) that can adopt different conformations, as a function of the environmental conditions experimented by the protein.

In a monomer, the domain(s) involved in the swapping leading to the oligomers formation create(s) contacts with a part of its body, in the so-called closed interface (C-interface)[87]. Mildly denaturing conditions, such as temperature or pH variations, as well as high protein concentration, allow a monomer to reach the necessary $\Delta G_{\ddagger}$ to switch its N- or C- terminal domain and form an "open" monomer. Two identical domains are reciprocally exchanged by different monomers, forming dimer(s) or oligomers in which the interfaces present in the native monomer are re-established (closed interface). Furthermore, in the resulting oligomer(s) a new, additional interface that is absent in the monomer, and is called Open interface (O-interface)[87], is formed between the two swapped subunits. The features of this interface vary from protein to protein and also within the same protein, such as is for RNase A. The type and the extension of this O-interface both contribute for the additional stabilization of the relative oligomer, while mutations may affect the stability of the O-interface.

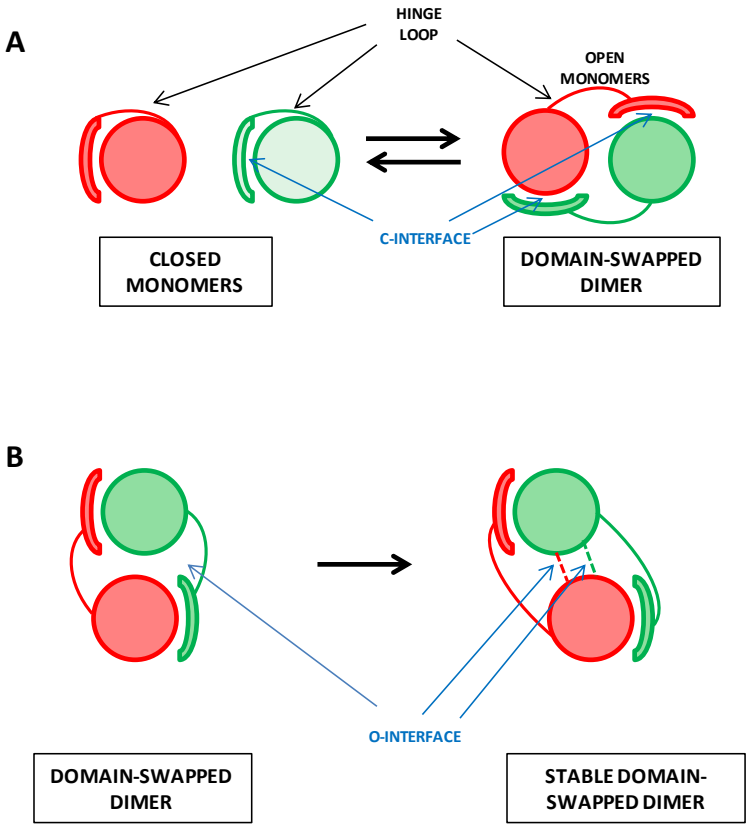

Figure 1.5. Formation of (A) metastable and (B) stable/covalent domain-swapped dimers. Closed monomers are composed by a protein body (circle) and by the swappable domain connected with a polypeptide linker (hinge loop). The interface existing between the protein body and the swappable domain present in both monomer and dimer is the C-interface. The open monomer dimerization through 3D-DS leads to the formation of an O-interface, not present in the monomer. (from Bennett et al., 1995[87])

When the $\Delta G^{\circ}_{oligomerization}$ is positive, metastable oligomers (such as for RNase A oligomers, or for the DT dimer[85]) are generated. Stable oligomers are formed, instead, when $\Delta G^{\circ}_{oligomerization}$ is negative (for example, in the case of BS-RNase, or IL-5). Three factors contribute to the Gibbs free energy differences existing among the monomer and the 3D-swapped oligomers: entropy makes the monomer thermodynamically favoured over the oligomer(s), while the new contacts, or links, generated in the swapped oligomers by the hinge loop(s) and/or by other region(s) of the protein (O-interface) can drive toward a favoured oligomerization over the native monomer[46,88–90].

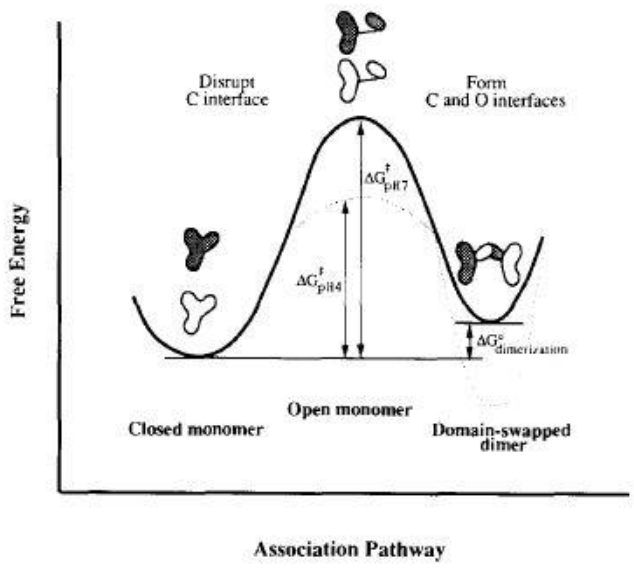

Figure 1.6. Free energy for the formation of a domain swapped dimer in DT (diphtheria toxin). The difference in the Gibbs free energy is positive, according to the metastable nature of the dimer formed. The dashed line refers to the formation of a stable domain swapped dimer favoured by a negative difference in Gibbs free energy (from Bennett et al., 1995[87]).

The swapping domain may be characterized by many different secondary structures: one α-helix, or β-strand, or also several α-helices or β-stands or even a mixture of α-helices and β-strands. Therefore, the 3D-DS mechanism does not require the involvement of a specific primary or secondary structure to occur[84]. Instead, the presence of a hinge loop connecting two domains is crucial. The flexibility of this loop permits its variable conformation. Indeed, it can also adopt a variety of secondary structures: some hinge loops are coils, other β-strands[45], while other can adopt a helical conformation in the oligomer(s).

The stabilization of the domain-swapped oligomers depends on various additional conditions, such as buffer type and concentration, pH, temperature, mutation(s) of key residue(s)[47,82,91–96,83–90]. 3D-DS may also occur as a consequence of single, or multiple mutations that destabilize the monomer. These mutations can be involved in hinge loop shortening, electrostatic repulsion occurring between the swapping domain and the protein body, etc[97–101].

Aminoacid substitution(s) could induce the formation of new contacts between the subunits constituting the oligomers, thus stabilizing the O-interface[87].

It has been proposed that 3D-DS is involved also in protein evolution: in fact, some proteins may acquire, upon oligomerization, different biological activity(ies) with respect to the monomer, and, the oligomers will be selected by in the process of natural evolution if this confers an advantage to the organism[87].

Importantly, in RNase A, as well as in BS-RNase, 3D-DS involves either N- or C-terminal domains, thus leading to a high number of dimeric or of larger oligomeric conformers.

1.2.5 RNase A 3D domain swapped N- and C-dimers

The two dimers are the most abundant species that RNase A forms upon its non covalent oligomerization. The crystallographic structures of both dimers have been solved, the N-swapped dimer (N_D) in 1998[45], while the C-swapped one (C_D) in 2001[46]. The active site of the native enzyme is reconstituted in both dimers, with the two His12/His119 residues being provided one each by the two subunits, so that the enzymatic activity is not lost[42,102]. RNase A constitutively forms traces of N-dimer (N_D)[43,77], where the swapped N-terminus of each monomer contacts the larger domain of the other (residues 23-124). The active site reconstitution is stabilized by the presence of phosphate ions in solution that interact with both the mentioned His residues to form a saline bridge allowing the oligomers formation and stabilization. If the phosphate bridge is absent no stabilizing interaction(s) occur(s) between the two subunits of the dimer that in turn results to be less stable, or even fails to be formed[44,103,104].

In the N_D, the two subunits interact through their three-stranded β-sheets, forming a six-stranded β-sheet region through an O-interface stabilized by six H-bonds[45]. These specific stabilizing contacts are warranted by the two subunits reciprocally disposed at approximately 160 degrees[45,105]. These contacts would be absent if symmetry would be 180°, and is instead 160° because the two hinge loops acquire different conformations: one forms an extended coil, whereas the other forms a helix[45]. On the contrary, the C-terminus of each protomer interacts

with the core of the other, forming a C-dimer (C_D) that is larger in size with respect to N_D. Indeed, it has a major surface area, 13411 $Å^2$ over the 12236 $Å^2$ of the N-swapped dimer[46]. In the C-terminal domain, two β-strands form a β-hairpin richer in hydrophobic residues with respect to the ones of the N-terminus, while molecular dynamics simulations suggest that the O-Interface permits the C_D to be more flexible than N_D[105,106]. Moreover, the less compact C_D structure lets this conformer to expose an overall higher positive charge than N_D[46,107].

Indeed, both different size and basic charge exposure of N- and C-dimers allow to separate them through size exclusion, or better, through cation exchange chromatographies[102,107].

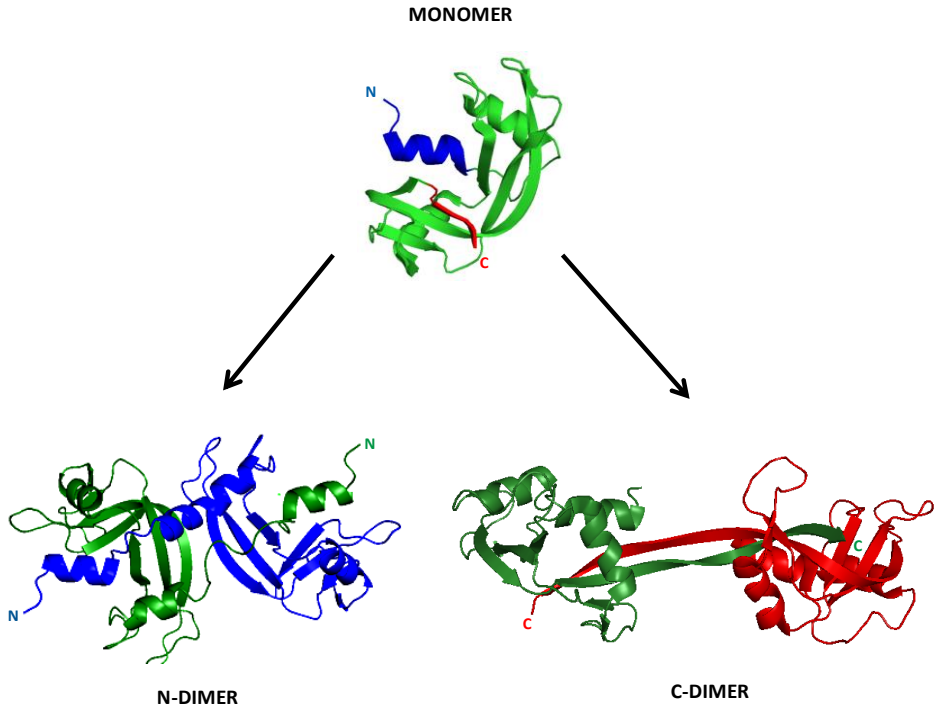

Figure 1.7. Crystal structures of the RNase A monomer and of the N-swapped and C-swapped dimers. Respectively, their PDB codes are: 5RSA.pdb, 1A2W.pdb, 1F0V.pdb.

1.2.6 RNase A 3D domain-swapped trimers, tetramers and larger oligomers

RNase A can form also oligomers larger than dimers. Indeed, two trimers have been isolated and characterized: one displaying both N- and C-swapping, called NC-trimer (NC_T), whose structure has been modeled [47,93], while the other swapped only the C-terminus, and called C-trimer (C_T), whose crystallographic structure has been solved[47]. According to a model whose validity has been experimentally confirmed, the NC-trimer forms when a central monomer simultaneously swaps both N- and C-termini with two other monomers to form a linear structure. Instead, the crystal structure of the C-trimer shows that the oligomer is cyclically generated through the swapping of the C-terminal domain of three monomers[47] into the core of the adjacent monomer, forming a structure similar to a propeller whose surface exposes more basic charges than the NC-trimer.

RNase A forms also low amounts of many tetrameric isoforms, but also the cationic exchange chromatography approach does not allow a complete purification[45–47,82,93,107,108]. However, some of them have been partially characterized and models have proposed, as reported in Figure 1.8 C-F. The possibility to simultaneously swap both N- and C-termini of RNase A leads to the formation of larger oligomers, definitely increasing the oligomerization tendency of the enzyme. In fact, D. Eisenberg and colleagues proposed in 2006 that a protein exponentially increases its self-association potential if it is able to swap more than one domain. They indicated the equation for the swapping capacity as $SC = N + N^2$, where N correspond to the number of swappable domains[109]. Indeed, in our case, also low amounts or traces of RNase A pentamers, hexamers and larger oligomers up to tetradecamers have been detected and partially characterized in the recent past[48,83,107,110].

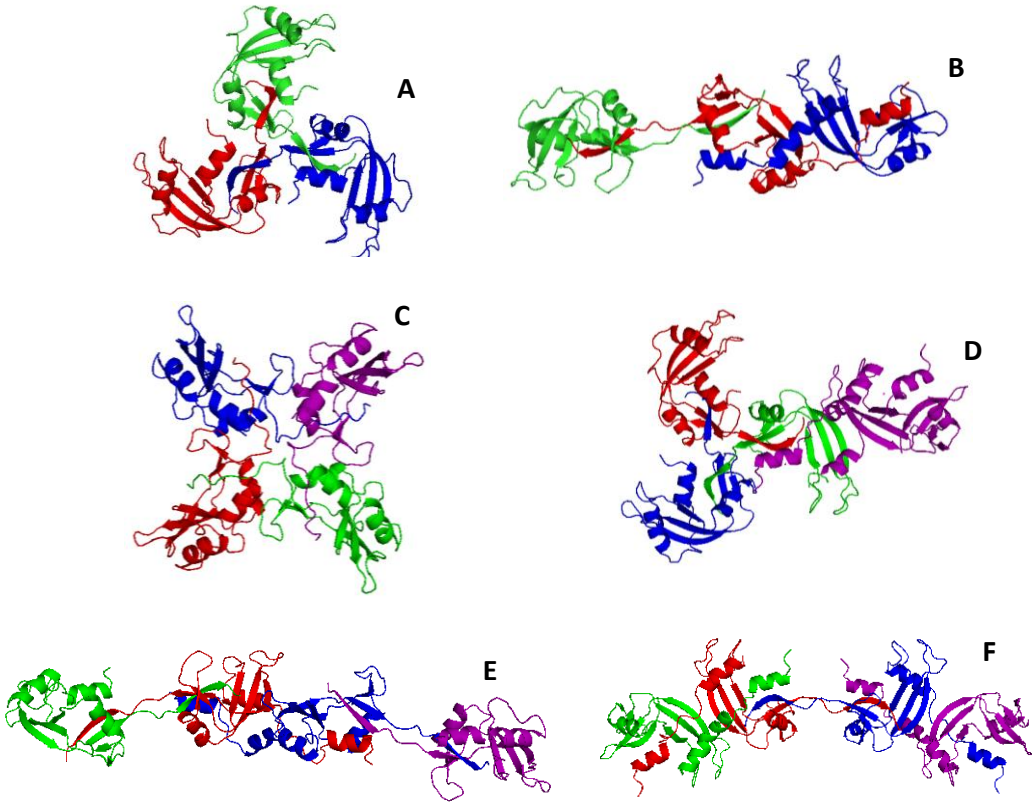

Figure 1.8. A. Structure of C-trimer. Model of: **B**. NC-trimer, C. C-tetramer, **D**. NCCC-tetramer, **E**. CNC-tetramer. **F**. NCN-tetramer. The "N"- or "C"- stands for the N- or C-terminus of the protein swapped (from Libonati and Gotte, 2004[44])

1.2.7 Catalytic activity of the RNase A oligomers

Covalently linked, but especially domain-swapped non covalent RNase A oligomers are enzymatically active thanks to the reconstitution of a composite enzyme active site[42,45,46,87,102]. No difference can be registered among monomer and oligomers activity against 2',3'-cyclic cytidylate[42,102,111], while against single-stranded (ss-RNA) yeast RNA as substrate oligomers display ribonucleolytic activity values that fall between 40% and 80% of the one displayed by monomeric RNase A[43,82,107,112], with a reduction of the catalytic activity with respect to the monomer that augments with the oligomer size. With polyuridylate (polyU) and polycytidylate (polyC) as substrates, the activity of the oligomers is comprised instead between 70% and 90% of that of the RNase A monomer[82,107]. However, if the activities of the oligomers are considered per mole of oligomeric molecule, the reduction can be considered linked to the fact that when more subunits are bound together they are not able to simultaneously bind the substrate, but only a fraction of them can interact and subsequently cleave it[44].

The higher catalytic activity that the oligomers display against poly(U) and poly(C) against yeast RNA could be due to the greater length and homogeneity of these substrates, that allow themselves to bind more efficiently the RNase A subsites[61,113,114]. Moreover, because of its heterogeneous sequence, yeast RNA could be attacked less efficiently by RNase A.

On the contrary, double-stranded RNA (ds-RNA) substrates are degraded less efficiently by RNase A monomer than by its oligomers[115]. Indeed, RNase A oligomerization leads to gain depolymerizing activity against double-stranded RNA, such as is the synthetic polyribonucleotide poly(A):poly(U). This activity increases with the size of oligomers, from dimers to trimers to tetramers, and so on[47,82,107,112]. Moreover, oligomers with the same size modulate their catalytic activity as a function of their positive charge exposition[107]. Therefore, the C-swapped oligomers are generally more active than the N-swapped ones. This is due to the different basicity exposed by the C-swapped oligomers than the N-swapped ones having the same size, with a consequent different interaction with the negative charges of the RNA phosphate groups.

Monomeric RNase A is not highly active against poly(A), likely because purine bases can bind only the B2 and B3 subsites, but not the B1[116]. On the contrary, RNase A oligomers are more active, and this activity increases with the size of the oligomers, probably because of their stronger electrostatic interaction with the substrate with respect to the monomer[82,107,117].

RNase A species	Specific activity (activity per nmol of enzyme species)				
	Poly(A) · poly(U)	Viral dsRNA	Poly(A)*	Poly(C)	Yeast RNA
Monomer	0.15 ± 0.03	0.44 ± 0.02	0.7 ± 0.03	933.3 ± 37.1	31.9 ± 1.9
N_D	0.33 ± 0.05	1.43 ± 0.19	3.8 ± 0.16	533.0 ± 131.5	16.5 ± 2.1
C_D	2.21 ± 0.01	1.37 ± 0.19	3.7 ± 0.30	–	15.3 ± 2.1
NC_T	2.21 ± 0.02	5.00 ± 0.24	5.5 ± 0.10	721.3 ± 116.1	13.7 ± 1.7
C_T	3.74 ± 0.17	5.52 ± 0.27	7.7 ± 0.08	606.5 ± 250.8	11.7 ± 1.6
NCN_{TT}	4.79 ± 0.58	11.72 ± 0.23	10.3 ± 0.55	804.3 ± 46.4	16.0 ± 1.7
CNC_{TT}	9.52 ± 0.27	10.86 ± 0.71	10.4 ± 0.33	674.0 ± 125.0	13.7 ± 0.8
P	20.47 ± 1.11	18.86 ± 0.29	17.1 ± 0.96	833.3 ± 96.9	18.7 ± 1.0

* Specific activity $\times 10^{-3}$.

Table 1.1. Specific activity of RNase A oligomers (from Libonati and Gotte, 2004[44]). N_D: N-dimer, C_D: C-dimer, NC_T: NC-trimer, C_T: C-trimer, NCN_{TT}: NCN-tetramer, CNC_{TT}: CNC-tetramer, P: pentamer(s).

1.2.8 Cytotoxic activity of RNase A oligomers

The catalytic activity of RNase A is responsible for its cytotoxicity that has been registered either *in vitro* or *in vivo* against some types of cancer[118]. Indeed, native monomeric RNase A demonstrated in the past to exert a weak antitumor activity, but only at high doses (above 10 mg/Kg), against Ehrlich carcinoma in mice[119,120]. Besides, RNase A oligomers are characterized by an *in vitro* and *in vivo* cytotoxic activity against some types of cancer cells, such as ML-2 (human myeloid leukemia) and HL-60 (human promyelocytic leukemia cells), as well by an aspermatogenic action that generally increases with the increasing size and the catalytic activity that is proportional with the basic charge of the oligomers[108].

The mechanism of endocytosis followed by the RNase A oligomers has not been completely clarified yet. However, it had been hypothesized that the high number of positive charges exposed allow the oligomers to interact with the negative surfaces of the target cells that successively incorporate them through endocytosis[108]. Once inside the cell, oligomers can attack various RNAs, such as mRNA, tRNA, rRNA, siRNA, and DNA:RNA hybrid duplexes. Putative targets of RNase A are also the RNAs circulating in the blood plasma, including pre-miRNAs and miRNAs implicated in the control of oncogenesis and invasion[121].

It was then supposed that the cytotoxicity of RNase A oligomers was principally ascribed to their partially ability to evade the cytosolic RNase A inhibitor (cRI)[19,122]. Their supramolecular structure, in fact, does not allow RI to completely retain them, contrarily to the RNase A monomer, for which RI shows a very high affinity[123–125]. The structures of the complexes formed between RI and the two dimers were modelled, with the C_D shape permitting a better interaction with two RI molecules than N_D. This could suggest that only one RI molecule can form a complex with one of the two N_D subunits, so that the other remains free to exert its activity[125].

As a support for this hypothesis, it was demonstrated that RNase A monomer acquires a significant antitumor activity when is conjugated with PEG[126], while RNase A mutants engineered to decrease the affinity interaction with RI are cytotoxic as well against K-562 cells. The cytotoxic activity of RNase A oligomers depends also on their stability, that is difficult to be analyzed either

in vitro or above all *in vivo*, and depends on several factors, such as buffer type or concentration, oligomer concentration itself, pH and temperature. In general, the higher the oligomer size, the lower its stability[93]. The possibility to stabilize the RNase A domain-swapped oligomers, as it was proposed by Lopez-Alonso et al. by using EDC, would certainly allow to increase their cytotoxic potential[127].

1.3 Onconase

Onconase (ONC) is a small monomeric enzyme extracted from oocytes and early embryos of the *Rana Pipiens* frog[128], and it belongs to the same secretory "pancreatic-type" ribonuclease super-family of RNase A. It was initially called ranpirnase, or also P30 protein, because of its low identity sequence (30%) with RNase A. However, now is commercially and commonly named onconase because of its remarkable cytotoxicity against cancer cells. ONC is polymorphic at the positions 11, 20, 25, 83 and 103, and *R. Pipiens* genome seems to contain four or more genes coding for ONC variants[129,130].

1.3.1 Onconase structure

ONC folds similarly to RNase A (Fig. 1.9) although it displays only 30% sequence identity, a lower MW (11.8kDa, 104 residues) and a higher basic charge than it. In particular, the two proteins share both α-helices and β-sheets locations, as well as the active site, the hydrophobic clusters and three out of four disulfide bonds; in particular Cys19-Cys68, Cys-30-Cys75 and Cys48-Cys90[131]. One important difference with respect to RNase A is that the ONC N-terminus displays a pyroglutamate residue formed by a spontaneous cyclization of the N-terminal glutamine residue, or as a product of glutaminyl cyclase. This derivatization connects the N-terminus to the protein body, therefore inducing a specific interaction with Lys9 that in turn influences the His10 residue of the active site[132]. The second difference is due to the presence of a disulfide bond at the C-terminus of the protein, linking Cys87 and Cys104. Both differences contribute to the ONC high thermal stability, since it displays a melting temperature of about 88-90°C, i.e., 25-30°C higher than RNase A[133,134]. Avoiding the formation of the mentioned pyro-Glu, if the starting N-terminal Met is not cleaved after protein expression, results in a decrease of ONC T_m of about 5°C, and in a 40-fold lower activity against yeast RNA with respect to the wt, due to the active role of pyroglutamate in the catalytic mechanism, since it interacts directly with Lys9 and indirectly with the two His of the active site[134]. Instead, the loss of the C-terminal disulfide

bond decreases the ONC melting temperature of 19°C, but does not affect its catalytic activity.

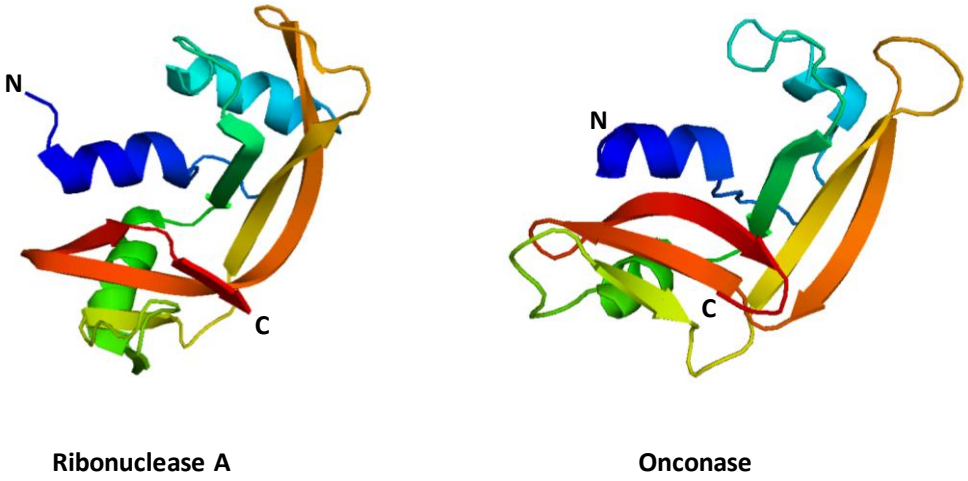

Figure 1.9 Comparison of the crystal structures of RNase A (5RSA.pdb) and of ONC (1ONC.pdb).

1.3.2 ONC enzymatic activity

The catalytic triad of ONC is composed by His10, Lys31, His97, similarly to RNase A His12, Lys41, His119. However, the enzymatic activity of ONC is generally about five order of magnitude lower than RNase A. In particular, the ONC target is the intracellular RNA, and there are evidences stating that ONC is able to principally cleave tRNAs[135]. ONC is 100-fold more active against polyuridylic acid than against polycytidilyc one, and 10-fold more active against uridylyl 3',5'guanosine than versus cytidilyl 3',5'guanosine[136].

The B1 subsite of ONC is composed by Thr35, Asp67 and Phe98, while the B2 subsite is supposed to be formed by Thr89 and Glu91[116]. Many RNase A homologs bind a pyrimidine residue on the 5'side of the phosphodiester bond, while ONC, and other frog ribonucleases, prefer to bind a guanine on the 3' side[59,68,70,132,137]. The cleavage of tRNA occurs between the guanosine-guanosine phosphodiester bond in the variable loop of the D-arm[138]. Furthermore, another

target of ONC is miRNA, with a consequent regulation of cell proliferation, migration, invasion and apoptosis, even though the exact mechanisms underlying these effects have not well understood yet[139].

1.3.3 ONC cytotoxicity

As mentioned before, and differently from most monomeric RNases, ONC can evade RI because it lacks many of the residues that are responsible for the RI-RNase A-like interaction[26,140].

The capability to avoid the RI interaction and its high basic surface charge make ONC cytotoxic and/or cytostatic against several tumor cell lines. Thus, ONC has been used in Phase II and IIIb clinical trials for the treatment of non-small cell lung cancer and unresectable malignant mesothelioma, respectively[141]. More recently, some studies have revealed that ONC is active toward other several human cancer cell types, such as glioma or, also, pancreatic adenocarcinoma cells through an autophagy-mediated and ROS-dependent pathway[142–144]. Its action is exerted by arresting the cell cycle in the G1 phase[15,145]. LC_{50} *in vitro* is about 10^{-7} M, but it depends on the cancer cell type treated. Moreover, ONC is able to inhibit human immunodeficiency virus type 1 replication[146,147]. Unfortunately, a prolonged ONC administration induces kidney toxicity, that makes the treatment dose-limiting, although this adversity can be overcome by discontinuing the treatments[148].

Like other cytotoxic RNases, ONC explicates its cytotoxicity after its cellular internalization, an event that occurs through endocytosis[149]. ONC can penetrate cancer cells thanks to its high basicity and favourable interaction with the sialic acid moieties present in the membranes of malignant cell[150]. The internalization mechanism has not been well characterized yet, but, after its releasing in the cytoplasm from the endosome, ONC is free to meet its target RNA. The reason proposed to justify ONC cytostatic and cytotoxic activity was the degradation of rRNA and the inhibition of protein synthesis[145], but ONC can cleave other RNAs as well. The cleavage of tRNA leads to the activation of the caspase cascade in mammalian cells, resulting in the activation of apoptosis[151].

Furthermore, the ONC generation of intracellular interfering RNAs (RNAi) could induce the apoptosis cascade[152].

One important aspect characterizing ONC activity is its ability to evade the cytosolic RNase inhibitor (RI). The K_i is about 10^{-6} M, ascribable, as already mentioned, to the lack of many residues that in RNase A are fundamental to mediate the interaction with RI[26,140].

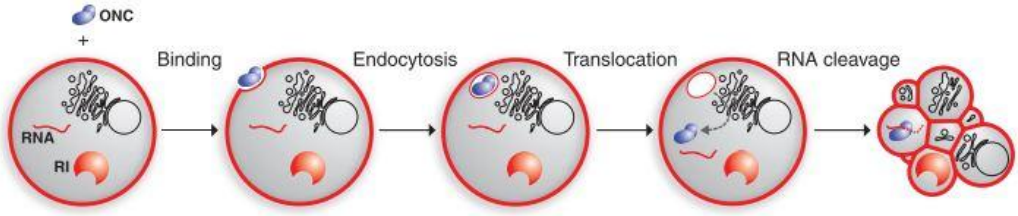

Figure 1.10. Proposed mechanism of ONC mediated cytotoxicity. ONC binds the cell surface and is internalized by endocytosis, and translocated into the cytosol where it evades RI and degrades RNA. RNA degradation results in cell death by apoptosis (from Turcotte et al., 2009[153]).

1.3.4 ONC dimerization

Recently, we observed that ONC can form a dimer after acid lyophilisation following the same protocol used for RNase A[42]. The structure of this dimer has been chromatographically and spectroscopically characterized, and a model has been proposed (Fig. 1.11), while its enzymatic activity has been measured on yeast RNA as a substrate.

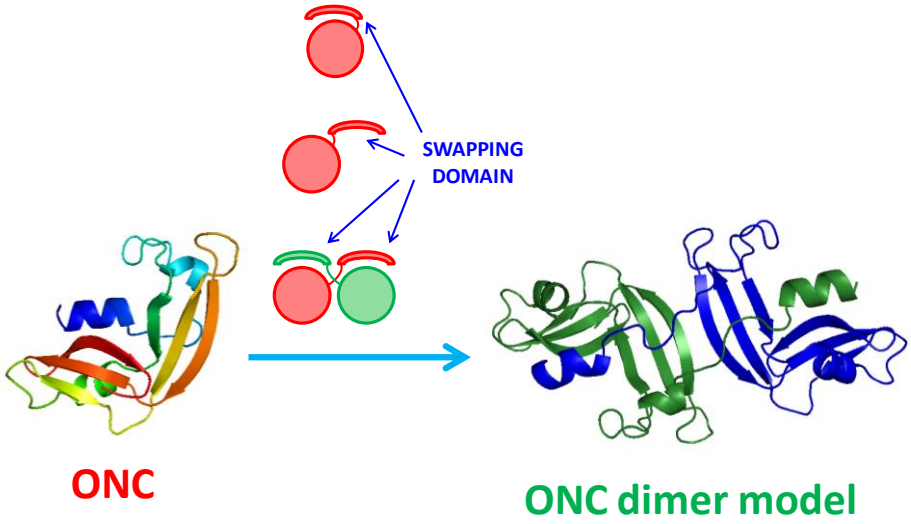

Figure 1.11. Molecular modelling of the N-swapped ONC dimer.

In addition, ONC cytotoxicity has been determined against pancreatic adenocarcinoma cells, finding that low dimer concentrations are more cytotoxic than the corresponding monomeric ones[154]. Thus, in the perspective of possible therapeutic applications, doses could be reduced and, consequently, also renal damage, to plan advantageous clinical applications to counteract this and/or other types of cancer as well.

1.4 Human Pancreatic Ribonuclease

1.4.1 HP-RNase structure

Human pancreatic ribonuclease (HP-RNase, or RNase 1) is a 128 AA residues RNase variant that is considered the homologue of RNase A in human[155]. These two enzymes share common characteristics, such as a high sequence identity (70%) and the same catalytic triad (His12, His119 and Lys41). As it is for RNase A, the human variant hydrolyzes 2',3'-cyclic phosphate nucleotides, and prefers poly(C) rather than poly(U)[156,157]. A remarkable difference characterizing the two mentioned variants is ascribable to the four residues elongation that HP-RNase displays at the C-terminus with respect to the bovine enzyme (total 128 vs 124 AA residues), as it is highlighted in Figure 1.12.

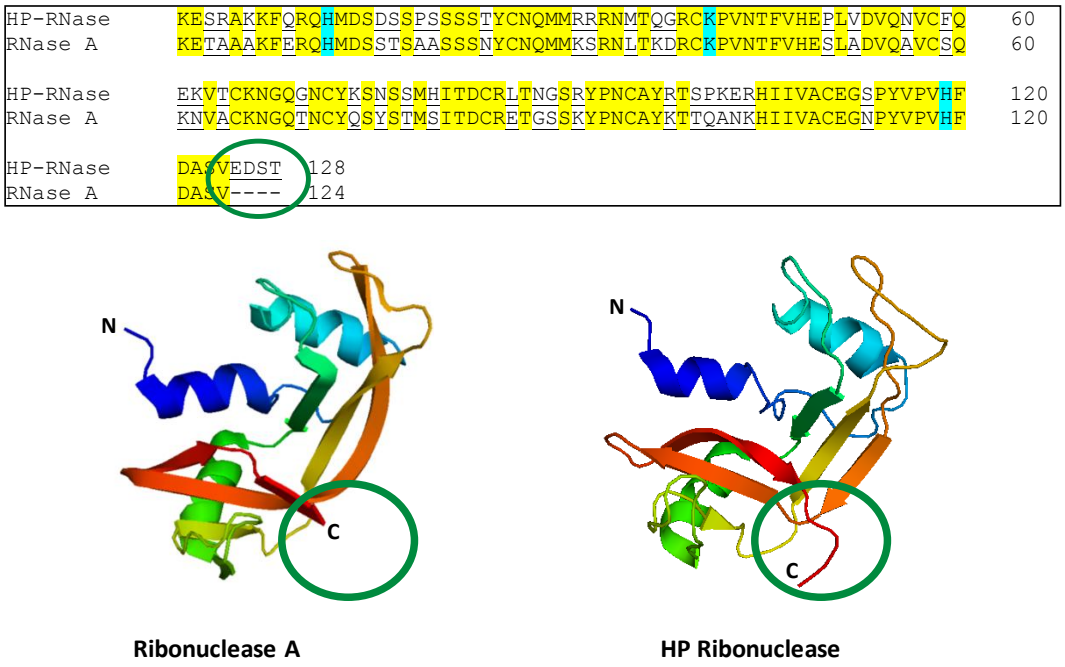

Figure 1.12 . Primary (upper panel) and three dimensional (lower cartoons) structures of RNase A and HP-RNase. (5RSA.pdb and 2K11.pdb). In the sequences the common residues are highlighted in yellow, while in light blue the catalytic triad. In the lower panels the green circles evidence the different length of the C-terminal tail of the two variants

1.4.2 HP-RNase activity and biological function

The hydrolytic cleavage mechanism of HP-RNase overlaps the one of RNase A. Also the substrate-binding subsite residues are the same, but the human variant displays more basic residues on its surface and this feature is related to its higher catalytic activities with respect to the bovine variant. HP-RNase can cleave dsRNA, poly(A), and the RNA component of RNA:DNA hybrids under physiological conditions[158]. Differently from RNase A, the human variant is capable to attack and efficiently cleave also dsRNA: this is due to the higher number of positive present in HP-RNase with respect to RNase A, and therefore to a higher interaction affinity of these charged residues with the polyanionic double helical substrate[9,159,160].

HP-RNase can be isolated from human pancreas, but its gene is present also in urine, seminal plasma, brain and kidney. Differential post-translational events occur at the expense of this enzyme, depending on the tissue origin. As an explanation of its presence in various organs, the protein may originate from the endothelium of arteries, vein and capillaries[161,162]. It has been suggested that HP-RNase might also be involved in the regulation of vascular homeostasis, because of its high expression level in endothelial cells[162]. Furthermore, HP-RNase might act as an extracellular RNA scavenger in order to normalize serum viscosity, and it may also be involved in the non specific response to pathogenic RNA molecules. This protein can also contribute to both inflammatory and immune responses, where this action is correlated to its ability to induce the maturation of dendritic cells and to the production of soluble mediators, such as cytokines, chemokines and growth factors[160,163].

Finally, it has been detected that HP-RNase can be also definitely cytotoxic, provided that it evades the interaction with RI, but this is not likely for the wt, unmodified form.

Like RNase A, HP-RNase forms a tight complex with RI ($K_d=10^{-15}M$)[124]. A recent study has shown that an engineered HP-RNase, in which two Arg residues have been mutated in cysteines (R31C and R32C), forms a covalent dimer that is toxic against various cell types. This new activity has been ascribed

to the resistance of the dimer to RI[164]. Therefore, we can envisage that a dimeric structure could be definitely advantageous for HP-RNase citotoxic activity.

Therefore, efforts to modify its structure and/or its steric hindrance have been performed in the recent past to let HP-RNase express its cytotoxic potential.

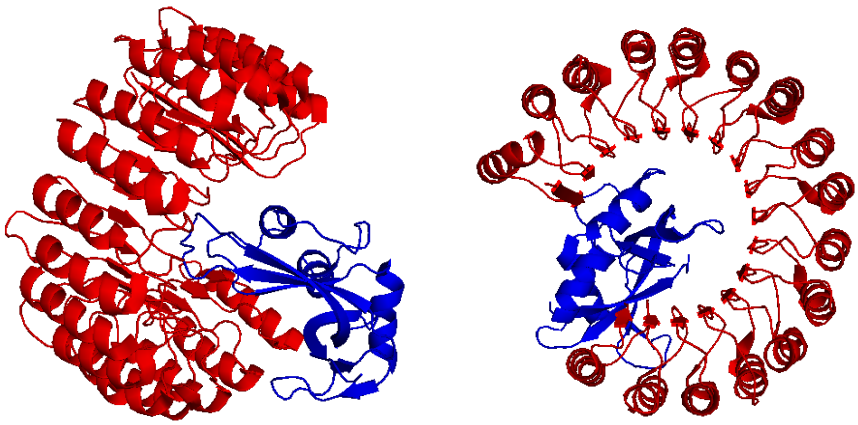

Figure 1.13. Crystal structure of human pancreatic ribonuclease (blue) in complex with ribonuclease inhibitor (red) (1Z7X.pdb).

1.4.3 HP-RNase dimerization

In the last two decades, some studies have been focused on HP-RNase dimerization, but they all involved mutants of the enzyme, not the wild-type. For example, efforts have been performed to produce covalently stabilized derivatives, as the HHP2-RNase variant, whose crystal structure has been solved[165]. It is a covalent, unswapped dimer in which some residues located in the helix-II of the HP-RNase were replaced by some other present in the natively dimeric BS-RNase (Q28L, R31C, R32C, N34K), and the negative charge on the surface was eliminated (E111G)[166]. This and other variants display two cysteine residues that form two antiparallel disulfide bonds between the monomers, like BS-RNase. Furthermore, the elimination of the E111 negative charge leads to an increase in the cytotoxicity of the protein[164–166]. Another engineered HP-RNase variant is PM8, in which some residues of the N-terminal have been replaced by the

corresponding ones of BS-RNase. Then, an additional P101Q mutation allowed this variant to form a domain-swapped dimer by reciprocally exchanging the N-termini[167]. However, this dimer is structurally different from the one of RNase A.

Other HP-RNase variants able to dimerize through 3D-DS were obtained by the deletion of some residues located in the connection loop between the N-terminal helix and the core of the protein[168,169]. This des(16-20)-HP-RNase variant spontaneously forms a dimer by exchanging its N-terminal domains, with no traces of residual monomer[168]. Also des(16-18)-HP-RNase is able to form a N-dimer eluted in a mixture with the monomer in a 4:1 ratio[168,169]. It was registered that this latter variant can evolve toward the association of two dimers that can form a tetramer, that in turn can further associate to evolve toward fibrillar aggregates[169].

1.5 Angiogenin

Angiogenin (ANG,) is another important member of the pancreatic-type ribonuclease superfamily, and for this reason is called also RNase 5. It was firstly discovered and isolated in the ‘80s from human adenocarcinoma cell conditioned medium. However, it is a secreted growth factor also in normal human tissues and fluids, such as plasma, amniotic fluid or cerebrospinal fluid[170–173]. It is called angiogenin because is involved in the neo-formation of vessels, but is also a ribonuclease because it exerts a ribonucleolytic activity.

1.5.1 ANG structure

ANG (Fig. 1.14) is a small RNase variant (123aa, 14.1kDa), that displays a low ribonucleic activity (10^{-5}/10^{-6} fold less than of RNase A). However, this activity is mandatory to exert its peculiar angiogenic activity. ANG displays only 33% sequence identity and 65% homology with bovine pancreatic RNase A, but is characterized by an identical catalytic triad (two His plus one Lys residues). An interesting feature that differentiates ANG from the other RNases of the superfamily is that its C-terminus displays an α-helix portion instead of a β-sheet.

```
RNaseA      -KETAAAKFERQHMDSSTSAASSSNYCNQMMKSRNLTKDRCKPVNTFVHESLADVQAVCS    59
wtANG       QDNSRYTHFLTQHYDAK-PQGRDDRYCESIMRRRGLT-SPCKDINTFIHGNKRSIKAICE    58

RNaseA      QKNVACKNGQTNCYQSYSTMSITDCRETGSSKYPNCAYKTTQANKHIIVACEGNPYVPVH    119
wtANG       NKNGNPH--RENLRISKSSFQVTTCKLHGGSPWPPCQYRATAGFRNVVVACENG--LPVH    114

RNaseA      FDASV----  124
wtANG       LDQSIFRRP  123
```

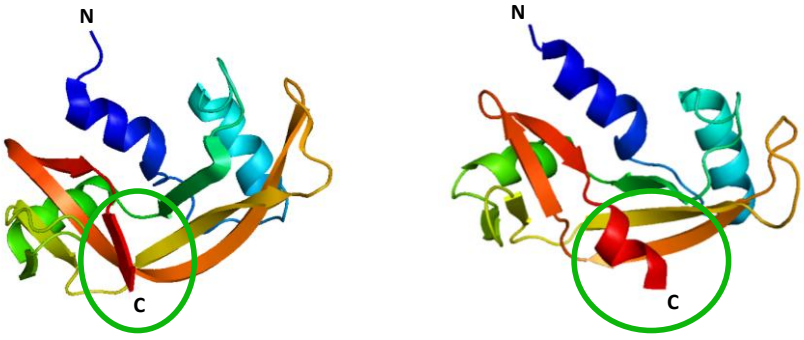

Ribonuclease A **Angiogenin**

Figure 1.14. Primary (upper panel) and 3D (lower cartoons) structures of RNase A and ANG. (5RSA.pdb and 5EOP.pdb, respectively). In the upper panel, the common residues are highlighted in green, while in cyan the catalytic triad. In the 3D structures the different conformations of the C-termini are inside a circle.

1.5.2 ANG enzymatic activity and biological functions

Angiogenin has the same RNase A catalytic triad, in particular H13, H114 and K40 in spite of H12, H119 and K41[170,174]. Like other pancreatic-type RNases, ANG cleaves the substrate preferentially on the 3' side of pyrimidine bases, and follows the same transphosphorylation/hydrolysis mechanism of RNase A (see Figure 1.3). However, ANG has a lower endonucleolytic activity than RNase A *versus* yeast RNA, resulting to be about 4-5 fold less potent than it. One of the reasons for this low activity is the presence of a Gln residue (Q117) located at the C-terminus which obstructs the pyrimidine binding site[174,175]. It has been observed that the substitution of the Q117 residue with alanine or glycine leads to an increase of its angiogenic activity, that results 18 to 30 folds more active versus tRNA, respectively[176]. ANG cleaves preferentially ss-RNA, although it has been observed that it binds also DNA *in vivo*, obviously without cleaving it[177,178].

ANG displays several biological functions, that can be exerted only if an at least minimal ribonucleolytic activity is present. One of the most important activities is the neovascularization of the central nervous system (CNS), but ANG is involved also in the embryonic development, in wound healing, as well as in new blood vessel formation, and so on[170]. Neo-angiogenesis is a complex and multistep process that involves a large amount of proteins, chemokines, factors and cells, and leads to the formation of new vascular structures[179]. In this complex scenario, after binding a 170 kDa transmembrane receptor of endothelial cells, ANG can trigger many signal transduction pathways, such as kinase 1/2 (ERK1/2), protein kinase B/Akt, and/or stress-associated protein kinase/c-Jun N-terminal kinase (SAPK/JNK)[180–182]. The activation of these patterns leads to the increase of endothelial cells growth, therefore stimulating angiogenesis[183]. ANG is able to bind endothelial cell surface, thanks to a 42 kDa receptor similar to the smooth muscle type α-actin[184]. This receptor seems to be involved in the

degradation of the basement membrane, and its complex with ANG accelerates the generation of plasmin from plasminogen catalyzed by a tissue-type plasminogen activator (tPA)[185]. This complex promotes also the degradation of the basement membrane and of the extracellular matrix, allowing endothelial cells to penetrate and migrate into the perivascular tissue, in order to create new vessels[186].

ANG can be internalized in endothelial cells to exert one of its numerous functions. The pathway followed is not completely known, but some evidences suggest that ANG enters the cells with a receptor-mediated endocytosis, and then is directed toward the nucleus through a microtubule and lysosome independent transport across the cell cytoplasm[187]. However, in the CNS cells, such as as neuronal, astrocytic and microglial ones, ANG is not internalized through an endosomes uptake which is clathrin/dynamin independent. Therefore, it is not still clear how ANG can move toward the nucleus after its cellular internalization[188].

Once inside the cell, ANG is able to translocate into the nucleus, in particular of endothelial and smooth muscle cells, following two mechanisms. The first is ascribable to a particular sequence called NLS, nuclear localization signal, containing three arginine residues (30-MRRRG-35)[189,190]. The second mechanism is represented instead by the passage through the nuclear pores, because ANG is definitely smaller than their size limit (50kDa)[191]. Inside the nucleus, ANG activates the transcription of some angiogenic factors, such as VEGF (vascular endothelial growth factor), EGF (epidermal growth factor), aFGF (acidic fibroblast growth factor) and bFGF (basic fibroblast growth factor)[192,193]. This mechanism takes place thanks to the ANG capability to bind some DNA promoter regions, in this way inducing rRNA transcription[194,195].

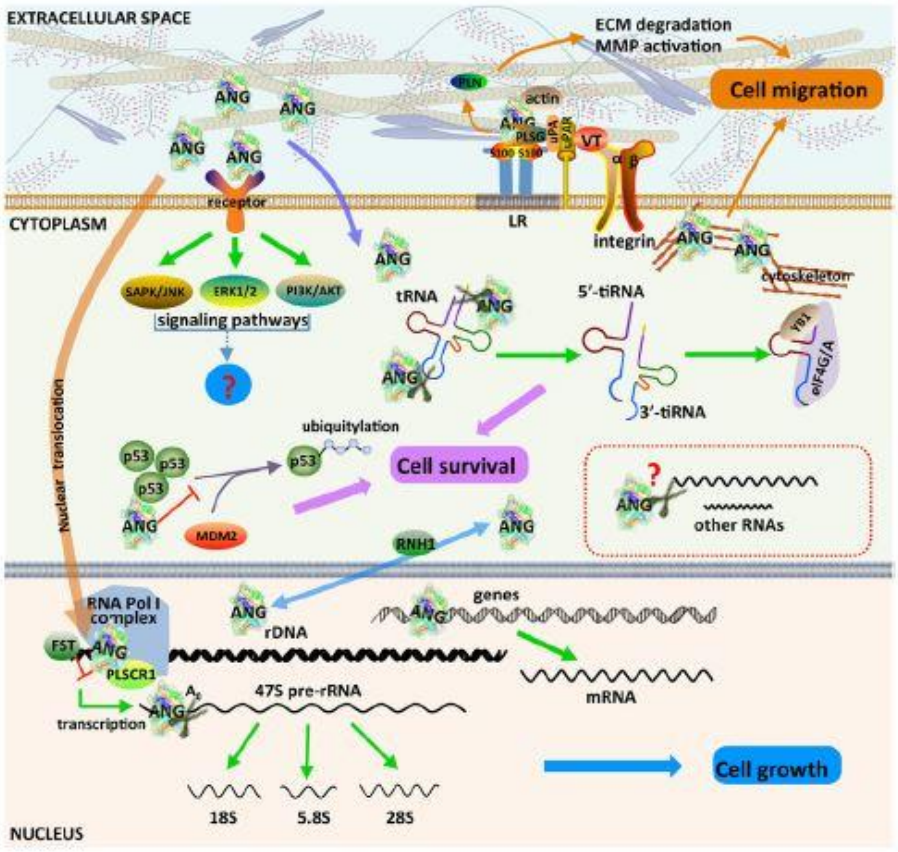

Figure 1.15. Schematic representation of the mechanisms of action of ANG. (from Sheng and Xu, 2016[183])

1.5.3 ANG and pathologies

The peculiar angiogenic activity of ANG is unfortunately involved also in the growth of solid tumors. This can occur thanks to the neovascularization induced around the malignant tissue mass. Indeed, an increased expression of ANG can be detected in many human cancer types, such as breast, cervical, colon, colorectal, prostate, endometrial, gastric, liver, kidney, ovarian, pancreatic, and urothelial cancers, lymphoma, melanoma, osteosarcoma, etc[196–198].

However, a positive effect of ANG is that it promotes a survival effect on the neuronal progenitors of CNS cells, and it protects motoneurons by increasing the neurovascular perfusion[175]. However, it is also known that many ANG mutants are implicated in neurodegenerative diseases, such as Amyotrophic Lateral Sclerosis (ALS), Parkinson's Disease (PD), and more recently also in

Alzheimer's Disease (AD)[199–203]. The majority of the mutants are linked to missense mutations located in the coding region of ANG gene that affect both neurite extension and the motor neurons survival, therefore inducing a decrease of tissues vascularisation and the motor neurons death for hypoxia[204]. As concerns ALS, different mutants have been detected in many cohorts of Italian, German, Irish, Scottish patients, etc[200,203,205–208]. Again, another study reported the presence of ANG genetic variants in both ALS and PD patients[183]. The ANG mutations involved in these neurodegenerative diseases generally influence not only the enzymatic activity of the protein, especially by affecting its binding to the substrate, but also its structure or its capability to be translocated into the nucleus[201,202,209].

In this complex scenario, a possible destiny for the pathogenic variants of ANG may be to oligomerize and form insoluble protein aggregates that could precipitate in the CNS (Central Nervous System) and contribute to the pathogenesis and developement of these multifactorial neurodegenerative diseases. Indeed, the fact that ANG mutants are involved in the onset of both ALS or PD, and that neurodegenerative diseases are related to uncontrolled protein aggregation events, suggests us to evaluate if this RNase variant might be prone to undergo controlled or, conversely, uncontrolled self-association.

Chapter 2

AIM

OF THE

THESIS

In my PhD course I was involved in the study of the oligomerization tendency of various pancreatic-type ribonucleases, such as amphibian onconase, human pancreatic RNase, and human angiogenin.

It is well known that RNase A can form dimers and larger oligomers through the 3D-DS mechanism if it undergoes two different incubation protocols. Therefore, in the first part of my thesis I analyzed if the two different methods could induce different structural or functional properties in the protein, or also in its two different N-terminus or C-terminus swapped dimers, called N_D and C_D respectively.

In the second part of my studies I continued the investigations started by my PhD predecessor and focused on the onconase (ONC) dimerization occurring through the domain swapping of its N-termini. In particular, the aim of my studies was to induce ONC to dimerize also through the swapping of its C-terminus, and to make the enzyme capable to oligomerize more extensively than its natural propensity and, thus to increase its cytotoxic potential. To do so, I designed and produced some ONC mutants in order to unlock the C-termini of the protein and allow its oligomerization through this domain, in addition to the N-terminal one. I produced initially two mutants lacking the disulfide bond C87-C104, where one Cys residue was substituted by a serine. Then, I designed two additional variants lacking one or two of the three C-terminal residues that make this domain longer than the one of RNase A. This elongation could somehow disturb the correct accommodation of the protein C-terminus after inducing its swapping, and it could influenced the ONC tendency to form stable oligomers.

Furthermore, the sequence alignment of RNase A, ONC, and also HP-RNase, shows that both the two last variants display a similar C-terminus elongation with respect to RNase A. Therefore, I investigated also the self-association propensity of HP-RNase, in parallel with its variant displaying the deletion of the mentioned C-terminus elongation. This should gain information on the general role of C-terminus elongation in its 3D-DS event, but would also allow to evaluate for the first time the general oligomerization propensity of HP-RNase. In fact, only some mutants at the expense of the N-terminus are known to form a N-swapped dimer, but not larger oligomers. Hence, considering that the

high cytotoxic potential of HP-RNase is frustrated by the formation of a tight complex with the ribonuclease inhibitor, the oligomers that it could form would become a useful tool against cancer, either *in vitro* or, hopefully, also *in vivo*.

Finally, I analyzed also the self-association propensity of human angiogenin (ANG). This particular RNase variant is a crucial factor for the neo-formation of vessels, but numerous variants were found in patients affected by neurodegenerative diseases, such as ALS, or PD. Although being, them, very complex and multifactorial pathologies, our aim is to investigate if the wild type and some pathogenic ANG variants as well might oligomerize like other RNases and possibly contribute for the onset and development of the mentioned pathologies.

Taken together, all the data emerging from the studies here described should certainly provide useful information to govern the activity(ies) of the mentioned RNases and drive their action toward more advantageous addresses than the native monomers. In addition, considering that these studies will involve four different RNases, the comparison of the relative results obtained will certainly provide general informations on the structural determinants favouring or, on the contrary, hindering the self-association through 3D-DS. Again, considering that the possibility for a protein to swap more than one domain can exponentially enhance its self-association propensity, the information collected on the possibility(ies) to swap the C-termini of these RNase variants, besides the corresponding N-terminal ones that can be more easily swapped, will certainly be precious to enhance the tendency of all pancreatic-type RNases to undergo extensive self-association.

Chapter 3

MATERIALS AND METHODS

3.1 Materials

RNase A type XII-A, polyadenylic acid-polyuridylic acid [poly(A):poly(U)] and subtilisin "Carlsberg" were purchased from Sigma. Yeast RNA was from Boheringer. HAc and EtOH were from Merck-Sigma. BMH, BMOE, $BM(PEG)_2$ were from ThermoScientific. All other chemicals were of the highest purity available.

The cDNA of wild type angiogenin was kindly provided br Dr. Eliodoro Pizzo (University of Naples, Federico II). The wt-ONC cDNA, inserted in the plasmidic vector pET-22b(+) between Nde I/Bam HI restriction sites, was kindly provided by Prof. D. Picone and Dr. E. Notomista (University of Naples, Federico II). Finally, the cDNA of human pancreatic RNase was provided by Dr. Ester Boix (Universitat Autonoma de Barcelona).

3.2 Mutants construction and production

The primers used are reported in following tables:

Onconase	
H10A	5'-TCCAGAAAAAAGCTATCACTAACACTCGTG-3' 5'-CACGAGTGTTAGTGATAGCTTTTTTCTGGA-3'
C87S	5'-TAACAAATTCAGCGTTACTTGCGAAAACCA-3' 5'-TGGTTTTCGCAAGTAACGCTGAATTTGTTA-3'
C104S	5'-GTTGGTGTTGGTTCTAGCTAGTAGGGATCC-3' 5'-GGATCCCTACTAGCTAGAACCAACACCAAC-3'
desC104	5'-CGTTGGTGTTGGTTCTTGATAGTAGGGATCC-3' 5'-GGATCCCTACTATCAAGAACCAACACCAACG-3'
desS103C104	5'-CATTTCGTTGGTGTTGGTTGATGCTAGTAGGGATCC-3' 5'-GGATCCCTACTAGCATCAACCAACACCAACGAAATG-3'
+ loop (QVVAG) +VV +G	5'-GCGAAAACCAGGTGGTGGCTCCGGTTCATTTCG-3' 5'-CGAAATGAACCGGAGCCACCACCTGGTTTTCGC
	5'-AACCAGGTGGTGGCTGGCCCGGTTCATTTC-3'

	5’-GAAATGAACCGGGCCAGCCACCACCTGGTT-3’
-GSC*	5’-TTCGTTGGTGTTTAGTCTTGCTAGTAGGG-3’ 5’-CCCTACTAGCAAGACTAAACACCAACGAA-3’

*these mutants are now under production

Angiogenin	
S28N	5'-GGACGATCGTTACTGCGAAAACATTATGAGACGCCGTGGG-3' 5’-CCCACGGCGTCTCATAATGTTTTCGCAGTAACGATCGTCC-3’
Q117G	5’-TCTGCCAGTCCATCTAGATGGCTCTATCTTCCGAAGGCC-3’ 5’-GGCCTTCGGAAGATAGAGCCATCTAGATGGACTGGCAGA-3’

H13A and C39W cDNA was provided by prof. D. V. Laurents (CSIC, Madrid).

Human Pancreatic RNase	
(-EDST) **des125-128**	5’-TGATGCTAGCGTTTAGGATTCTACTTAAGGATCCGGC-3’ 5’-GCCGGATCCTTAAGTAGAATCCTAAACGCTAGCATCA-3’
H12A*	5’-AGTTCCAAAGACAAGCGATGGACTCTGATAGC-3’ 5’-GCTATCAGAGTCCATCGCTTGTCTTTGGAACT-3’
R4A*	5’-GAAAGAATCTGCGGCTAAAAAGTTCCAAAGAC-3’ 5’-GTCTTTGGAACTTTTTAGCCGCAGATTCTTTC-3’
S113N*	5’-TTGTTGCTTGTGAAGGTAACCCTTACGTTCC-3’ 5’-GGAACGTAAGGGTTACCTTCACAAGCAACAA-3’

*these mutants are now under production

The polymerase chain reaction (PCR) was carried out by using the QuickchangeII (Agilent) mutation kit or Phusion Hot Start II DNA Polymerase (ThermoFisher Scientific). The reaction mixtures were prepared in different way depending on the polymerase used. For the QuickchangeII kit: 0.5µl of plasmidic

DNA, 5µl of 10X buffer, 1µl of 10mM dNTPs mix, 1.25µl of primers ([stock solution]= 25µM), 1µl of PFU polymerase, and 40µl of ddH_2O. PCR was performed using the following cycles: 30" at 95°C, 16 x (30" at 95°C, 1min at 57°C, 12min at 68°C), 12" at 68°C. For the Phusion polymerase: 1µl of plasmidic DNA, 10µl of 5X buffer, 1µl of 10mM dNTPs mix, 1.25µl of primers ([stock solution]= 25µM), 0.5µl of polymerase, and 35.5µl of ddH_2O. In this case the PCR cycles are: 30" at 98°C, 30 x (10" at 98°C, 1min at 57°C, 5min at 72°C), 12" at 72°C.

The amplification product was detected through electrophoresis on a 0.8% agarose gel with 1/10'000 SYBR® dye solution, and successively digested with DpnI at 37°C, for 1h, in order to eliminate the original cDNA.

As for H10A-ONC, C97S-ONC and C104S-ONC mutants, TOP10 cells with 5µl of PCR product, transferred in ice bath for 30min, then for 30sec at 42°C and again for 2 min in ice-bath. Successively, 250µl of SOC medium were added and the sample was incubated at 37°C for 1h. 80µl of bacteria were grown overnight on a "Petri" plate, in 15ml of LB-agar containing 15mg of ampicillin (AMP). Two colonies were separately collected, amplificated in 5ml of LB medium containing 5mg AMP, and grown at 37°C. The plasmidic DNA was purified, sequenced, and the one extracted from a selected colony was used to transform BL21(DE3) cells, following the procedure described below.

For all other mutants, DH5α cells were incubated with 5µl of PCR product, transferred in ice bath for 30min, then for 20 sec at 42°C and again for 2 min in ice-bath. Then, 250µl of LB medium were added and the sample was incubated at 37°C for 1h. 100µl of bacteria were grown overnight on a "Petri" plate, in 15ml of LB-agar containing 15mg of ampicillin (AMP). Two colonies were separately collected, amplificated in 5ml of LB medium containing 5mg AMP, and grown at 37°C. The plasmidic DNA was purified, sequenced, and used to transform BL21(DE3) cells.

3.3 Competent cells transformation

BL21(DE3) cells were incubated with 100ng of plasmidic DNA, transferred in ice-bath for 30min, and then incubated at 42°C for 2 min, and lastly other 2 min on ice. Then, 200µl LB were added and the mixtures was incubated at 37°C for 1h. Later, 50µl of this solution were transferred in a "Petri" plate containing 15ml of LB-agar and 15mg AMP. The plate was kept at 37°C overnight. A colony was then collected, transferred in 5ml LB containing 5mg AMP, and grown at 37°C overnight. Subsequently, 500µl of culture were mixed with 500µl glycerol and immediately frozen to -80°C.

3.4 Protein expression and purification

Competent cells (BL21(DE3)) were grown for 6h in 5ml of TB medium and 0.5mg AMP, at 37°C, and then overnight in 150ml of the same broth, at the same temperature. The inoculum was subsequently mixed with 1L of TB, 0.1g AMP, incubated at 37°C, and protein production was induced with 0.4mM IPTG when OD_{600} reached the value of 2.4. Then, it was left overnight at 37°C, and under agitation. Cell lysis was performed resuspending the pellet in 10ml of 0.1M Tris-acetate pH 8.4, 5mM protease inhibitor phenylmethylsulfonyl fluoride (PMSF), and 2g of lysozyme, for 30 min. After this step, the pellet can be conserved at -80°C or conversely, it can be treated with deoxycholic acid, and with the other passages previously reported. Then, 30mg of deoxycholic acid were added, and the solution was transferred at 37 °C for 40-60 min. After that, 320 Kunitz Units of DNase and 5mM $MgCl_2$, final concentration, were added, and the solution was incubated for 30min at room temperature. The mixture was then centrifuged at 16.000rpm for 30min and the resulting pellet solubilized in 0.1M Tris-acetate, pH 8.4, 10mM EDTA, 2% Triton X and 2M Urea. After 30min incubation, the washing was repeated three times, one with the same buffer and two with only 0.1M Tris-acetate, pH 8.4, 10mM EDTA. The pellet was subsequently redissolved in 0.1 M Tris-acetate, pH 8.4, 10 mM EDTA, 6M GdnHCl, and 100mM DTT, saturated in nitrogen, and the solution incubated for 3h at 37°C. The reaction mixture was then dialyzed twice against 2L of 20mM

acetic acid, for 3h, and finally against 5L, overnight. After pellet removal, the solution was diluted in 200ml of 0.1M Tris-acetate, 0.5M L-arginine, pH 8.4. A mix of reduced and oxidized glutathiones (3mM/0.6mM) was added to the protein extract with no free Cys, and saturated with nitrogen for 20-24 h. After protein renaturation, the solution containing the protein was transferred in a 0.2M potassium phosphate pH 8.0, 2mM $ZnSO_4$ solution containing aminopeptidase extracted from *Aeromonas proteolytica* (AAP). AAP:protein molar ratio was 1:1000, and the protein was incubated for 96h at 37°C. Subsequently, EDTA was added at a final concentration of 10mM. The protein was further purified using a Superdex 75 HR 10/300 column, connected to an ÄKTA-FPLC system (GE-Healthcare), in 0.1M Tris-acetate pH 8.4, 0.3M NaCl, at a flow rate of 0.3ml/min. After the final purification step, the protein amount was spectrophotometrically determined at 280nm, and the protein absorbance ($A_{280}^{0.1\%}$) was calculated with ProtParam tool, with a Jasco V-650 spectrophotometer, and the protein lyophilized from ddH_2O. Ten µg of protein sample were resuspended in 100µl of 0.1% HCOOH and analyzed with a high-resolution mass spectrometry on a Xevo G2-S Q-TOF instruments (Waters, MA, USA) with the collaboration of Dr. G. Pontarollo, Dr. D Peterle of the University of Padua. The mass versus charge signals, visualized as BPI (base peak intensity) by the program MassLynx V4.1, were deconvoluted by the software MaxEnt1 to achieve the peaks average masses. Other MS analysis were obtained by a Bruker Ultraflextreme MALDI-TOF/TOF instrument of "Centro Piattaforme Tecnologiche" (CPT), University of Verona, with the technical assistance of Dr. D. Sorio.

3.5 Induction of oligomerization through lyophilization of 40% acetic acid solutions and purification of the oligomers

Purified proteins were dialyzed against MilliQ water and lyophilized as 0.2-1mg aliquots. The powder was aliquoted to prepare oligomers by lyophilization after resuspension in 40% aqueous acetic acid solution, and then following the same protocol used for RNase A (Cresfield et al. 1962).

The powder resulting after acidic lyophilisation was solubilised in 0.4M sodium phosphate (NaPi), pH 6.7, and analyzed in size exclusion chromatography (SEC) using a Superdex 75 Increase 10/300 GL column attached to an ÄKTA-FPLC Purifier System (GE-Healthcare). The column was equilibrated with the same buffer (0.4M NaPi, pH 6.7) and the sample eluted at 0.3mL/min.

Only for RNase A, the resulting powder was then solubilised in 50mM sodium phosphate (NaPi), pH 6.7, and analyzed with cation exchange chromatography using a Source 15S column attached to an ÄKTA-FPLC Purifier System (GE-Healthcare). A NaPi gradient from 70mM to 200mM was applied to elute the monomer and, progressively, to separate all RNase A oligomers [44]. This technique permits to well separate the two dimers and the major oligomers that have the same molecular weight but different ionic charge exposure. Firstly was eluted the monomer, and in sequence, at higher concentration of phosphate ion, the N-dimer, and successively the C-dimer, which has a major positive charge exposure than the other two species analyzed. Finally were eluted the other major oligomers, trimers, tetramers, etc.

3.6 Thermally-induced oligomerization

The lyophilized powder of RNase A was dissolved in 40% EtOH (final concentration 200mg/ml) and incubated at 60°C for 90min. The reaction was stopped adding 500µl of 50mM NaPi, pH 6.7 pre-heated at 60°C [43]. Then, samples were put in an ice-bath before the cation exchange analysis performed under the same conditions used upon acetic acid lyophilisation.

This protocol was applied also to RNase A and some ONC variants and analyzed by SEC. The lyophilized powder of purified protein was dissolved in 5µl of a 40% EtOH (final concentration 200mg/ml) and incubated at 70°C for 80min. The reaction was stopped by adding 500µl 0.2M NaPi, pH 6.7 pre-heated at 70°C. Then, samples were put in an ice-bath before performing SEC analysis under the same conditions used with oligomers mixtures obtained lyophilising the proteins from 40% acetic acid solutions.

3.7 Nondenaturing cathodic PAGE

Nondenaturing cathodic PAGE was performed with 12.5 and 15% acrylamide gels, in 0.35% β-alanine and acetic acid buffer, pH 4.0 [104]. The purified species were desalted, and 5µg of each sample analyzed without boiling them. The Sample Loading Buffer (SLB) was composed of 0.04% methyl green dissolved in a 50% glycerol solution. Gels were stained with 0.1% Coomassie Brilliant Blue, and destained with 10% CH_3COOH, 20% EtOH solution.

3.8 Enzymatic activity assays

3.8.1 Single stranded RNA (ss-RNA)

The activity of the proteins (RNase A monomers and dimers, wild type ONC and some of its variants) was analyzed using yeast RNA single stranded (ss-RNA) as substrate, following the protocol of Kunitz[210]. Assays were performed with a substrate concentration of 0.6mg/mL in 0.1M sodium acetate buffer, pH 5.0. The final protein concentration in the reaction mixture was 12.5ng/µL for ONC species. The catalytic activity was determined at 300nm, measuring the absorbance decrease with time. Negative controls were performed by measuring the absorbance of yeast RNA solution without the addition of enzymes.

The kinetic analyses of RNase A monomers and dimers were performed by using a substrate concentration from 0.02 to 0.8mg/mL. The enzyme

concentration was 0.8ng/μL for the monomers and 1.5ng/μL for the dimers. The calculated specific catalytic activity corresponded to the Abs_{300} decrease per min per μg of enzyme[210].

3.8.2 Double stranded RNA (ds-RNA)

The activity against ds-RNA was tested using poly(A):poly(U) as substrate, in concentration range between 0.02 to 0.2 mg/mL in 0.15M NaCl / 0.015M sodium citrate buffer, pH 7.0[211]. Higher substrate concentrations could not be explored for the incoming of an excessive spectrophotometric error. In these assays, was added 10μg for the monomers, 4μg for N_D and 2μg for C_D. The volume reaction was 300μL, and the absorbance was recorded at 260nm. The calculated catalytic activity was the Abs_{260} decrease per min per μg of enzyme[211].

3.9 Circular dichroism spectroscopy

The far and near UV CD spectra of the proteins performed at 25°C in 10mM NaPi buffer, pH 6.7, from 190 to 240nm and from 240 to 350nm, respectively, using a Jasco J-710 spectropolarimeter. Protein concentration was comprised between 0.3 and 1.0 mg/ml for near-UV analysis, and between 0.15 to 0.25mg/ml for far-UV spectra. Spectra were normalized against concentration and the far-UV analysis converted to molar ellipticity. Deconvolutions of far-UV-CD spectra were performed in the 190-240nm range using the DichroWeb software online tools [212].

3.10 Intrinsic fluorescence

Intrinsic fluorescence emission spectra of RNase A monomers and dimers were registered with a Jasco FP-750 spectrofluorimeter, using a 1cm path length quartz cuvette at 25°C. Spectra were acquired from 290 to 500nm upon excitation

at 280nm with 5nm bandwidth. Monomers and dimers samples concentration was 0.1mg/mL, with the species dissolved in 10mM NaPi, pH 6.7.

3.11 Mass Spectrometry of the RNase A monomers

The molecular weight of each RNase A monomer recovered upon the different incubations was determined, including the untreated monomer, with ESI-TOF Mass Spectrometry. Measures were performed with a MICROTOF Bruker Daltonics Spectrometer in the "Centro Piattaforme Tecnologiche" (CPT) of the University of Verona. Each monomeric sample recovered was desalted and lyophilized, successively suspended with aqueous acetonitrile (ACN) solution (30:70 v/v ACN: 0.1% aqueous TFA), and incubated at RT for 30 min. The resulting solution was mixed at 1:1 (v/v) ratio with the sinapinic acid (trans-3,5-dimethoxy-4-hydroxycinnamic acid) matrix (10 mg/mL in ACN:H_2O 1:1 with 0.1% TFA). Then, 1 μl of sample/matrix solution was spotted in triplicate onto a Ground Steel MALDI target plate (Bruker Daltonics, Billerica, MA, USA), allowed to dry at RT. MS analysis was performed again on a Bruker Ultraflextreme MALDI-TOF/TOF instrument (Bruker Daltonics) of the "Centro Piattaforme Tecnologiche" (CPT), the University of Verona. Mass spectra were collected in the m/z range of 5000 to 20000 in positive linear mode. Mass calibration was performed with a protein standard mixture of myoglobin, cytochrome C, ubiquitin I and insulin. Instrument settings were: ion source 1: 19.93 kV; ion source 2: 18.77 kV; lens: 8.57 kV; delay time: 104 ns with a scale factor of 800; acceleration voltage: 20 kV; number of shots: 2000 in six different positions for one spectrum. All data were analyzed with the Flex Analysis Software (Bruker Daltonics).

3.12 Thermal denaturation analyses of the RNase A monomers

The thermal denaturations of the RNase A monomers were measured following the 218 nm far-UV CD signal, with the same Jasco J-710 spectropolarimeter equipped with a Peltier thermostatic device. The temperature of each sample dissolved in 10mM NaPi was increased, at 1.5 °C/min speed, from 20 to 90°C. The signal was recorded every 0.5°C, with a 2 nm bandwidth and the T_m of each monomer was derived from the 50% far-UV CD signal.

Furthermore, to investigate the degree of reversibility of the process, native RNase A was incubated at 90°C for times ranging from 10 to 240 min and then cooled to 25°C to measure its near-UV CD spectrum and compare it with the one of the untreated RNase A monomer. In addition, each sample was analyzed through catodic PAGE to investigate the possible formation of deamidated species upon a long-time 90°C incubation.

3.13 Limited proteolysis with subtilisin

All RNase A species (monomers and N- or C-terminus swapped dimers) were dissolved in 10mM NaPi pH 6.7 and subtilisin "Carlsberg" was added in a 1:1000 molar ratio. The reaction was stopped by adding 1.5mM PMSF at different times, and the products present in the mixture were analyzed with SDS-PAGE under reducing conditions. The incubation time of the N-dimers was shorter than the ones relative to the other species, due to the higher susceptibility of N_D to the protease with respect to the monomer and the C_D[213].

3.14 Divinylsulfone (DVS) cross-linking reaction

RNase dimers were incubated with DVS cross-linker, useful to link the active-site His residues of the proto-type RNase [214]. If 3D-DS had occurred, the cross-linking should provide a covalently stabilized dimer, connecting the core of one monomer to the swapped domain of the other.

Protein dimers at a concentration of 0.25mg/ml in 0.1M NaAc/HAc buffer, pH 5.0. 10% DVS was added in a DVS:protein molar ratio of 1:1000. The reaction was stopped by adding β-mercaptoethanol at the desired times, up to 96h, and the time-course of the cross-linking analyzed with SDS-PAGE.

Chapter 4

RIBONUCLEASE A

4.1 Results

As it has been already reported in the Introduction section, RNase A can form domain-swapped oligomers if it is forced to follow two different protocols: i. lyophilisation from 40% acetic acid solutions, or ii. thermal aggregation of high concentrations of the enzyme in various solvents. Considering that a detailed analysis of the differences that could emerge in the species formed or recovered from the two different protocols had never been performed, a study to better elucidate these aspect has been planned. To do so, the thermal aggregation conditions chosen were the ones involving ethanol, whose action provides satisfactory yields of the two N- or C-swapped RNase A dimers[43].

4.1.1 RNase A oligomerization and purification of the oligomers

The monomers and the two dimers of RNase A recovered after acidic lyophilization or the two thermal incubations were separately collected and stored at 4°C in the presence of 50mM phosphate until further analyses had to be performed.

Each monomer, and N- or C-dimers formed through the two mentioned protocols were purified through a cation-exchange Source 15 S HR 10/10 column. The chromatographic patterns (Fig. 4.1) show different dimers amounts depending on the type of incubation, in line with previous reports[43]. To better define the species analyzed and to avoid confusing assignments, we call X_H, X_{20}, X_{40} (X = M, N_D, C_D) the monomers, the N- and C-dimers obtained after acid lyophilization or upon thermal incubations with EtOH 20% or 40% respectively. Therefore, the specie analyzed will be three N-dimers and three C-dimers; then three monomers plus the native one. Thus, a total of four monomers.

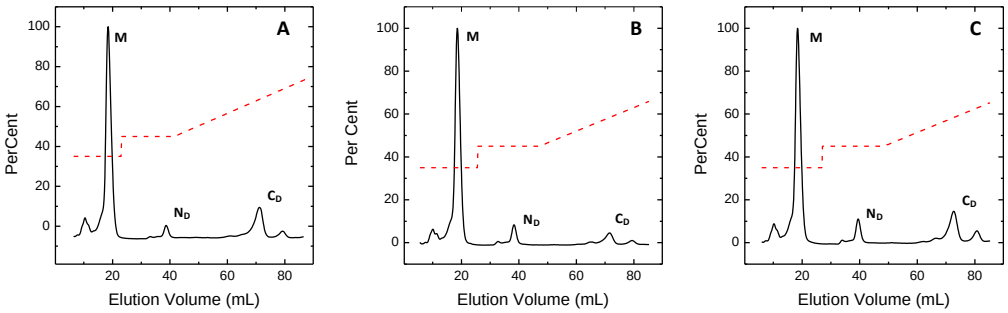

Figure 4.1. Cation exchange chromatographic patterns of RNase A oligomers formed upon A: lyophilizaton from 40% HAc solution, B: thermal treatment in 20% EtOH, C: thermal treatment in 40% EtOH.

4.1.2 Mass Spectra analysis and deamidation detection of RNase A monomers

We started the analysis by measuring if the acid or thermal incubations at 60°C may have induced some perturbations in RNase A. We investigated firstly if deamidation occurred and might have affected the N67 residue, the most sensitive Asn out of the many present in the protein. This should induce an Asn to Asp 1Da difference the MW. Monomers were analyzed with Mass Spectrometry and we found no dramatic changes in the MW of native RNase A ± 1 Da (MW = 13683Da). However, a possible 1Da difference could have not been visible with MS. Therefore, to better detect if deamidation occurred, cation exchange analysis did not show the presence of deamidated monomers after all the treatments suffer by the protein (Fig. 4.2)[215,216].

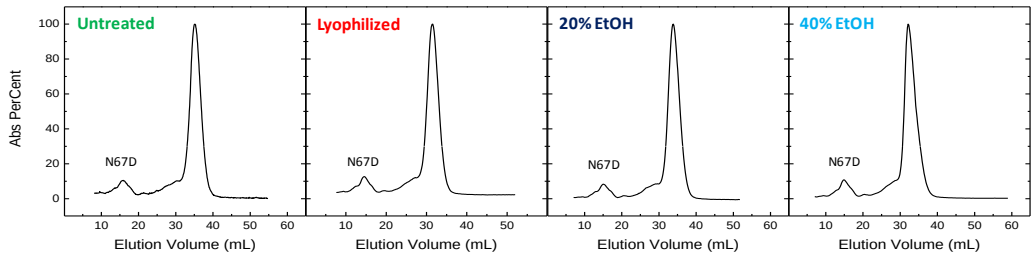

Figure 4.2. Cation exchange chromatographic patterns of each RNase A monomer recovered after the mentioned incubation, and compared with the untreated sample. The conditions to separate N67D-RNase from the native enzyme had been setted as reported in.

Species	Molecular weight (Da)
Untreated	13682.2 ± 1
Lyophilized	13684.2 ± 1
40% EtOH	13682.5 ± 1

Table 4.1. Molecular weight values measured by MS analyses of the different monomers.

4.1.3 Native cathodic PAGE of monomers and dimers

All monomers and dimers were analyzed through non denaturing cathodic PAGE (Fig. 4.3). No differences emerged within the four monomers, confirming that incubations did not induce RNase A deamidation[216]. As expected, the N-dimers displayed instead a different mobility from the corresponding C-dimers, due to their different conformation and basic charge exposure[104,107]. Within the same species, in some experiments we found only a very slight, not significant and not constantly reproducible, difference of the mobility of N_{DH} obtained upon HAc lyophilization with respect to the two thermally-obtained same N_D species, as visible in panel A.

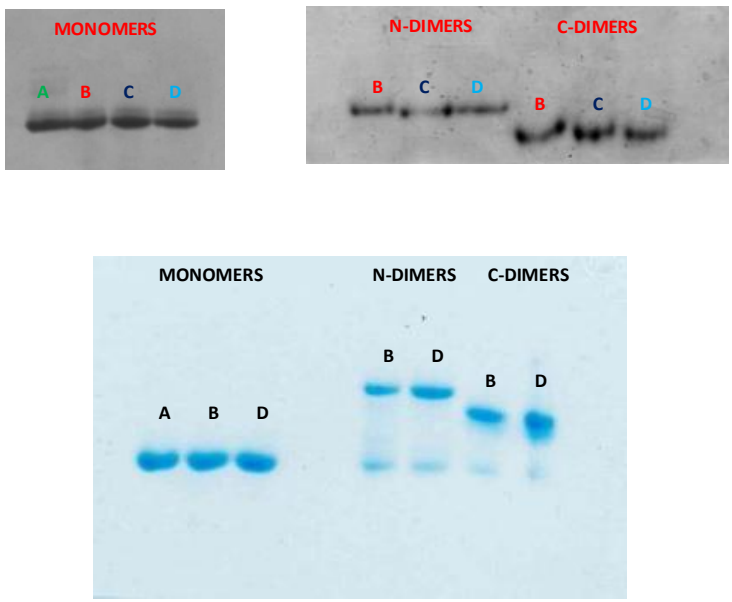

Figure 4.3. Gel electrophoresis under non denaturing condition of RNase A species. A: untreated, B: lyoph., C: 20% EtOH, D: 40% EtOH.

4.1.4 Thermal denaturation of the RNase A monomers

The thermal denaturation of each monomer was followed by monitoring the relative 218 nm far-UV CD signal with the 1.5°C/min increase of the temperature from 25 to 90°C. Figure 4.4 shows the denaturation curves and Table 1 reports the relative calculated T_m values: the melting temperature of the untreated monomer is about 4-5°C higher than the ones of the other species.

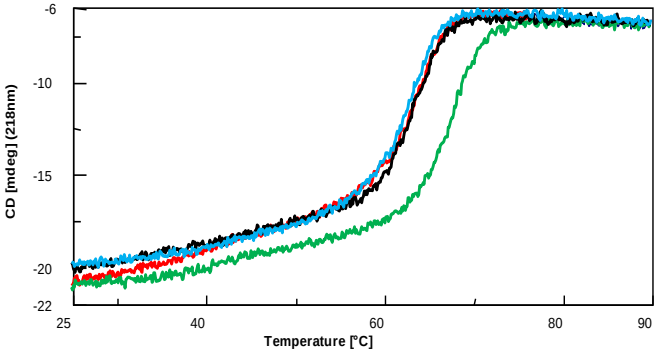

Monomers	T_m (°C)
Untreated (uM)	67
Lyophilized	63
20% EtOH	63
40% EtOH	62

Figure 4.4. Thermal denaturation of monomers: far-UV CD signal at 218 nm vs temperature. Untreated monomer: green curve. Lyoph. M, 20% EtOH M, 40% EtOH M: red, blue and light blue curve respectively.

Table 4.2. Melting temperatures of RNase A monomer recovered after the different incubations reported.

Furthermore, we analyzed if the thermal denaturation is reversible for all the monomers recovered after applying the mentioned HAc, or 20% EtOH, or also 40% EtOH incubations. To do so, we measured if native RNase A is influenced by a prolonged incubation at 90°C: far UV-CD spectra confirmed that the protein is not affected after recooling within the first ten minutes after having reached 90°C, while progressively loses its native structure with the increase of the time of incubation at 90°C (Figure 4.5A). Samples incubated at 90°C for increasing times were analyzed also with non-denaturing cathodic PAGE: the different mobility of the species recovered after 10 min incubation indicates that RNase A suffers a progressively increasing deamidation[216] (Figure 4.5B). The band relative to RNase A monomer increases its fading and progressively disappears after 90°C

incubation time, thus suggesting that an increase of the deamidation content causes a progressive precipitation of the protein, as was already envisaged in the recent past (Fagagnini et al BBA 2017[216]).

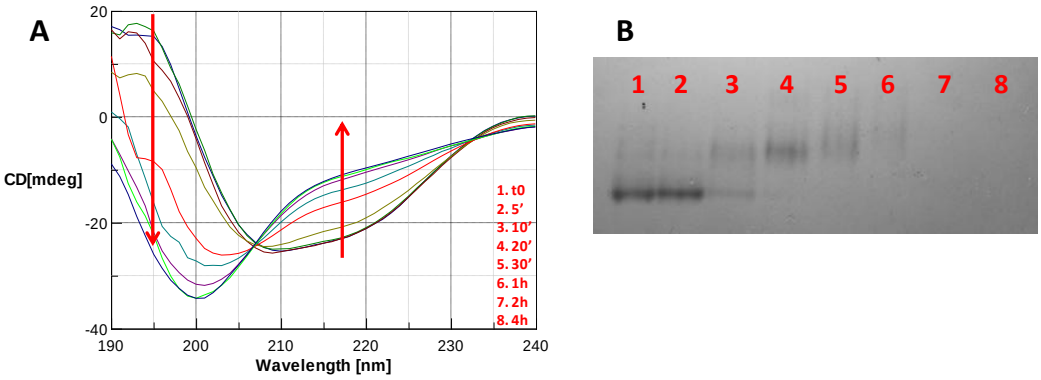

Figure 4.5. A: Far-UV CD spectra of RNase A untreated monomer after incubation at 90°C un to 4h. Arrows indicate the increasing incubation time. **B:** Gel electrophoresis under non denaturing condition of native RNase A untreated monomer after incubation at 90°C for different times. Deamidation induces a decrease of the electrophoretic mobility of the protein[216].

4.1.5 Kinetics of the limited proteolysis of RNase A monomers and of the domain-swapped dimers

Subtilisin, a serine protease, specifically hydrolyses the RNase A peptide bonds connecting A20-S21 and S21-S22, producing the S-peptide (1-20/21) and S-protein (20/21-124). Therefore, possible conformational changes occurring in the RNase A N-terminal region may be related to a different N_D-subtilisin interaction with respect to the same proteolytic action against C_D. The proteolysis kinetics of the monomers and C-dimers were analyzed for 24h (1440 min), while the ones of N-dimers only for 1h, being N_D more susceptible than the other two species certainly because the region suffering the proteolysis changes conformation upon N-terminus swapping[213]. Figure 4.6 shows the region of the protein that suffers the subtilisin reaction and the SDS-PAGE analyses of the mentioned reaction kinetics: some little differences are visible within the

monomers, especially the one that suffered harsh incubations (40% HAc or 40% EtOH). Instead, no significant differences emerged within the C-dimers. While, only the N_D formed upon 40% EtOH thermal incubation showed to be slightly less susceptible to subtilisin than the other two N-dimers.

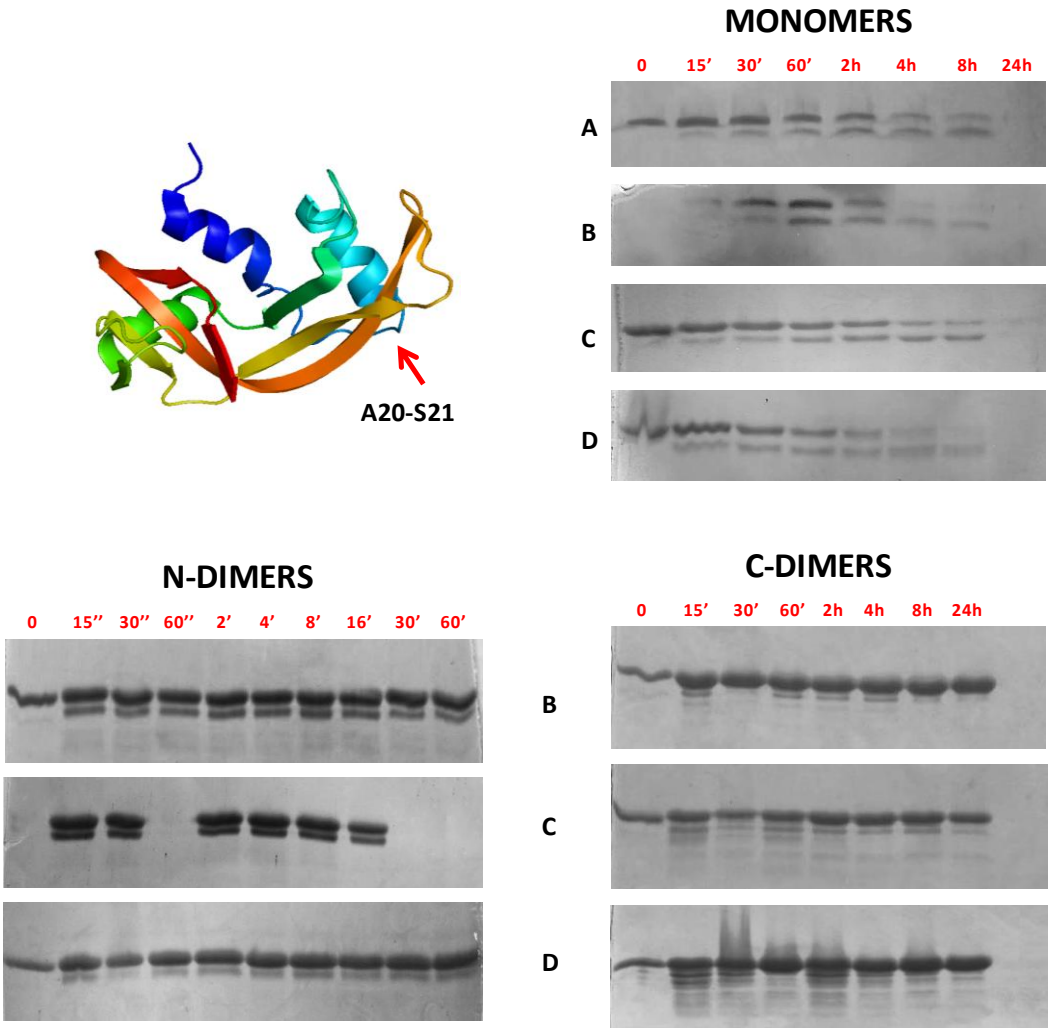

Figure 4.6. SDS-PAGE of the products formed upon limited subtilisin proteolysis performed on differently treated RNase A species. A: untreated, B: lyoph. HAc, C: 20% EtOH, D: 40% EtOH.

4.1.6 Intrinsic fluorescence of monomers and dimers

The intrinsic fluorescence emission spectra of all monomer species showed no significant differences, with and emission maximum always centered at 305nm.

For what regards the dimers, we did not analyzed the species derived from thermal incubation in 20% EtOH solution for their very low yield. The N_{DH} and C_{DH} showed similar emission spectra, with a maximum again centered at 305nm,. Then, the N_{D40} obtained after thermal treatment has the same spetra respect to the two dimers from lyophilization, while C_{DH} and C_{D40} showed a different emission profile with maxima at 305 and 306nm, respectively, therefore with C_{D40} displaying a 1nm red-shift. This variation suggests that this latter species undergoes a slight conformational change in its tertiary structure in a different way from C_{DH}. This could be due to some differences induced in the microenvironment of one or more aromatic residues.

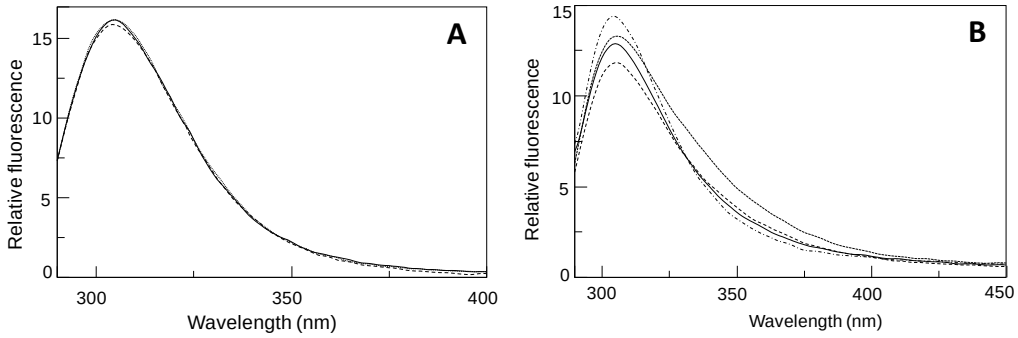

Figure 4.7. Intrinsic fluorescence of RNase A monomers (A) and dimers (B). **A.** Emission spectra of native RNase (—), M_H (····), M_{40} (-----). **B.** Emission spectra of N-dimers obtained from N_{DH} (—), N_{D40} (−−−) and C-dimers C_{DH} (-·-·-), C_{D40} (-----). Spectra were registered upon excitation at 280 nm, at a protein concentration of 0.1mg/mL in 20mM NaPi.

4.1.7 Enzymatic activity assays

The enzymatic activity of all RNase A monomers and dimers was measured against ss-RNA, using yeast RNA as substrate, by performing a "Kunitz" spectrophotometric assays at 300nm[210]. The monomers were more active than the N- and C-dimers, as expected. The different monomers recovered after they suffered the various treatments showed no significant differences within each other. However the native, untreated monomer, is slightly more active than the monomers recovered upon the mentioned incubations.

Species	V_{max} (ΔAbs_{300}/min/µg)	K_M (mg/mL)
uM	0.151 ± 0.006	0.087 ± 0.013
M_H	0.152 ± 0.005	0.147 ± 0.015
M_{40}	0.160 ± 0.005	0.156 ± 0.016
N_{DH}	0.079 ± 0.002	0.132 ± 0.012
N_{D40}	0.076 ± 0.004	0.111 ± 0.018
C_{DH}	0.041 ± 0.001	0.130 ± 0.012
C_{D40}	0.030 ± 0.001	0.109 ± 0.011

Table 4.2. Kinetic parameters of the RNase A species activity vs ss-yeast RNA.

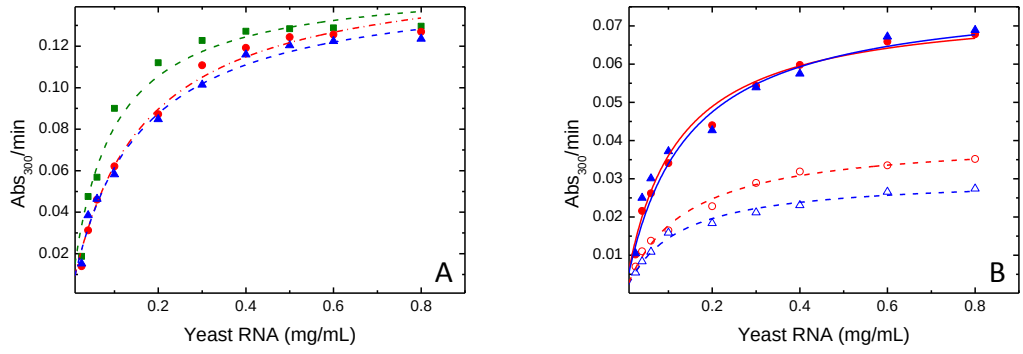

Figure 4.7. Kunitz activity curves of monomers and dimers *vs* yeast RNA (ss-RNA) as a function of substrate concentration. **A.** Monomers, green: uM, red: M_H, blue: M_{40}. **B.** Dimers. Solid line N_D, dashed line C_D. Red: lyoph.; blue: 40% EtOH.

The activity of RNase A against ds-RNA is known to be low, but it increases proportionally with the size of the oligomers and to the increase of their basic charge density upon the enzyme self-associates. As visible in Figure 4.8, significant differences between the different species analyzed appear. We measured the activity of all RNase A species against increasing concentrations of the synthetic poly(A):poly(U) ds-RNA substrate. We investigated only the initial linear part of the Michaelis-Menten curve in order to avoid an excessive photometric error. The monomeric species displayed no significant differences in the activity from one another. Instead, the N_{DH} appeared to be slightly more active than the N_{D40}. Finally, the C_{DH} appears to be significantly more active than the other C-dimer, C_{D40}.

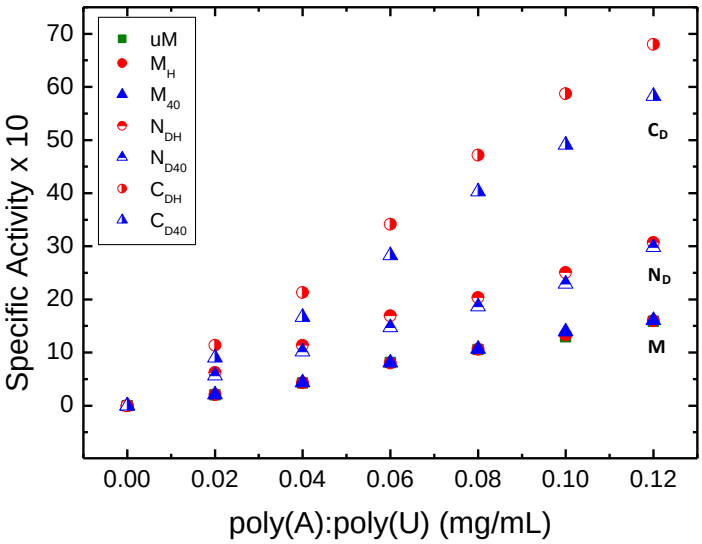

Figure 4.8. Initial, linear part of enzymatic activity *vs* ds-RNA monomers and dimers. Curves were plotted as a function of increasing poly(A):poly(U) substrate concentrations. Each reaction kinetics was followed at 260 nm in the linearity range, and the specific activity activity is expressed as $Abs_{260}/\mu g*min$.

4.2 Discussion

The RNase A oligomerization event occurring through 3D-DS has been deeply studied over the last decades, but no studies were performed to evaluate if different methods applied to obtain the oligomers could affect the properties of the species produced. Therefore, we investigated here if different conditions used to induce its oligomerization may affect the properties of the RNase A monomer and of the resulting dimers.

To do so, we performed many different investigations with different techniques: non-denaturing cathodic PAGE did not show differences related to the type of incubation suffered by the protein.

Then, we investigated the melting temperature of RNase A monomers recovered after the different treatments: the harsh incubations (HAc lyophilization or 40% EtOH thermal incubation) promotes only a partial destabilization of the enzyme. In fact, the T_m of the untreated, native, RNase A monomer is only few degrees higher than the one of the other species, i.e., 67°C instead of 62-63°C. Moreover, we analyzed the renaturation capability of native RNase A after incubating the protein at 90°C for prolonged times. The protein is able to regain its native folding only within a few minutes after reaching 90°C. Indeed, the increase of incubation time induce also a partial precipitation of the protein and a deamidation, an event confirmed by the progressive disappearance with time of the protein electrophoretic band. This analysis confirmed that the 60°C incubation in 20% or 40% aqueous EtOH and the lyophilization from acetic acid solution induced a only a reversible destabilization of the protein that can disappear by re-dissolving the protein in "benign" buffers, such as phosphate. However, in all the oligomerization treatments analyzed, a variable percentage of the protein formed insoluble precipitates that could not be redissolved in NaPi buffer before SEC.

The limited proteolysis of the monomers with subtilisin showed some differences between the native monomer and the ones that underwent incubations in harsh conditions. No detectable differences appeared within the C-dimers, and this it could be due to the intrinsically high resistance of these dimers to subtilisin. Instead, the N-dimer obtained by the 20% EtOH thermal treatment seems to be

slightly more susceptible to the protease than the other two species, but this difference cannot be considered significant.

The intrinsic fluorescence spectra of the various monomers and N-dimers showed no significant relative differences within one another. Instead, the two C-dimers, C_{DH} and C_{D40} showed an emission maximum with a difference of 1nm. This suggests that that the two different treatments induced a slight but not negligible difference in the structural determinants involving the aromatic Tyr or Phe residues of these dimers. This variations could affect the side chain of the Phe120 catalytic subsite, that could undergo a re-orientation upon suffering conditions inducing RNase A oligomerization, and this rearrangement could be distinct as a function of the type of incubation. Therefore, this could differently affect also the catalytic activity of the two C-dimers and explain the different activity values obtained with C_{DH} and C_{D40}.

Concerning the catalytic activity versus ss-RNA of the various RNase A species studied, the K_M value of the two monomers analyzed after the two treatments doubles up the one of the untreated one, therefore indicating that the enzyme affinity for the yeast RNA substrate is affected by all the treatments. Both N-dimers showed instead to have about the same activity, but the V_{max} values are about half the ones of the untreated monomer. This difference could be due to its quaternary structure, that leads to a different number of active sites available per N-dimer along the ss-RNA substrate filament with respect to the monomer. Again, the C-dimers display a V_{max} lower than the N-dimers, and the C_D obtained from thermal treatment in 40% ethanol is less active than the one withdrawn from acid lyophilisation. The potentially available active sites per molecule are the same for N_D and C_D, so that the significant activity difference between these species seems not be easily evaluable. However, as shown in Figure 4.9, the two active site are “cis-oriented” in N_D, while “trans-oriented” in C_D. Hence, this different orientation could make the interaction of the substrate with the second active site more favourable for N_D than for C_D, therefore justifying the lower activity values measured for the latter.

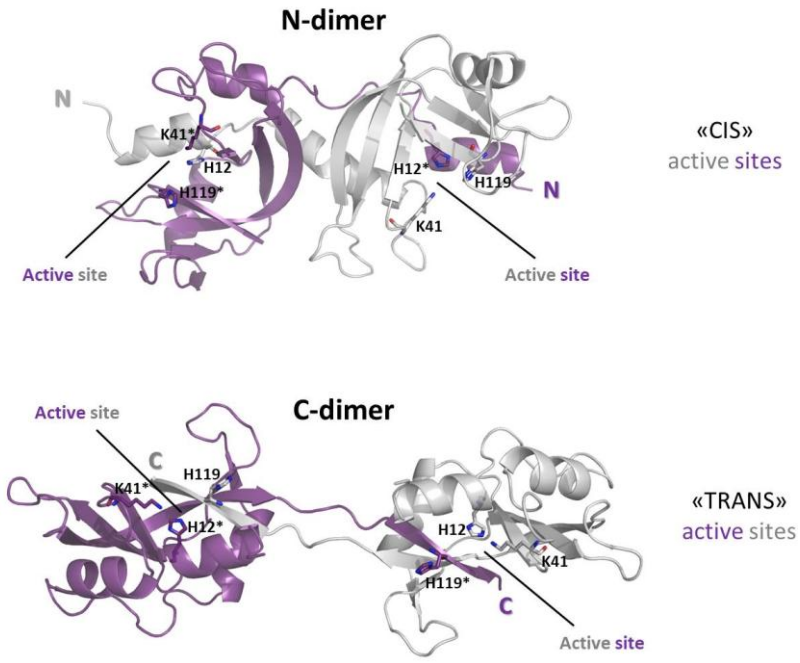

Figure 4.9. Relative orientation of the two active sites in the two domain-swapped RNase A dimers, respectively 1.A2W.pdb and 1F0V.pdb. The active site residues His12, Lys41 and His119 are highlighted.

As regards the data obtained with ds-RNA as substrate, no differences were registered within the monomers, being all of them are less active than the dimers. The two N-dimers display only slight differences within one another; instead, the C-dimers are both more active than all monomers and N-dimers, and C_{DH} is more active than C_{D40}. C_{D40} results to be less active than C_{DH} also on ss-RNA. These differences support the idea that the two different incubation methods applied to make RNase A oligomeric may affect the tertiary structure of the C-dimer in different ways, and this argument is enforced by the florescence spectra registered for the two C-dimers. Concerning the N-dimers, the activity differences registered are not as significant as are within the C-dimers. It has to be mentioned that the ds-RNA kinetic parameters of all RNase A species vs the ds-RNA poly(A):poly(U) could not be calculated because the progressive increase of the substrate concentration induced a too large spectrophotometric error. However, the data collected with low substrate concentrations enforces the idea

that EtOH thermal incubation might alter the RNase A dimeric structures in a different way respect to the acid lyophilisation.

Chapter 5

ONCONASE AND HUMAN PANCREATIC RIBONUCLEASE

5.1 Results

5.1.1 Expression and production of ONC and HP-RNase variants

Recombinant variant of the two ONC and HP-RNase species were expressed from *E. coli*, and the protein of interest was detectable in the insoluble inclusion bodies. The SEC purifications (Figure 5.1) showed that all variants were the sole species present in solution after the expression and production protocols used and MS confirmed that it corresponded to the protein that had to be expressed. The elution volume was about 14.5mL for both ONC and HP-RNase, even if they have a different molecular weight. This result could be related to the fact that they could have a similar hydration sphere that confer them the same elution volume in SEC analysis, similarly to what was already detected in the recent past for ONC and RNase A[154].

We obtained an almost pure protein for wt-ONC, H10A-ONC, C87S-ONC, C140S-ONC, C87S/C104S-ONC, dC104-ONC and dS103C104-ONC, even if the expression of the last two variants produced very low quantities.

Both chromatograms of wt and of the C-terminal truncated des125-128 (–EDST) HP-RNase variant showed two peaks (Figure 5.1): we collected the most abundant one that corresponded to the elution volume of a RNase and to the correctly expressed protein, as confirmed by further analyses. Unfortunately, we obtained low yields for both wild type and truncated HP-RNase in two out of three different preparations

All variants were then processed with AAP for a successful cleavage of the starting N_{term}-Met (Met(-1)). The correct expression of was confirmed by subsequent electrophoretic, MS, and enzymatic analyses.. Then, the chromatogram of C87S-QVVAG-ONC showed its principal peak at an elution volume of 12.2mL instead of about 14mL. However, we collected and analyzed it with MS and SDS-PAGE. Both analyses revealed the presence of more than one species characterized by different MW values.

ONC mutant sequence:

EDWLTFQKKHITNTRDVDCDNIMSTNLFHCKDKNTFIYSRPEPVKAICKGIIASK
NVLTTSEFYLSDCNVTSRPCKYKLKKSTNKFCVTCENQVVAGPVHFVGVGSC

In this sequence, the Gln and Ala residues were already present. Therefore, we inserted the codons corresponding to the two Val residues and, subsequently, the sequence coding for the Gly. Unfortunately, we did not obtain certain data about the correctness of protein expression and about the possibility of this ONC variant to be more inclined to 3D-DS self-association than the WT.

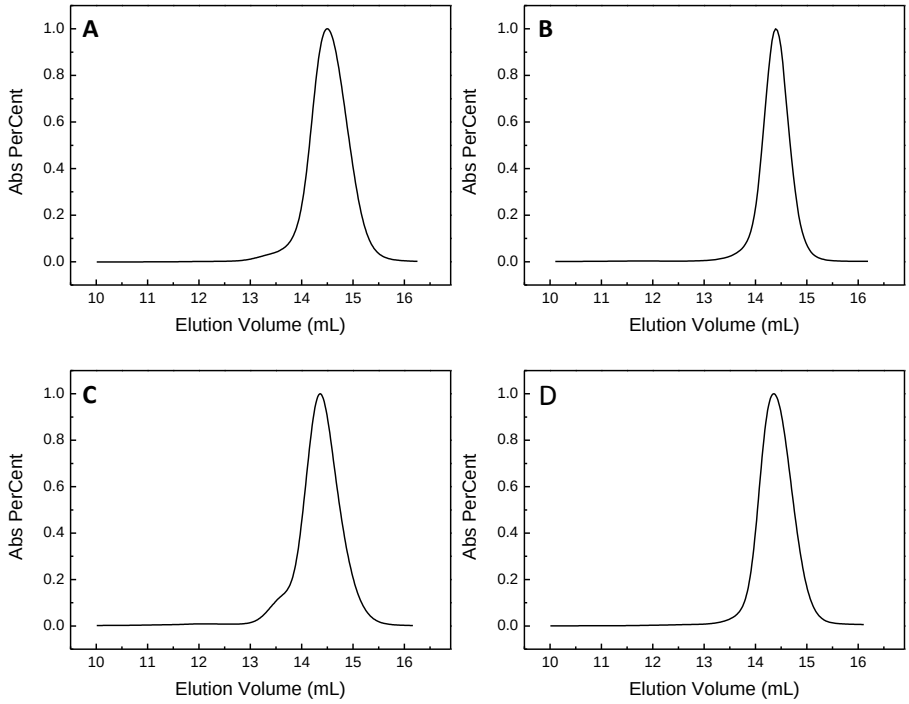

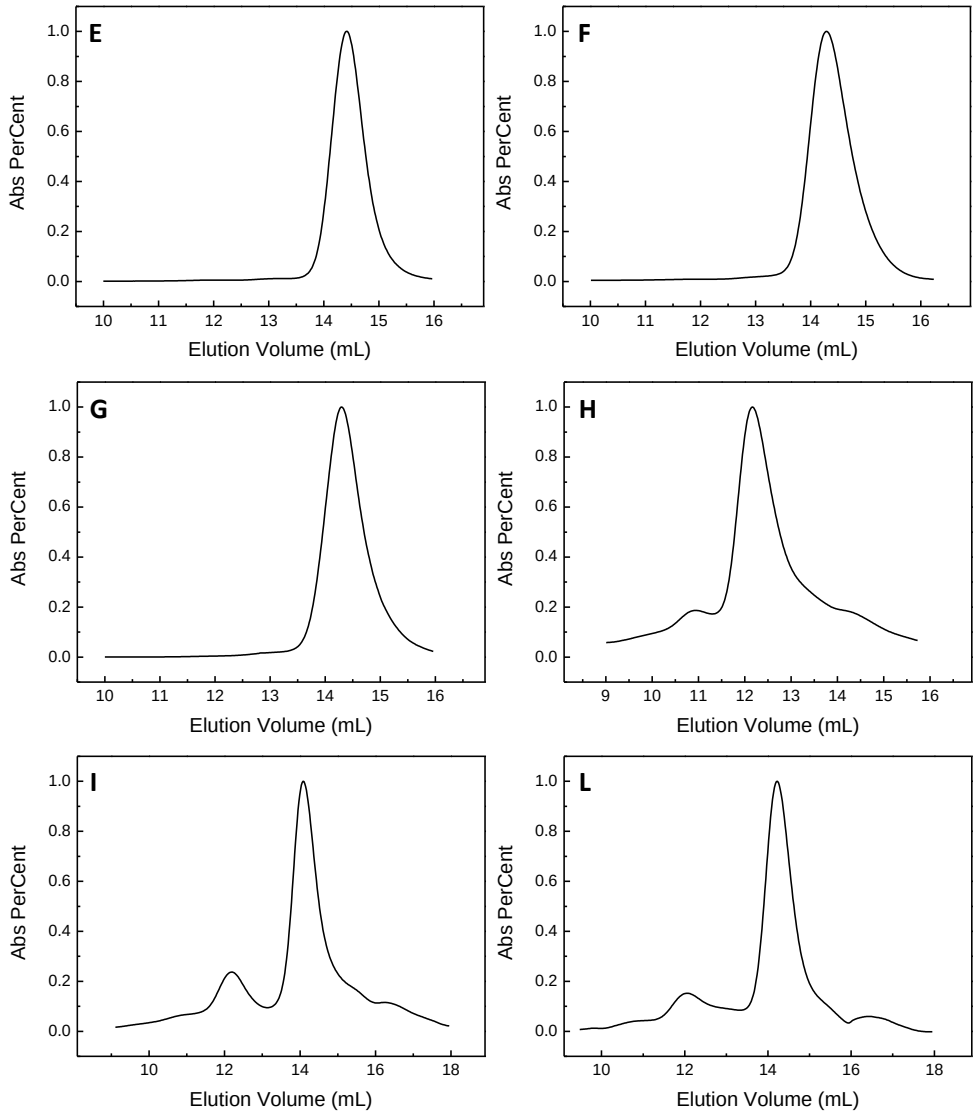

Figure 5.1. SEC patterns of the last purification step for the expression of **A**: wt-ONC, **B**: H10A-ONC, **C**: C87S-ONC, **D**: C104S-ONC, **E**: C87S/C104S-ONC, **F**: dC104-ONC, **G**: dS103C104-ONC, **H**: C87S-loop-ONC, **I**: HP-RNase, **L**: (-EDST)-HP-RNase. Chromatographies were performed with a Superdex 75 HR 10/300 column equilibrated with 0.1M Tris-acetate, 0.3M NaCl, pH 8.4. Each pattern was modified and normalized to the monomer area of wt-ONC with Origin 7 Software.

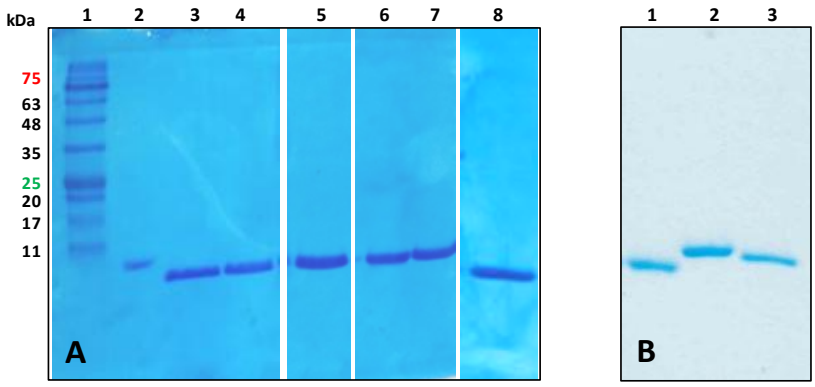

Figure 5.2. SDS-PAGE analyses of the main peak of ONC and HP-RNase SEC purification. **A.** lane 1 standard molecular weight, lane 2 RNase A, lane 3 wt-ONC, lane 4 dC104-ONC, lane 5 dS103C104-ONC, lane 6 C87S-ONC, lane 7 C104S-ONS, lane 8 C87S-C104S-ONC. **B.** lane 1 RNase A, lane 2 wt-HP-RNase, lane 3 (-ESDT)-HP-RNase.

5.1.2 Induction of the oligomerization of ONC and HP-RNase, and purification of their oligomers

We applied the HAc lyophilization method either with ONC or with HP-RNase. We also applied the thermal method with ONC but the dimerization yield was definitely lower than the one obtained with lyophilization.

After lyophilization from 40% acetic acid the protein samples were analyzed through SEC (Figure 5.3), using the well known oligomerization pattern of RNase A as a standard. ONC (wild type and mutants) formed a dimer that has been demonstrated to be swapped through its N-termini (Figure 5.3 A)[154]: indeed, the chromatographic pattern of wt-ONC obtained after acidic lyophilization showed a peak corresponding to the ONC dimer that is eluted to a volume that is comparable to the one of the RNase A N-dimer.

To evaluate if the variants oligomerize through the 3D-DS mechanism, we performed a crosslinking reaction with DVS, in order to covalent bind the two His of the active site[154]. Furthermore, as shown in Figure 5.3 B, the H10A-ONC variant, that lacks one of the two His residue of the active site, does not form a domain-swapped dimer: this His residue located the N-terminal domain is necessary to form a saline bridge with the phosphate ion and the other His residing in the C-terminus of the second monomer. Therefore, the presence of

only one peak corresponding to the monomer, without any trace of dimer, indirectly confirms that the ONC dimer forms through the 3D-DS mechanism.

Then, we designed and produced some mutants in order to unlock and shorten the C-terminal end of the protein. This was planned to induce ONC oligomerization also through the swapping of its C-terminus. However, the chromatographic patterns show that these variants do not form a C-dimer (Figure 5.3 C). Furthermore, and unfortunately, all the mutants produced less N-dimer than the wild type.

All wild-type and ONC mutants form instead traces of a species that could be a trimeric form of the protein, considering that its elution volume falls between the ones of the RNase A trimer and C-dimer, but the quantity was too low to be successfully analyzed.

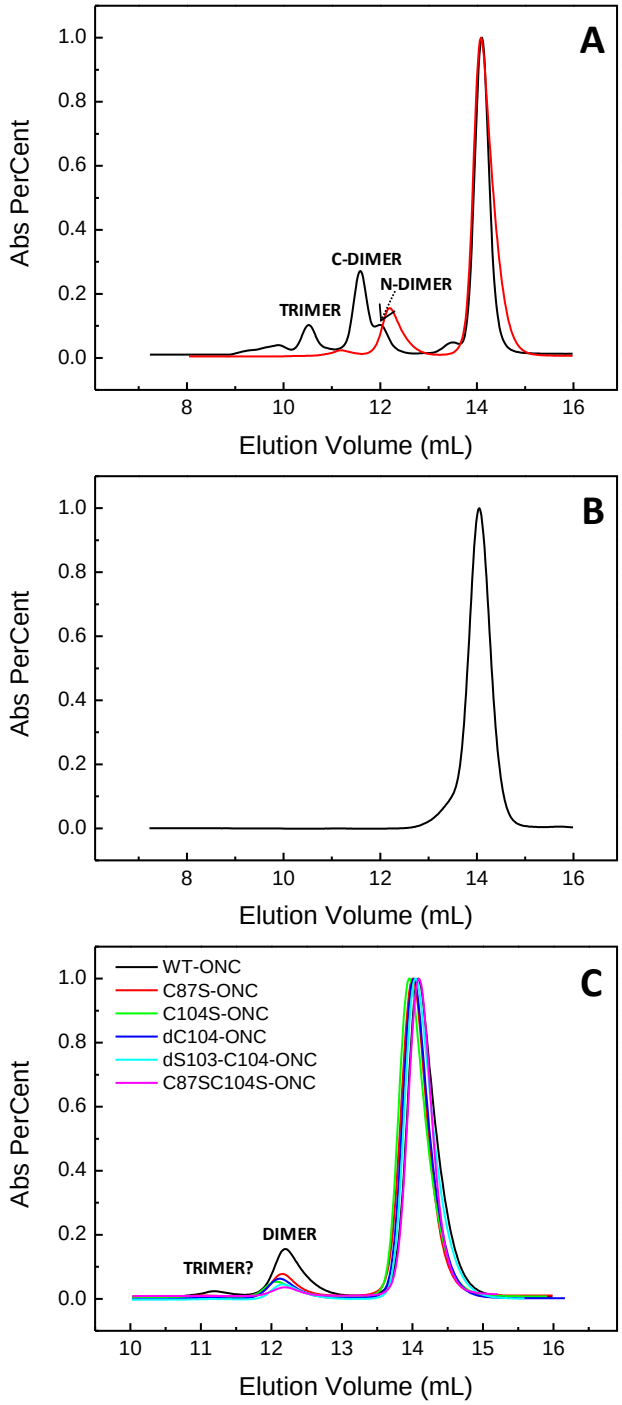

Figure 5.3. SEC analysis of ONC samples lyophilized from 40% acetic acid. Chromatograms were performed with a Superdex 75 10/300 Increase SEC column equilibrated with 0.4M NaPi, pH 6.7. Each pattern was normalized to the monomer area with the Origin 7 Software. **A**. black line: RNase A, red line wt-ONC. **B**. H10A-ONC. **C.** Other ONC variants compared to wt-ONC.

5.1.3 Nondenaturing cathodic PAGE

The nondenaturing cathodic PAGE analysis of the ONC species showed that the monomers of the two C87S-ONC and C104S-ONC mutants display the same relative electrophoretic mobility within each other but different from the wild type (Figure 5.4). We analyzed only these species because we did not collected enough quantities of the others, where a large amount of them precipitated after the lyophilization from 40% acetic acid solution.

The electrophoretic mobility measured under nondenaturing conditions is influenced by dimension and MW of the species analyzed, but also by the conformation and charge exposure of the protein. Therefore, the C87S-ONC and C104S-ONC monomers could have different conformations and different charge exposure that induced their lower electrophoretic mobility with respect to the wild type. Furthermore, lacking one cysteine residue, these mutants could undergo to different disulfide bridge formation during the refolding process.

All dimeric samples showed also the concomitant presence of the monomer, due to a partial dissociation related to their metastability. Then, also the desalting process, necessary to reduce NaPi concentration, can lead to a decrease of the dimer's amount[44]. Moreover, we observed that the dimers obtained from different species show different mobility from one another, suggesting that they may assume different three dimensional conformations.

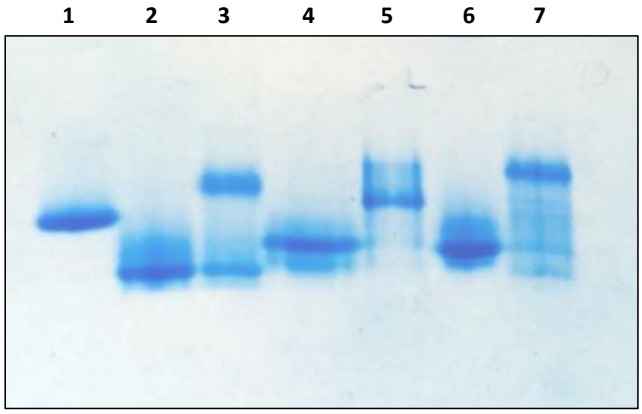

Figure 5.4. 15% acrylamide nondenaturing cathodic PAGE of ONC monomers and dimers obtained after 40% acetic acid lyophilization of the protein. Lane 1: RNase A monomer (13.7 kDa), used as a standard; Lane 2: wt-ONC monomer; Lane 3: wt-ONC dimer; Lane 4: C87S-ONC monomer; Lane 5: C87S-ONC dimer; Lane 6: C104S-ONC monomer; Lane 7: C104S-ONC dimer.

5.1.4 Human pancreatic RNase aggregation

We produced also the recombinant human pancreatic RNase in order to understand if it is able to oligomerize through the 3D-DS mechanism, similarly to RNase A, since they share similar folds and 70% sequence identity. As shown in Fig 5.6, panel A, we observed that HP-RNase pattern is very similar to the RNase A one and, surprisingly, it forms a larger percentage of oligomers than the bovine variant. Moreover, observing the SEC pattern, it is possible to suppose that HP-RNase almost certainly form two type of dimer, the N-dimer and the C-dimer, as RNase A. But their separation and purification need to be better investigate with cation exchange chromatography, which conditions are not easy to set up.

Observing the alignment of RNase A, HP-RNase and ONC, we note a difference in the C-terminal domain (Fig. 5.5). HP-RNase displays a four aminoacid elongation with respect to RNase A, while ONC three. Therefore, we designed and produced truncated ONC, as explained before, and HP-RNase mutants in order to analyze the oligomerization ability after lyophilization from 40% acetic acid solutions.

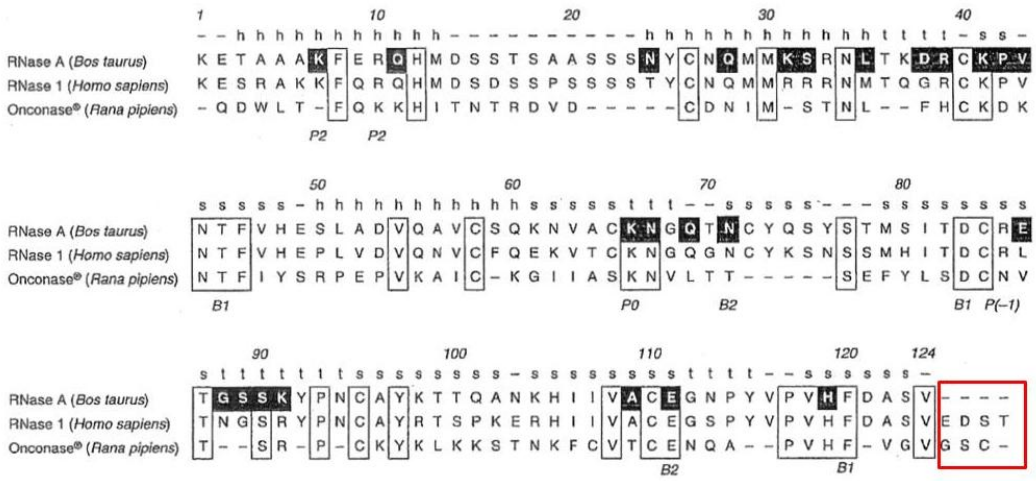

Figure 5.5. Primary structures of RNase A, HP-RNase and ONC. (from Leland et al., 2001[217]). The C-terminal elongations of HP-RNase (residues 125-128) and ONC (residues 102-104), with respect to RNase A, are highlighted in the red square.

The structural and functional features of the both wt and des125-128-HP-RNase mutant that carries the deletion of the four C-terminal residues (EDST) had been already studied [218], but the oligomerization propensity of both variants, and the role of this elongation in this tendency was not analyzed yet. Therefore, we produced this mutant in order to understand if the C-terminal tail deletion would negatively or positively affect the tendency of the protein to dimerize through 3D-DS mechanism in comparison with the wild type and with RNase A. These results should also indirectly help to understand if the self-association tendency of ONC would have been significantly affected by its C-terminal three residues elongation.

The chromatographic patterns reported in Figure 5.6, panels B and C, show that the des125-128-HP-RNase variant displays a behavior qualitatively analogous to the wild type. However, the percentage of oligomers formed by the mutant seems to be slightly little more abundant than the wt. Both proteins display a behavior very similar respect to RNase A pattern, showed in dashed line in Figure 5.6 A. Surprisingly, both human variants show a larger self-aggregation propensity than bovine RNase A.

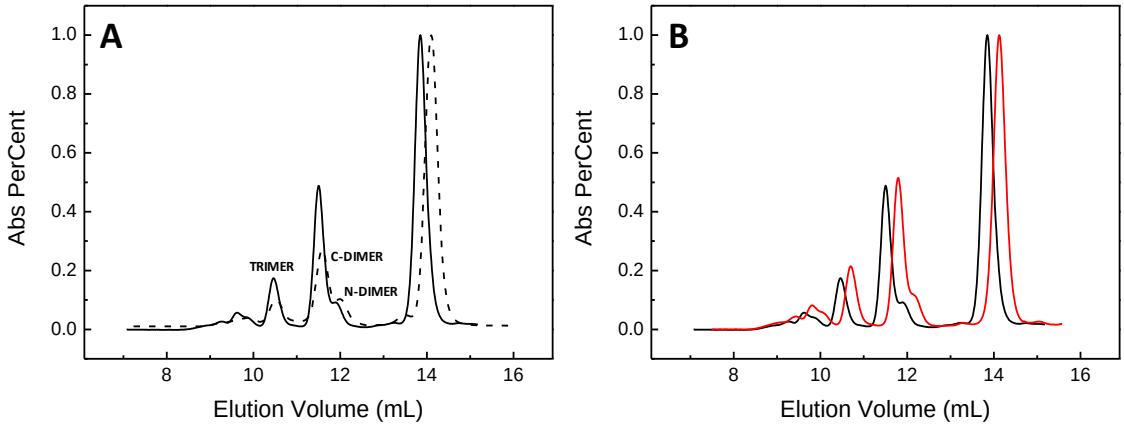

Figure 5.6. SEC analysis of samples lyophilized from 40% acetic acid. Chromatographies were performed with a Superdex 75 10/300 Increase column equilibrated with 0.4M NaPi, pH 6.7. Each pattern was normalized to the monomer area with the Origin 7 Software. **A**: RNase A (dash line), HP-RNase (solid line). **B**: HP-RNase (black line), (-EDST)-HP-RNase (red line), powder lyoph. from 40% acetic acid solution and then resuspended in NaPi buffer.

	Monomer	Dimers	Trimers
RNase A	63.33 ± 0.40	24.34 ± 0.90	7.36 ± 0.43
wt-HP-RNase	56.26 ± 1.34	27.54 ± 1.18	9.70 ± 0.36
(-EDST)-HP-RNase	49.05 ± 2.32	28.45 ± 0.44	11.26 ± 0.39

Table 5.1. Percentage of monomers and dimers of wild type and truncated human pancreatic ribonuclease.

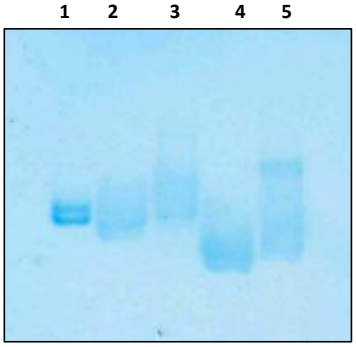

Figure 5.7. 15% acrylamide nondenaturing cathodic PAGE of HP-RNase monomers and dimers obtained after 40% acetic acid lyophilization of the protein. Lane 1: RNase A monomer (13.7 kDa), used as a standard; Lane 2: wt-HP-RNase monomer; Lane 3: wt-HP-RNase dimer; Lane 4: (-EDST)-HP-RNase monomer; Lane 5: (-EDST)-HP-RNase dimer.

We separately collected the oligomers formed by both HP-RNase variants and we focused our attention especially on their dimers. The species were then analyzed with nondenaturing cathodic PAGE (Figure 5.7). The analysis display that the electrophoretic mobility of the truncated variant is higher than the one of the wild type protein, due to the deletion of two negatively charged residues, E125 and D126. Furthermore, both dimers show a not well defined, smeared band, but they have at the same time a different mobility with respect to each other and to each relative monomer.

In order to detect the 3D-DS presence, we performed the DVS cross-linking reaction also with HP-RNase dimers but the products did not show any trace of covalent dimer (Figure 5.8). DVS is a bifunctional crosslinker that can covalently bind the two His of the active site (numbered 12 and 119 in HP-RNase) that in pancreatic-type RNases belong to the two N- and C-termini of the protein,

respectively[214]. Thus, if 3D-DS took place, the cross-linking of the two His residues would produce a covalently stabilized dimer as it occurs with all other pancreatic-type ribonuclease oligomers forming through the 3D-DS mechanism[40,45,219].

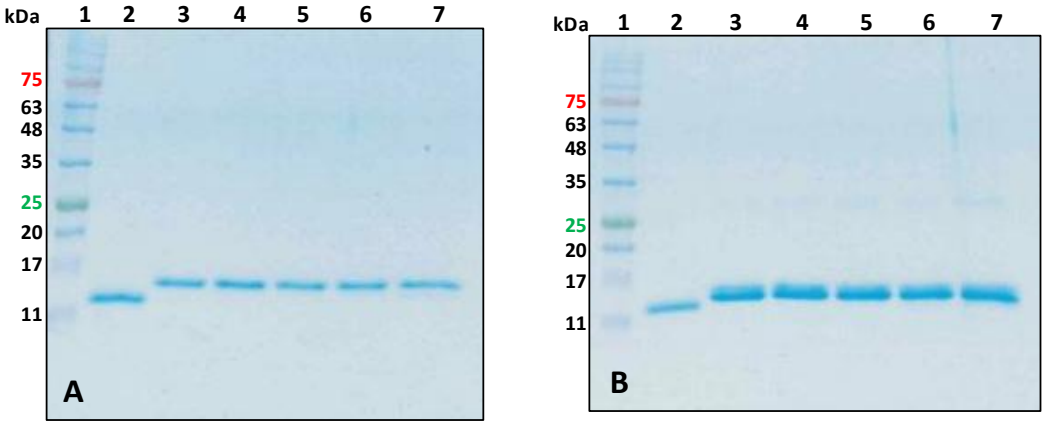

Figure 5.8. SDS-PAGE analyses of the products obtained from DVS reaction with HP-RNase dimer. **A**: wild type. **B**: truncated. Lane 1: standard of molecular weight. Lane 2: RNase A monomer (MW 13.7kDa). Lanes from 3 to 7: 0h, 6h30, 24h, 30h, 96h.

We could envisage that this could be due to the intrinsic instability of the dimer, and/or of the reaction conditions (0.1M sodium acetate buffer, pH 5.0) could induce its destabilization. However, another hypothesis could be that 3D-DS did not occur.

To investigate if 3D-DS actually takes place we re-suspended the acidic lyophilized powder in ddH_2O instead of in NaPi and we performed the SEC analysis visible in Figure 5.9: in the chromatographic patterns any trace of oligomers is absent. This indicates that the absence of the phosphate does not allow to create a saline connection between two His in the dimer active site and does not permit the 3D-DS swapped oligomers to be formed and stabilized.

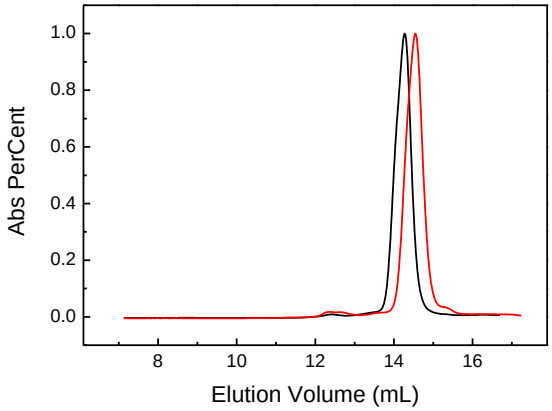

Figure 5.9. SEC analysis of HP-RNase samples lyophilized from 40% acetic acid. Chromatographies were performed with a Superdex 75 Increase 10/300 column equilibrated with 0.4M NaPi, pH 6.7. Each pattern was normalized to the monomer area with the Origin 7 Software. wt HP-RNase (black line), (-EDST)-HP-RNase (red line), powder lyoph. from 40% acetic acid solution and then resuspended in ddH_2O.

Another method to indirectly confirm this hypothesis could be linked to the production of H12A mutant: lacking one of the two His of the catalytic site, this variant should not be able to produce dimers and larger oligomers. This is because, being His12 is in the swapped domain that interact after 3D-DS with the His119 of the core of the other monomer, the lack of one of the two His residues may not permit the His12-His119 interaction mediated by phosphate that stabilizes the domain-swapped dimers.

5.2 Discussion

We previously demonstrated that ONC can oligomerize through the 3D-DS mechanism[154]. In order to enlarge the propensity of ONC to self-associate, in this work we tried to unlock the C-terminal domain to verify if it is able to oligomerize by exchanging also this domain.

To do so, we firstly eliminated the disulfide bond between Cys87 and Cys104, substituting one of the two cysteine residues with a serine, in a way to induce the minimal chemical perturbation. We produced, therefore, the mutants C87S, C104S, C87S/C104S, and after lyophilization from acetic acid solution their SEC pattern showed that they can dimerize, but without forming an additional, C-swapped, dimeric variant, and, surprisingly, at a lesser extent than the wild type. However, C87S-ONC produced a slightly higher dimeric amount than the C104S variant. In addition, we tried to oligomerize them by applying the same thermal incubations used with RNase A, but we did not obtained better results.

Subsequently, for the same reasons, we designed two truncated variants, the first upon deleting the C104 residue, the other by eliminating both S103 and C104 terminal residues. Again, after lyophilization from acetic acid solution we did not obtain larger amount of dimers than the wt. Instead, even for both these variants, the peak corresponding to the dimer is smaller than the one obtained with the C87S and C104S mutants evaluated before.

The last ONC variant we analyzed was the C87S-C104S double mutant, and also in this case, its SEC pattern after lyophilization did not provide satisfactory results.

All these results suggest that, very likely, the unlock of the C-terminus influenced also the ability of the protein to undergo N-domain swapping. We can suppose that a cross-talk between the N- and C-termini occurs also for ONC, as it is known for RNase A and B[215].

However, and finally, within all the mentioned variants, C87S-ONC showed the highest dimeric yield, even if it dimerized less abundantly than the wild type protein. For this reason, and for the presence of the unlocked C-

terminus, we chose to start from this mutant to produce other variants such as the one, successively, engineered with the insertion of the QVVAG loop.

By observing the alignment of RNase A, HP-RNase and ONC, it is clear that both HP-RNase and ONC show a C-terminus elongation, of four and three aminoacidic residues respectively, more than RNase A.

The aggregation propensity of wild type HP-RNase had never been studied before. Thus, we evaluated its self-association tendency, together with the aggregation propensity of a truncated variant, in which we expressed the protein without the four EDST residues forming the C-terminal elongation tail.

We observed that both the wild type and the truncated HP-RNase mutant display SEC patterns similar to the one of RNase A, but both human variants are able to produce larger amounts of oligomers than RNase A with a significant reproducibility. In particular, the high qualitative similarity of both HP-RNase SEC profiles with the RNase A one suggests that also the human variant can form two dimers, i.e. N- or C-dimers. Then, thanks to the presence of C-swapping, it can form also definitive amounts of trimers and tetramers, as visible in table 5.1.

We to analyzed the possible presence of 3D-DS in the dimers with the DVS cross-linker, but we did not obtain positive results. This could be due at the intrinsic instability of the dimer or the instability in the DVS reaction conditions. Therefore, to certainly probe the presence of 3D-DS, the H12A HP-RNase variant is now under production: this mutant, lacking one His of the active site that is necessary for the dimer stabilization in the domain swapping mechanism, should do not form any oligomer.

However, we recall here that HP-RNase displays, in both N- and C-termini some different AA residues with respect to RNase A,. We suppose that the intrinsic instability of the oligomers of the human variant could be ascribable to the presence of the basic residues that probably induce a repulsive force between the monomers composing them[220]. Again, this instability can be related to the presence of some residues which could create a steric obstruction in the N-terminus and avoid the accommodation of the swapped domain, destabilizing the oligomers as is visible in Figure 5.9. For this reason, after observing the sequence

alignment existing between the bovine and the human variants, we designed the two R4A and S113N mutants that are now under production.

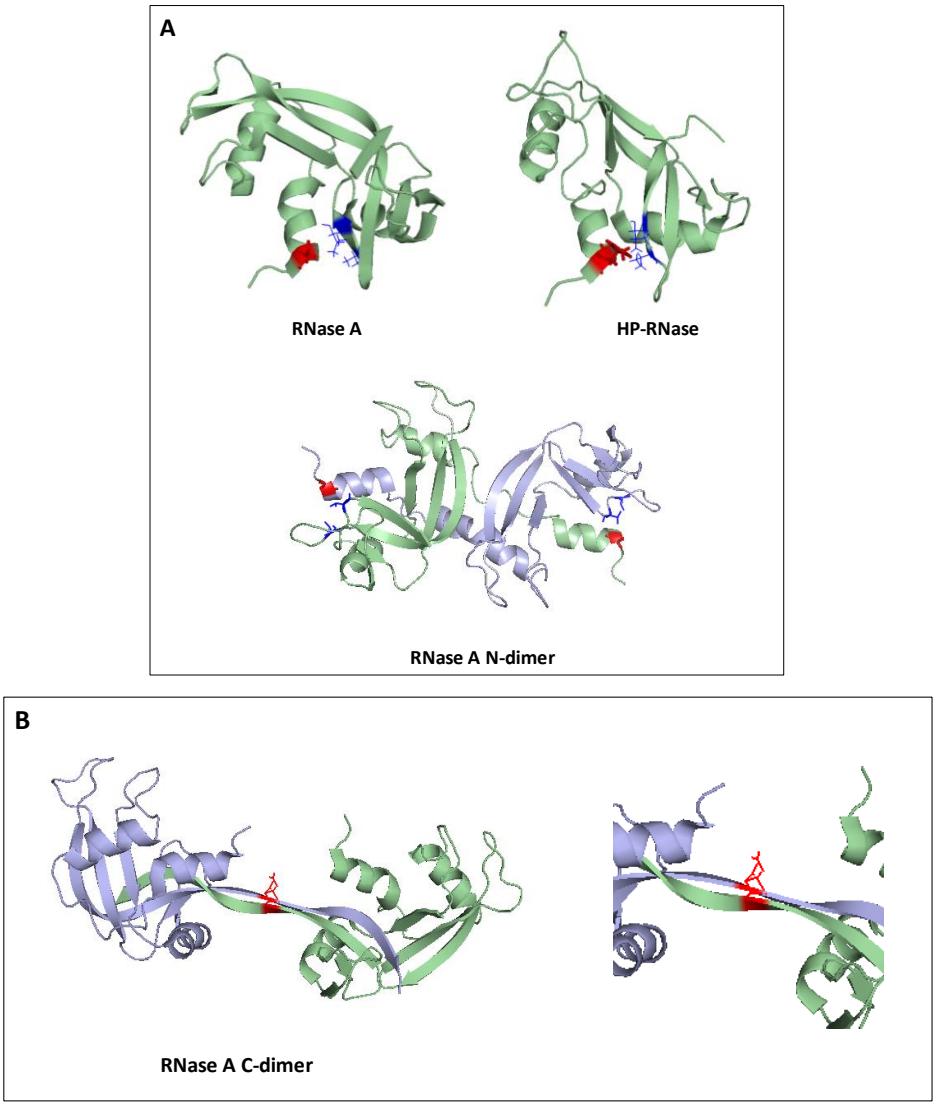

Figure 5.9. A. Residues located in the position 4 in RNase A and in HP-RNase, Ala and Arg respectively (in red). In the RNase A N-dimer, Ala4 interacts with the two Val residues located in the C-terminal domain of the protein, V116 and V118 (in blue). **B.** RNase A C-dimer, in which the two stabilizing N113 residues (Liu et al Nat Struct Biol 2001) are visible in red.

In conclusion, the results registered here with HP-RNase could be indirectly useful also to understand if the tendency of ONC to self associate would be affected by its three residues C-terminal elongation. For this reason, also the truncated ONC variant, lacking all three C-terminal GSC residues is now under production.

Chapter 6

ANGIOGENIN

6.1 Results

6.1.1 Expression and production of angiogenin and of its variants

After the expression of each ANG variant, i.e. the wild-type, the Q117G more active and the additional H13A and S28N pathogenic mutants, a final purification step has been performed with SEC, whose relative patterns are shown in Figure 6.1. The elution volume of ANG is about 15mL. We obtained an almost pure protein with the two wt-ANG and S28N variants with which, only one peak is visible, corresponding to the desired protein. This has been confirmed also by the subsequent electrophoretic and MS analyses. Hence, the species detected are the only ones present in solution and visible in the SEC patterns.

Instead, the chromatograms of H13A-ANG, and Q117G-ANG showed the presence of another peak eluted before the more abundant one which corresponded to the desired ANG species. However, upon collecting the most abundant peak, we obtained an almost pure protein with small amounts of impurities, as it can be visible in the SDS-PAGE analysis (Figure 6.2). The other peak present in the purification step of these variants showed a lower SDS-PAGE electrophoretic mobility, with an estimated molecular weight of approximately 16-17 kDa. Therefore, we confirmed the molecular weights of the proteins with MS analyses, as shown in table 6.1. Unfortunately, we could not successfully produce great difficulties the C39W-ANG, even. after changing the expression and renaturation protocol many times. Therefore, a SEC peak eluted at an elution volume of about 12 mL is visible in Figure 6.1 E. This peak corresponds to the impurity found in the chromatograms of the other ANG mutants. This peak has been collected and analyzed with SDS-PAGE, and is visible in the lane 7 of Figure 6.2: many impurities are present, together with a major band at about 25kDa. For all these reasons, we did not perform further analyses and we abandoned the study of this mutant.

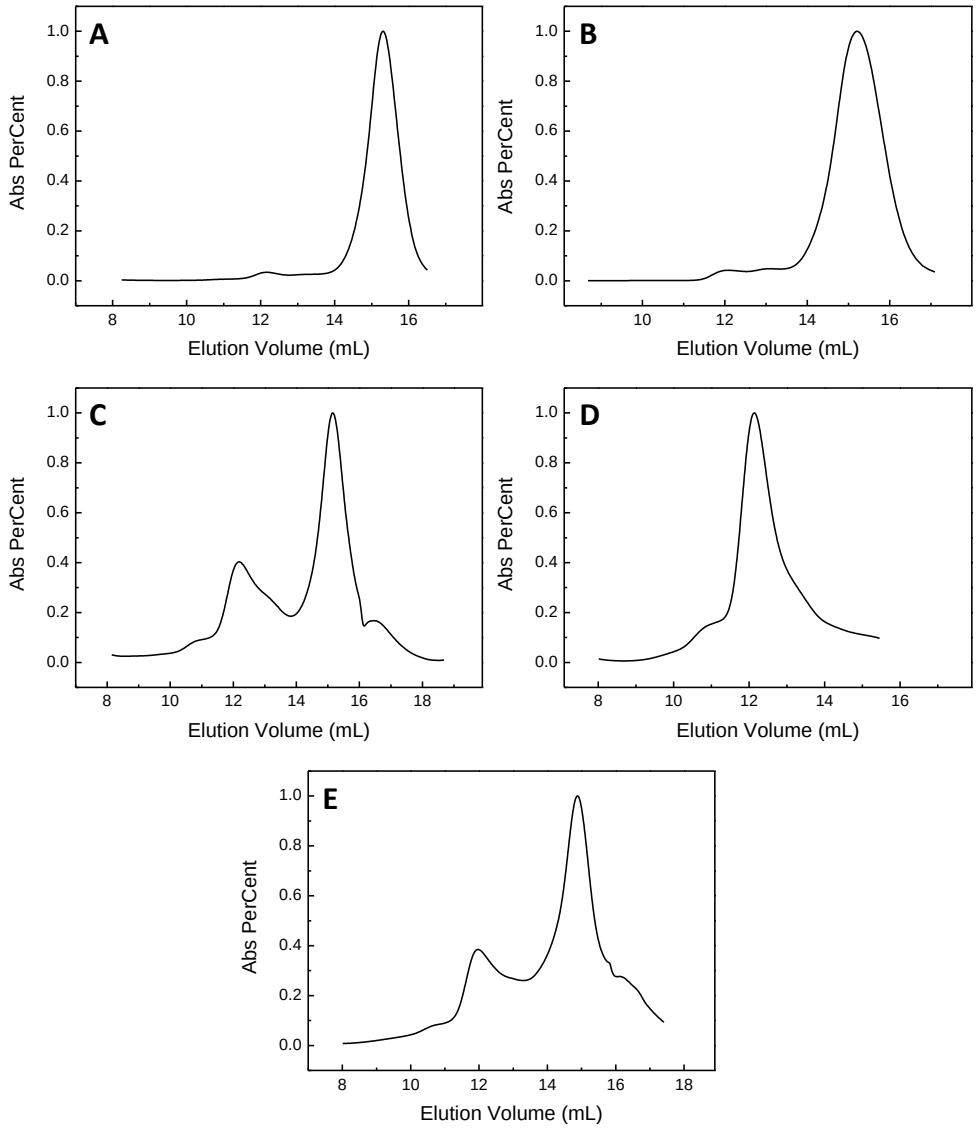

Figure 6.1. SEC patterns relative to the last purification step performed upon the expression of each ANG variant. Chromatographies were performed with a Superdex 75 HR 10/300 column equilibrated with 0.1M Tris-acetate, 0.3M NaCl, pH 8.4. Each pattern was normalized with Origin 7 Software. A: wt-ANG. B: S28N-ANG. C: H13A-ANG. D: C39W-ANG. E:Q117G-ANG.

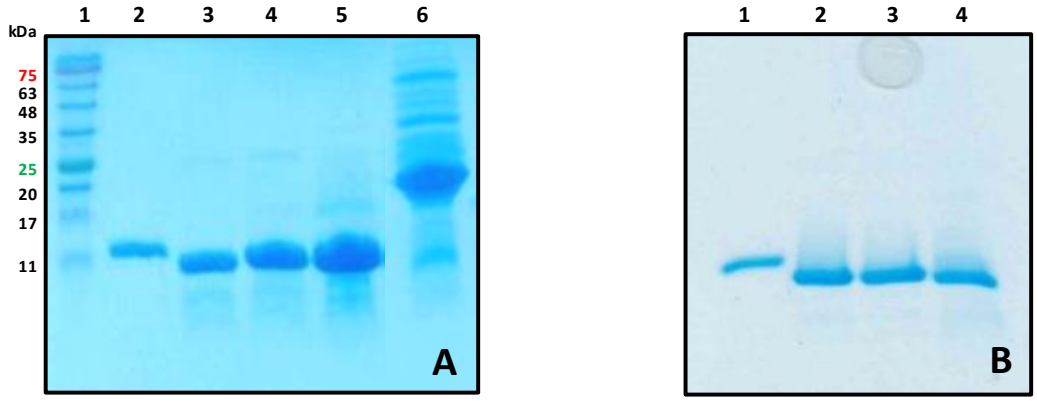

Figure 6.2. SDS-PAGE analyses of the main peak of ANG SEC purification. **A.** lane 1 standard molecular weight, lane 2 RNase A, lane 3 wt-ANG, lane 4 S28N-ANG, lane 5 H13A-ANG, lane 6 C39W-ANG. **B.** lane 1 RNase A, lane 2 wt-ANG, lane 3 S28N-ANG, lane 4 Q117G-ANG.

Variants	Theoretical MW (Da)	Experimental MW (Da)
WT	14120.9	14121.0 ± 1
S28N	14150	14148.2 ± 1
H13A	14054.0	14055 ± 1
Q117G	14049	14041 ± 1

Table 6.1. Molecular weight of ANG variants.

6.1.2 Circular dichroism spectroscopy

In order to investigate the goodness of the refolding step of the species produced, circular dichroism (CD) analyses have been performed with the ANG variants obtained with the highest yield and purity. Informations concerning the secondary and the tertiary structures of the ANG wild-type and of its mutants have been withdrawn. The far- and near-UV CD spectra of wt-ANG and S28N-ANG showed no differences within one another (Figure 6.3 A and B). This suggests that the S28N mutation, although being located in a α-helix, does not affect the whole secondary structure of the protein. The near-UV spectra indicate

that the conformation of the regions in which the aromatic residues are located are not perturbated by the mutation, suggesting that S28N-ANG retains the global tertiary structure of the wt.

The H13A-ANG mutant displayed some differences in both far and near-UV spectra. These differences suggest that the mutation provokes a modification in the α-helix where the aminoacid is located. Moreover, the variation in the region below 200nm indicates that there is a difference in a β-sheet of the protein, far from the mutation. However, maybe the His residue is crucial for some stabilizing interactions occurring with the aminoacids that are involved in the formation of this β-sheet. Near-UV spectra suggest that some variations in the environment of aromatic aminoacids may have took place.

The near-UV spectrum of the Q117G variant showed no significant differences with the one of the wt. Instead, the far-UV spectrum is shifted to the left with respect to the wild type protein, and this could be ascribable to differences at the expense of the β-sheet region.

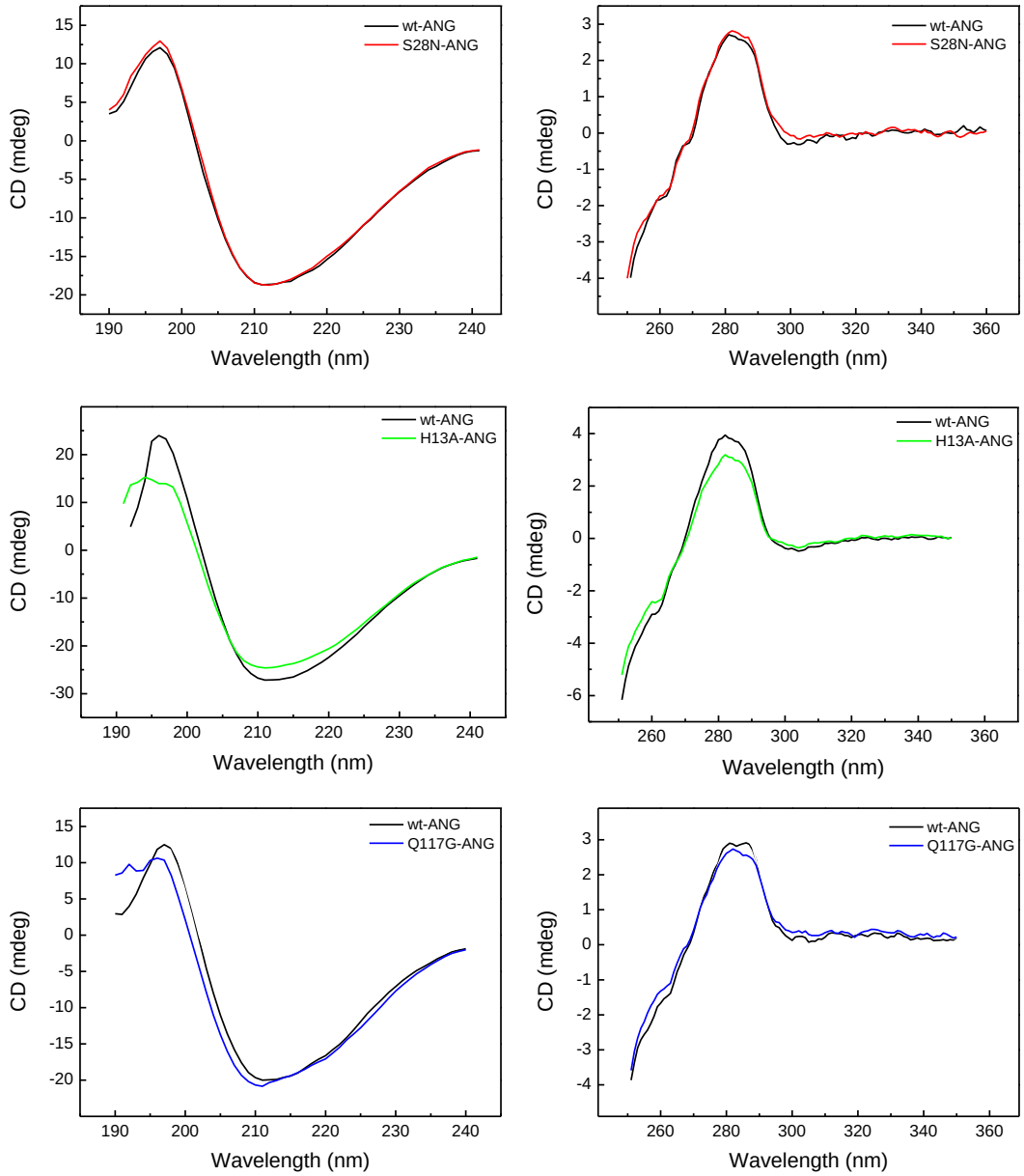

Figure 6.3. Far- and near-UV CD spectra of wt-ANG, S28N-ANG, H13A-ANG and Q117G-ANG.

6.1.3 Induction of oligomerization and dimer purification

After lyophilization from 40% acetic acid protein samples were redissolved in NaPi and analyzed through SEC (Figure 6.4). We focused our studies especially on the WT and S28N-ANG mutant. Both variants form a species that elutes before the monomer in SEC. This species, considering also the behavior of other RNase variants, is very probably a dimer. The pathogenic S28N variant shows to have a slightly higher propensity to form a dimer than the WT. This difference has been confirmed by repeated experiments. Indeed, Table 6.2 reports the average values of 5 different chromatographic analyses and shows that the S28N mutant forms more than 14% dimer, while the wt only 10%. The remaining ANG species is a monomer for both variants. The absolute values are not highly remarkable, but the relative differences emerging between the two ANG species are significant. The reason that could underpin this result could be due to the substitution, in the S28N-ANG mutant, of a serine with an asparagine, which might lead to the creation of a novel additional H-bond between the two domains, not present in the wild-type ANG dimer. Again, like HP-RNase and all other domain-swapped RNase oligomers, the formation of a dimer form was not possible upon resuspending the wt-ANG and S28N-ANG in ddH_2O instead of NaPi buffer. As explained in the previous chapters, the phosphate ion is necessary for RNases to permit the dimerization through 3D-DS mechanism, because it connects two histidines of the active site, one from the core and the other from the swapped N-terminal domain, and this can indirectly suggest that the ANG dimer forms through the 3D-DS mechanism.

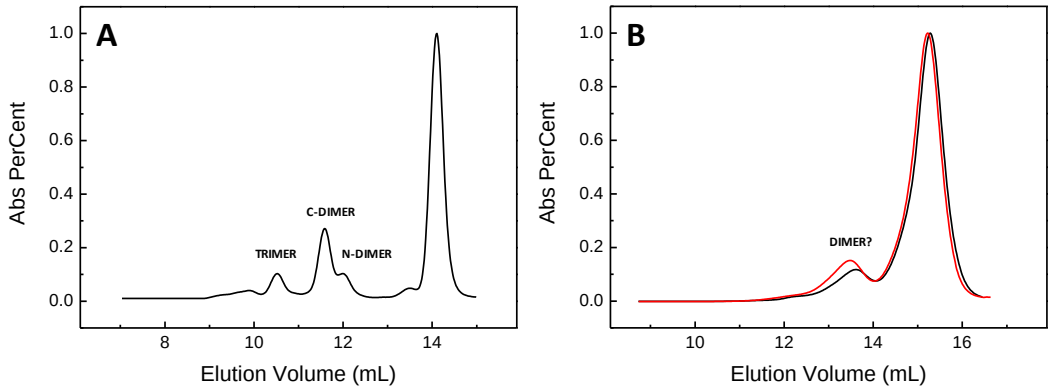

Figure 6.4. SEC parallel analysis of RNase A and ANG samples lyophilized from 40% acetic acid and redissolved in NaPi buffer. Each pattern was normalized to the monomer area with the Origin 7 Software. **A**: RNase A. **B**: wt-ANG (black line) and S28N-ANG (red line).

	%M	%D
wt	89.4 ± 1.2	10.1 ± 1.0
S28N	84.6 ± 1.0	14.8 ± 0.9

Table 6.2. Percentage of monomers and dimers of wild type and S28N angiogenin.

6.1.4 Cross-linking with divinyl sulfone (DVS) of ANG dimers

If also ANG would dimerize through 3D-DS, like other RNases, the DVS reaction should cross-link the two mentioned His residues to covalently stabilize the dimer, thus becoming capable to resist to the denaturing conditions induced by SDS-PAGE. Instead, as it is reported in figure 6.5, the SDS-PAGE analysis of the DVS reaction did not show the presence of a covalently stabilized dimer, both with wt-ANG and S28N-ANG. This result has been confirmed also after exploring the reaction using different DVS:protein ratios, and different reaction times. Therefore, no certainties could be reached about the mechanism through which ANG dimerization occurs. Maybe, the DVS stabilization did not occur for the intrinsic instability of the dimers in the reaction conditions experimented. Moreover, another possibility to be considered could be that the DVS cannot enter the ANG active site for the steric hindrance of Q117.

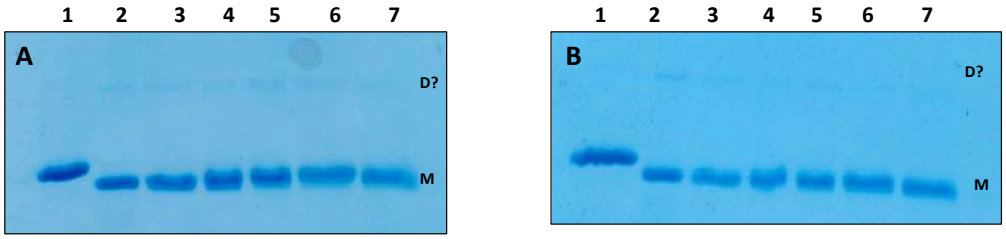

Figure 6.5. SDS-PAGE analyses of the products obtained from DVS reaction with ANG dimer. A: wt-ANG. B: S28N-ANG. Lane 1: RNase A monomer used as a standard (MW 13.7kDa). Lanes from 2 to 7: 0h, 6h, 24h, 48h, 72h, 96h.

6.1.5 H13A and Q117G variants

The analysis of the H13A-ANG should indirectly confirm that the species other from the monomer and visible in the chromatographic profiles is actually a domain-swapped dimer. Upon inducing the dimerization of this mutant by lyophilizing its 40% acetic acid solution, the SEC analysis shows no dimer (Figure 6.6 A). Thus, also H13A-ANG, as well other RNases lacking one His residue of the active site, is not able to form a dimer, therefore strongly indicating that the 3D-DS mechanism is the one followed by the wt.

We then produced the Q117G-ANG mutant in order to understand if the steric hindrance of glutamine in the active site could prevent the dimer formation[177]. We obtained only preliminary data to date, because we encountered some problems with the mutagenesis and the production of this mutant. Nevertheless, as shown in Figure 6.6 B, the monomer's peak is not well defined.

Furthermore, the low purification yield of Q117G-ANG did not permit us to perform additional .

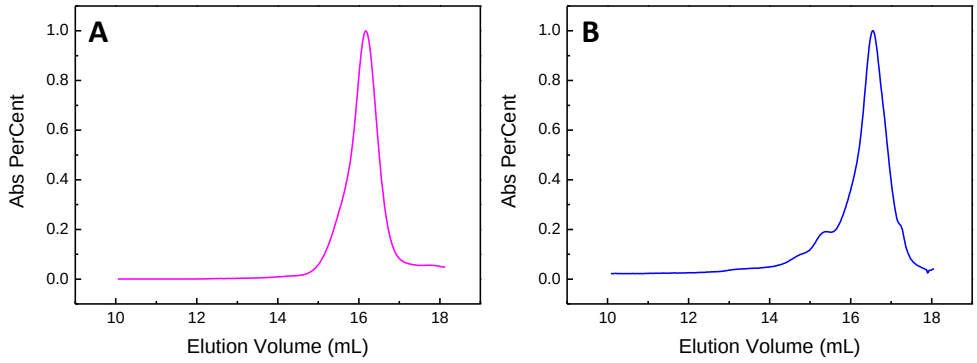

Figure 6.6. SEC analysis of RNase A and ANG samples lyophilized from 40% acetic acid and redissolved in NaPi buffer. Each pattern was normalized to the monomer area with the Origin 7 Software. **A**: H13A-ANG **B**: Q117G-ANG.

6.2 Discussion

In this thesis, the ANG self-aggregation propensity has been analyzed for the first time. Some variants of this protein are involved in neurodegenerative diseases, such as ALS and PD, and we wanted to investigate if they tend to aggregate to gain informations that could become useful in these complex and multifactorial pathologies.

We produced and analyzed the self-association capability of the wild type, and of the H13A, S28N and Q117G-ANG mutants. Concerning S28N and Q117G variants, their CD spectra showed no significant differences with respect to the wild type protein. This indicates that these mutations do not alter both the secondary and the tertiary structure of the protein. Instead, the spectrum of H13A displays some differences in both far and near-UV, suggesting that this inactive mutant could reach different secondary and tertiary structures with respect to the wild type.

We first analyzed the aggregation propensity of the wild type and S28N variants, choosing this mutant because it had been previously considered to be intrinsically prone to dimerize[201]. The chromatographic aggregation patterns of wt and S28N-ANG showed that, upon lyophilisation from 40% acetic acid solutions and resuspension in 0.4M NaPi (pH 6.7), a species was eluted before the monomer peak, which should correspond to a dimer. We have performed several aggregation tests, and the S28N variant seems to be slightly more prone to dimerize than the wild type (see Table 6.2). This could be ascribable to the Asn residue that might lead to the formation of a new additional H-bond between the two domains than the wt.

We tried to covalently stabilize the dimer with DVS, but we detected only traces of covalent dimers in SDS-PAGE analyses. This negative results could be due at different reasons: *i*. the 3D-DS does not occur, *ii*. the dimers are intrinsically unstable and they return to the monomeric form, *iii*. the dimer instability in the reaction conditions (0.1M NaAc, pH 5), *iv*. the active site is sterically occupied by the Gln117 residue that hinders the DVS accommodation and consequently its reaction. Therefore, we investigated if the protein dimerize

through the 3D-DS mechanism by redissolving the powder obtained after acid lyophilization in ddH_2O instead of NaPi buffer. As reported in the Introduction section, the phosphate ion create a saline bond between two His resides, one from the core of one monomer, and the other from the swapped domain of the second monomer. Thus, without phosphate, this saline bond is absent, so that the dimer formation and stabilization are not possible. In these experiments both wt and S28N patterns did not show the presence of any dimer, thus indirectly, but strongly, suggesting that ANG dimerizes through the 3D-DS mechanism.

A second, indirect indication of the presence of 3D-DS was provided by the H13A mutant. This pathogenic variant, lacking one of the His residues that allow the dimer formation and stabilization, do not show any dimeric trace in SEC.

Concerning the steric hindrance of Gln117, we obtained only a single indication about its self-association propensity, because of its low production yields. Moreover, the Q117G chromatographic pattern obtained after acid lyophilization is not so clear and well-defined, as visible in Figure 6.6.

After these preliminary investigations, we can envisage that the species present in SEC analyses of wt and S28N could be dimers formed through the 3D-DS mechanism, however, obviously, further investigations are required.

Furthermore, considering the numerous ANG variants involved in neurodegenerative diseases such as ALS, AD and PD, the analysis of their aggregation propensity *in vitro* could be definitely interesting.

Chapter 7

CONCLUSION AND FUTURE PERSPECTIVES

The first part of my PhD thesis was dedicated to evaluate if different methods used to induce the RNase A oligomerization may affect the properties of the RNase A monomer and of its domain-swapped dimers. We concluded that the differences detected in the structural properties of the RNase A species were definitely low, while the enzymatic activities were more significantly, although not vastly modulated as a function of the type of incubation suffered by the protein.

Concerning onconase (ONC), the experimental strategy followed to form, beyond the known N-swapped dimer, a C-swapped dimer did not show positive results, either upon mutating the C-terminal Cys residue or after deleting the two residue elongation that the protein displays with respect to RNase A. However, other mutants that could be useful to increase the self-association tendency of ONC are presently under production in the laboratory in which I performed my studies. Furthermore, if it will be possible to obtain large amounts of stable dimer(s) through the 3D-DS mechanism, or upon the introduction of covalent cross-links, the products could be used *in vitro* to investigate their cytotoxicity against different cancer cell lines. In this way, we could design more cytotoxic ONC variants in order to decrease the relative doses to be used *in vivo*, and consequently to lower or totally delete the concomitant undesired nephrotoxicity.

The experimental data obtained with human pancreatic ribonuclease highlighted for the first time that also the human pancreatic RNase variant can undergo extensive self-association. I recall here that some data were present in literature about the spontaneous dimerization of some HP-RNase mutants, but nothing concerning the wt protein, and all the data collected here strongly suggest that the HP-RNase dimers and larger oligomers form through the 3D-DS mechanism. However, further investigations are necessary to definitely confirm this. It is also important to underline that the human variant can self-associate at a higher extent than the bovine one. This evidence might be used to create a "chimera" with ONC in order to obtain a an antitumor protein with new or enhanced biological properties. To this regard, also the HP-RNase oligomers themselves could become useful tools in a therapeutic strategy perspective.

Indeed, considering that already the native monomer would be cytotoxic if it were able to avoid the RI mortal embrace, the oligomeric HP-RNase species could actually exert a potent cytotoxic action if they were intrinsically stable, or somehow stabilized, for example with carbodiimides, like EDC.

Finally, also angiogenin (ANG) was detected for the first time to be able to dimerize, in particular either the wild-type or, especially, its pathogenic S28N-ANG mutant. This dimer has been only partially characterized and we were not able to directly demonstrate if it forms through the 3D-DS mechanism or not. Probably, its stability is not sufficient to better characterize it. However, by producing and analyzing the H13A mutant behaviour, we indirectly confirmed that ANG dimerizes through 3D-DS. A more detailed characterization of this dimer, and the study of other ANG mutants present in the cohort of patients affected by serious diseases as ALS or PD, will help to better understand the role of these mutants and of their tendency to self-associate in the incoming and development of the mentioned neurodegenerative diseases.

8. Bibliography

1. Sierakowska H, Shugar D. Mammalian nucleolytic enzymes. *Prog Nucleic Acid Res Mol Biol*. 1977;20:59-130.
2. Weickmann JL, Elson M, Glitz DG. Purification and characterization of human pancreatic ribonuclease. *Biochemistry*. 1981;20(5):1272-1278. doi:10.1021/bi00508a035
3. Weickmann JL, Glitz DG. Human ribonucleases. Quantitation of pancreatic-like enzymes in serum, urine, and organ preparations. *J Biol Chem*. 1982;257(15):8705-8710.
4. Morita T, Niwata Y, Ohgi K, Ogawa M, Irie M. Distribution of two urinary ribonuclease-like enzymes in human organs and body fluids. *J Biochem*. 1986;99(1):17-25. doi:10.1093/oxfordjournals.jbchem.a135456
5. De Prisco R, Sorrentino S, Leone E, Libonati M. A ribonuclease from human seminal plasma active on double-stranded RNA. *Biochim Biophys Acta*. 1984;788(3):356-363. doi:10.1016/0167-4838(84)90049-9
6. Chu TM, Wang MC, Kuciel R, Valenzuela L, Murphy GP. Enzyme markers in human prostatic carcinoma. *Cancer Treat Rep*. 1977;61(2):193-200.
7. Kurihara M, Ogawa M, Ohta T, Kurokawa E. Purification and Immunological Characterization of Human Pancreatic Ribonuclease. *Cancer Res*. 1982;42(November):4836-4841. http://cancerres.aacrjournals.org/content/42/11/4836.short.
8. Sorrentino S, De Prisco R, Libonati M. Human seminal ribonuclease. Immunological quantitation of cross-reactive enzymes in serum, urine and seminal plasma. *Biochim Biophys Acta*. 1989;998(1):97-101. doi:10.1016/0167-4838(89)90125-8
9. Sorrentino S, Libonati M. Structure-function relationships in human ribonucleases: main distinctive features of the major RNase types. *FEBS Lett*. 1997;404(1):1-5. doi:10.1016/s0014-5793(97)00086-0
10. Benito A, Ribo M, Vilanova M. On the track of antitumour ribonucleases. *Mol Biosyst*. 2005;1(4):294-302. doi:10.1039/b502847g
11. Rybak SM, Newton DL. Natural and engineered cytotoxic ribonucleases: therapeutic potential. *Exp Cell Res*. 1999;253(2):325-335.

doi:10.1006/excr.1999.4718

12. Ilinskaya O, Decker K, Koschinski A, Dreyer F, Repp H. Bacillus intermedius ribonuclease as inhibitor of cell proliferation and membrane current. *Toxicology*. 2001;156(2-3):101-107.
13. Sevcik J, Urbanikova L, Leland PA, Raines RT. X-ray structure of two crystalline forms of a streptomycete ribonuclease with cytotoxic activity. *J Biol Chem*. 2002;277(49):47325-47330. doi:10.1074/jbc.M208425200
14. Olmo N, Turnay J, Gonzalez de Buitrago G, Lopez de Silanes I, Gavilanes JG, Lizarbe MA. Cytotoxic mechanism of the ribotoxin alpha-sarcin. Induction of cell death via apoptosis. *Eur J Biochem*. 2001;268(7):2113-2123. doi:10.1046/j.1432-1327.2001.02086.x
15. Juan G, Ardelt B, Li X, et al. G1 arrest of U937 cells by onconase is associated with suppression of cyclin D3 expression, induction of p16INK4A, p21WAF1/CIP1 and p27KIP and decreased pRb phosphorylation. *Leukemia*. 1998;12(8):1241-1248.
16. Arnold U, Ulbrich-Hofmann R. Natural and engineered ribonucleases as potential cancer therapeutics. *Biotechnol Lett*. 2006;28(20):1615-1622. doi:10.1007/s10529-006-9145-0
17. Arnold U. Aspects of the cytotoxic action of ribonucleases. *Curr Pharm Biotechnol*. 2008;9(3):161-168.
18. Di Donato A, Cafaro V, D'Alessio G. Ribonuclease A can be transformed into a dimeric ribonuclease with antitumor activity. *J Biol Chem*. 1994;269(26):17394-17396.
19. Leland PA, Schultz LW, Kim BM, Raines RT. Ribonuclease A variants with potent cytotoxic activity. *Proc Natl Acad Sci U S A*. 1998;95(18):10407-10412. doi:10.1073/pnas.95.18.10407
20. Gaur D, Swaminathan S, Batra JK. Interaction of human pancreatic ribonuclease with human ribonuclease inhibitor. Generation of inhibitor-resistant cytotoxic variants. *J Biol Chem*. 2001;276(27):24978-24984. doi:10.1074/jbc.M102440200
21. Leland PA, Staniszewski KE, Kim BM, Raines RT. Endowing Human Pancreatic Ribonuclease with Toxicity for Cancer Cells. *J Biol Chem*. 2001;276(46):43095-43102. doi:10.1074/jbc.M106636200
22. Bosch M, Benito A, Ribo M, Puig T, Beaumelle B, Vilanova M. A nuclear localization sequence endows human pancreatic ribonuclease with cytotoxic activity. *Biochemistry*. 2004;43(8):2167-2177. doi:10.1021/bi035729+

23. Futami J, Maeda T, Kitazoe M, et al. Preparation of potent cytotoxic ribonucleases by cationization: enhanced cellular uptake and decreased interaction with ribonuclease inhibitor by chemical modification of carboxyl groups. *Biochemistry*. 2001;40(25):7518-7524. doi:10.1021/bi010248g
24. Futami J, Kitazoe M, Maeda T, et al. Intracellular delivery of proteins into mammalian living cells by polyethylenimine-cationization. *J Biosci Bioeng*. 2005;99(2):95-103. doi:10.1263/jbb.99.095
25. De Lorenzo C, Arciello A, Cozzolino R, et al. A fully human antitumor immunoRNase selective for ErbB-2-positive carcinomas. *Cancer Res*. 2004;64(14):4870-4874. doi:10.1158/0008-5472.CAN-03-3717
26. Boix E, Wu Y, Vasandani VM, et al. Role of the N terminus in RNase A homologues: differences in catalytic activity, ribonuclease inhibitor interaction and cytotoxicity. *J Mol Biol*. 1996;257(5):992-1007. doi:10.1006/jmbi.1996.0218
27. Sorrentino S, Libonati M. Human pancreatic-type and nonpancreatic-type ribonucleases: a direct side-by-side comparison of their catalytic properties. *Arch Biochem Biophys*. 1994;312(2):340-348. doi:10.1006/abbi.1994.1318
28. Sorrentino S, Tucker GK, Glitz DG. Purification and characterization of a ribonuclease from human liver. *J Biol Chem*. 1988;263(31):16125-16131.
29. Ohta T, Ogawa M, Kurihara M, Kitahara T, Kosaki G. Purification, characterization and development of radioimmunoassay of human liver ribonuclease. *Clin Chim Acta*. 1982;124(1):51-62.
30. Yasuda T, Mizuta K, Sato W, Kishi K. Purification and characterization of a ribonuclease from human spleen. Immunological and enzymological comparison with nonsecretory ribonuclease from human urine. *Eur J Biochem*. 1990;191(2):523-529. doi:10.1111/j.1432-1033.1990.tb19152.x
31. Mizuta K, Awazu S, Yasuda T, Kishi K. Purification and characterization of three ribonucleases from human kidney: comparison with urine ribonucleases. *Arch Biochem Biophys*. 1990;281(1):144-151. doi:10.1016/0003-9861(90)90424-w
32. Iwama M, Kunihiro M, Ohgi K, Irie M. Purification and properties of human urine ribonucleases. *J Biochem*. 1981;89(4):1005-1016.
33. Liang CJ, Yamashita K, Kobata A. Structural study of the carbohydrate moiety of bovine pancreatic ribonuclease B. *J Biochem*. 1980;88(1):51-58.
34. Rudd PM, Scragg IG, Coghill E, Dwek RA. Separation and analysis of the glycoform populations of ribonuclease B using capillary electrophoresis. *Glycoconj J*. 1992;9(2):86-91.

35. Fu D, Chen L, O'Neill RA. A detailed structural characterization of ribonuclease B oligosaccharides by 1H NMR spectroscopy and mass spectrometry. *Carbohydr Res*. 1994;261(2):173-186.
36. Plummer THJ. Glycoproteins of bovine pancreatic juice. Isolation of ribonucleases C and D. *J Biol Chem*. 1968;243(22):5961-5966.
37. Baynes JW, Wold F. Effect of glycosylation on the in vivo circulating half-life of ribonuclease. *J Biol Chem*. 1976;251(19):6016-6024.
38. HIRS CH, MOORE S, STEIN WH. The sequence of the amino acid residues in performic acid-oxidized ribonuclease. *J Biol Chem*. 1960;235:633-647.
39. SMYTH DG, STEIN WH, MOORE S. The sequence of amino acid residues in bovine pancreatic ribonuclease: revisions and confirmations. *J Biol Chem*. 1963;238:227-234.
40. Kartha G, Bello J, Harker D. Tertiary structure of ribonuclease. *Nature*. 1967;213(5079):862-865. doi:10.1038/213862a0
41. Leland PA, Raines RT. Cancer chemotherapy - Ribonucleases to the rescue. *Chem Biol*. 2001;8(5):405-413. doi:10.1016/S1074-5521(01)00030-8
42. CRESTFIELD AM, STEIN WH, MOORE S. On the aggregation of bovine pancreatic ribonuclease. *Arch Biochem Biophys*. 1962;Suppl 1:217-222.
43. Gotte G, Vottariello F, Libonati M. Thermal aggregation of ribonuclease A. A contribution to the understanding of the role of 3D domain swapping in protein aggregation. *J Biol Chem*. 2003;278(12):10763-10769. doi:10.1074/jbc.M213146200
44. Libonati M, Gotte G. Oligomerization of bovine ribonuclease A: structural and functional features of its multimers. *Biochem J*. 2004;380(Pt 2):311-327. doi:10.1042/BJ20031922
45. Liu Y, Hart PJ, Schlunegger MP, Eisenberg D. The crystal structure of a 3D domain-swapped dimer of RNase A at a 2.1-A resolution. *Proc Natl Acad Sci U S A*. 1998;95(7):3437-3442.
46. Liu Y, Gotte G, Libonati M, Eisenberg D. A domain-swapped RNase A dimer with implications for amyloid formation. *Nat Struct Biol*. 2001;8(3):211-214. doi:10.1038/84941
47. Liu Y, Gotte G, Libonati M, Eisenberg D. Structures of the two 3D domain-swapped RNase A trimers. *Protein Sci*. 2002;11(2):371-380. doi:10.1110/ps.36602
48. Gotte G, Laurents D V, Libonati M. Three-dimensional domain-swapped

oligomers of ribonuclease A: identification of a fifth tetramer, pentamers and hexamers, and detection of trace heptameric, octameric and nonameric species. *Biochim Biophys Acta*. 2006;1764(1):44-54. doi:10.1016/j.bbapap.2005.10.011

49. Klink TA, Woycechowsky KJ, Taylor KM, Raines RT. Contribution of disulfide bonds to the conformational stability and catalytic activity of ribonuclease A. *Eur J Biochem*. 2000;267(2):566-572. doi:10.1046/j.1432-1327.2000.01037.x
50. Laity JH, Shimotakahara S, Scheraga HA. Expression of wild-type and mutant bovine pancreatic ribonuclease A in Escherichia coli. *Proc Natl Acad Sci U S A*. 1993;90(2):615-619. doi:10.1073/pnas.90.2.615
51. Shimotakahara S, Rios CB, Laity JH, Zimmerman DE, Scheraga HA, Montelione GT. NMR structural analysis of an analog of an intermediate formed in the rate-determining step of one pathway in the oxidative folding of bovine pancreatic ribonuclease A: automated analysis of 1H, 13C, and 15N resonance assignments for wild-type and [C65S, C72S] mutant forms. *Biochemistry*. 1997;36(23):6915-6929. doi:10.1021/bi963024k
52. Ui N. Isoelectric points and conformation of proteins. I. Effect of urea on the behavior of some proteins in isoelectric focusing. *Biochim Biophys Acta*. 1971;229(3):567-581.
53. FELSENFELD G, SANDEEN G, VONHIPPEL PH. THE DESTABILIZING EFFECT OF RIBONUCLEASE ON THE HELICAL DNA STRUCTURE. *Proc Natl Acad Sci U S A*. 1963;50:644-651. doi:10.1073/pnas.50.4.644
54. Kelly RC, Jensen DE, von Hippel PH. DNA "melting" proteins. IV. Fluorescence measurements of binding parameters for bacteriophage T4 gene 32-protein to mono-, oligo-, and polynucleotides. *J Biol Chem*. 1976;251(22):7240-7250.
55. Record MTJ, Lohman ML, De Haseth P. Ion effects on ligand-nucleic acid interactions. *J Mol Biol*. 1976;107(2):145-158.
56. McPherson A, Brayer G, Cascio D, Williams R. The mechanism of binding of a polynucleotide chain to pancreatic ribonuclease. *Science*. 1986;232(4751):765-768. doi:10.1126/science.3961503
57. Aguilar CF, Thomas PJ, Mills A, Moss DS, Palmer RA. Newly observed binding mode in pancreatic ribonuclease. *J Mol Biol*. 1992;224(1):265-267.
58. Katoh H, Yoshinaga M, Yanagita T, et al. Kinetic studies on turtle pancreatic ribonuclease: a comparative study of the base specificities of the B2 and P0 sites of bovine pancreatic ribonuclease A and turtle pancreatic ribonuclease. *Biochim Biophys Acta*. 1986;873(3):367-371. doi:10.1016/0167-4838(86)90085-3

59. RUSHIZKY GW, KNIGHT CA, SOBER HA. Studies on the preferential specificity of pancreatic ribonuclease as deduced from partial digests. *J Biol Chem*. 1961;236:2732-2737.

60. Irie M, Watanabe H, Ohgi K, et al. Some evidence suggesting the existence of P2 and B3 sites in the active site of bovine pancreatic ribonuclease A. *J Biochem*. 1984;95(3):751-759. doi:10.1093/oxfordjournals.jbchem.a134666

61. Raines RT. Ribonuclease A. *Chem Rev*. 1998;98(3):1045-1066.

62. delCardayre SB, Ribo M, Yokel EM, Quirk DJ, Rutter WJ, Raines RT. Engineering ribonuclease A: production, purification and characterization of wild-type enzyme and mutants at Gln11. *Protein Eng*. 1995;8(3):261-273.

63. Panov KI, Kolbanovskaya EY, Okorokov AL, et al. Ribonuclease A mutant His119 Asn: the role of histidine in catalysis. *FEBS Lett*. 1996;398(1):57-60. doi:10.1016/s0014-5793(96)01173-8

64. Trautwein K, Holliger P, Stackhouse J, Benner SA. Site-directed mutagenesis of bovine pancreatic ribonuclease: lysine-41 and aspartate-121. *FEBS Lett*. 1991;281(1-2):275-277. doi:10.1016/0014-5793(91)80410-5

65. Thompson JE, Raines RT. Value of general Acid-base catalysis to ribonuclease a. *J Am Chem Soc*. 1994;116(12):5467-5468. doi:10.1021/ja00091a060

66. Thompson JE, Kutateladze TG, Schuster MC, Venegas FD, Messmore JM, Raines RT. Limits to Catalysis by Ribonuclease A. *Bioorg Chem*. 1995;23(4):471-481. doi:10.1006/bioo.1995.1033

67. Messmore JM, Fuchs DN, Raines RT. Ribonuclease a: revealing structure-function relationships with semisynthesis. *J Am Chem Soc*. 1995;117(31):8057-8060. doi:10.1021/ja00136a001

68. Wlodawer A, Miller M, Sjolin L. Active site of RNase: neutron diffraction study of a complex with uridine vanadate, a transition-state analog. *Proc Natl Acad Sci U S A*. 1983;80(12):3628-3631. doi:10.1073/pnas.80.12.3628

69. FINDLAY D, HERRIES DG, MATHIAS AP, RABIN BR, ROSS CA. The active site and mechanism of action of bovine pancreatic ribonuclease. *Nature*. 1961;190:781-784. doi:10.1038/190781a0

70. delCardayre SB, Raines RT. Structural determinants of enzymatic processivity. *Biochemistry*. 1994;33(20):6031-6037. doi:10.1021/bi00186a001

71. Lee FS, Vallee BL. Structure and action of mammalian ribonuclease (angiogenin) inhibitor. *Prog Nucleic Acid Res Mol Biol*. 1993;44:1-30.

72. Shapiro R. Cytoplasmic ribonuclease inhibitor. *Methods Enzymol*. 2001;341:611-

628.

73. Klink TA, Raines RT. Conformational stability is a determinant of ribonuclease A cytotoxicity. *J Biol Chem*. 2000;275(23):17463-17467. doi:10.1074/jbc.M001132200
74. Kobe B, Deisenhofer J. A structural basis of the interactions between leucine-rich repeats and protein ligands. *Nature*. 1995;374(6518):183-186. doi:10.1038/374183a0
75. Monti DM, Montesano Gesualdi N, Matousek J, Esposito F, D'Alessio G. The cytosolic ribonuclease inhibitor contributes to intracellular redox homeostasis. *FEBS Lett*. 2007;581(5):930-934. doi:10.1016/j.febslet.2007.01.072
76. Gotte G, Laurents D V, Merlino A, Picone D, Spadaccini R. Structural and functional relationships of natural and artificial dimeric bovine ribonucleases : New scaffolds for potential antitumor drugs N-swapping. *FEBS Lett*. 2013;587(22):3601-3608. doi:10.1016/j.febslet.2013.09.038
77. Park C, Raines RT. Dimer formation by a "monomeric" protein. *Protein Sci*. 2000;9(10):2026-2033. doi:10.1110/ps.9.10.2026
78. D'Alessio G. Oligomer evolution in action? *Nat Struct Biol*. 1995;2(1):11-13.
79. D'alessio G. Evolution of oligomeric proteins. The unusual case of a dimeric ribonuclease. *Eur J Biochem*. 1999;266(3):699-708. doi:10.1046/j.1432-1327.1999.00912.x
80. Rutkoski TJ, Kink JA, Strong LE, Schilling CI, Raines RT. Antitumor activity of ribonuclease multimers created by site-specific covalent tethering. *Bioconjug Chem*. 2010;21(9):1691-1702. doi:10.1021/bc100292x
81. Gotte G, Testolin L, Costanzo C, Sorrentino S, Armato U, Libonati M. Cross-linked trimers of bovine ribonuclease A: activity on double-stranded RNA and antitumor action. *FEBS Lett*. 1997;415(3):308-312. doi:10.1016/s0014-5793(97)01147-2
82. Libonati M, Bertoldi M, Sorrentino S. The activity on double-stranded RNA of aggregates of ribonuclease A higher than dimers increases as a function of the size of the aggregates. *Biochem J*. 1996;318 (Pt 1):287-290. doi:10.1042/bj3180287
83. Lopez-Alonso JP, Gotte G, Laurents D V. Kinetic analysis provides insight into the mechanism of ribonuclease A oligomer formation. *Arch Biochem Biophys*. 2009;489(1-2):41-47. doi:10.1016/j.abb.2009.07.013
84. Liu Y, Eisenberg D. 3D domain swapping: as domains continue to swap. *Protein Sci*. 2002;11(6):1285-1299. doi:10.1110/ps.0201402

85. Bennett MJ, Choe S, Eisenberg D. Domain swapping: entangling alliances between proteins. *Proc Natl Acad Sci U S A*. 1994;91(8):3127-3131. doi:10.1073/pnas.91.8.3127

86. Gronenborn AM. Protein acrobatics in pairs--dimerization via domain swapping. *Curr Opin Struct Biol*. 2009;19(1):39-49. doi:10.1016/j.sbi.2008.12.002

87. Bennett MJ, Schlunegger MP, Eisenberg D. 3D domain swapping: a mechanism for oligomer assembly. *Protein Sci*. 1995;4(12):2455-2468. doi:10.1002/pro.5560041202

88. Kuhlman B, O'Neill JW, Kim DE, Zhang KY, Baker D. Conversion of monomeric protein L to an obligate dimer by computational protein design. *Proc Natl Acad Sci U S A*. 2001;98(19):10687-10691. doi:10.1073/pnas.181354398

89. Rousseau F, Schymkowitz JW, Wilkinson HR, Itzhaki LS. Three-dimensional domain swapping in p13suc1 occurs in the unfolded state and is controlled by conserved proline residues. *Proc Natl Acad Sci U S A*. 2001;98(10):5596-5601. doi:10.1073/pnas.101542098

90. Schymkowitz JW, Rousseau F, Wilkinson HR, Friedler A, Itzhaki LS. Observation of signal transduction in three-dimensional domain swapping. *Nat Struct Biol*. 2001;8(10):888-892. doi:10.1038/nsb1001-888

91. Ercole C, Colamarino RA, Pizzo E, Fogolari F, Spadaccini R, Picone D. Comparison of the structural and functional properties of RNase A and BS-RNase: a stepwise mutagenesis approach. *Biopolymers*. 2009;91(12):1009-1017. doi:10.1002/bip.21176

92. Gotte G, Donadelli M, Laurents D V, Vottariello F, Morbio M, Libonati M. Increase of RNase a N-terminus polarity or C-terminus apolarity changes the two domains' propensity to swap and form the two dimeric conformers of the protein. *Biochemistry*. 2006;45(36):10795-10806. doi:10.1021/bi060933t

93. Nenci A, Gotte G, Bertoldi M, Libonati M. Structural properties of trimers and tetramers of ribonuclease A. *Protein Sci*. 2001;10(10):2017-2027. doi:10.1110/ps.14101

94. Vottariello F, Giacomelli E, Frasson R, Pozzi N, De Filippis V, Gotte G. RNase A oligomerization through 3D domain swapping is favoured by a residue located far from the swapping domains. *Biochimie*. 2011;93(10):1846-1857. doi:10.1016/j.biochi.2011.07.005

95. Ercole C, Lopez-Alonso JP, Font J, et al. Crowding agents and osmolytes provide insight into the formation and dissociation of RNase A oligomers. *Arch Biochem*

Biophys. 2011;506(2):123-129. doi:10.1016/j.abb.2010.11.014

96. Bucci E, Vitagliano L, Barone R, Sorrentino S, D'Alessio G, Graziano G. On the thermal stability of the two dimeric forms of ribonuclease A. *Biophys Chem*. 2005;116(2):89-95. doi:10.1016/j.bpc.2005.03.002
97. Murray AJ, Lewis SJ, Barclay AN, Brady RL. One sequence, two folds: a metastable structure of CD2. *Proc Natl Acad Sci U S A*. 1995;92(16):7337-7341. doi:10.1073/pnas.92.16.7337
98. Green SM, Gittis AG, Meeker AK, Lattman EE. One-step evolution of a dimer from a monomeric protein. *Nat Struct Biol*. 1995;2(9):746-751.
99. Kortt AA, Malby RL, Caldwell JB, et al. Recombinant anti-sialidase single-chain variable fragment antibody. Characterization, formation of dimer and higher-molecular-mass multimers and the solution of the crystal structure of the single-chain variable fragment/sialidase complex. *Eur J Biochem*. 1994;221(1):151-157. doi:10.1111/j.1432-1033.1994.tb18724.x
100. Perisic O, Webb PA, Holliger P, Winter G, Williams RL. Crystal structure of a diabody, a bivalent antibody fragment. *Structure*. 1994;2(12):1217-1226.
101. Trinkl S, Glockshuber R, Jaenicke R. Dimerization of beta B2-crystallin: the role of the linker peptide and the N- and C-terminal extensions. *Protein Sci*. 1994;3(9):1392-1400. doi:10.1002/pro.5560030905
102. Fruchter RG, Crestfield AM. Preparation and properties of two active forms of ribonuclease dimer. *J Biol Chem*. 1965;240(10):3868-3874.
103. Gotte G, Libonati M. Oligomerization of ribonuclease A under reducing conditions. *Biochim Biophys Acta*. 2008;1784(4):638-650. doi:10.1016/j.bbapap.2007.12.013
104. Gotte G, Libonati M. Two different forms of aggregated dimers of ribonuclease A. *Biochim Biophys Acta*. 1998;1386(1):106-112.
105. Merlino A, Vitagliano L, Ceruso MA, Mazzarella L. Dynamic properties of the N-terminal swapped dimer of ribonuclease A. *Biophys J*. 2004;86(4):2383-2391. doi:10.1016/S0006-3495(04)74295-2
106. Merlino A, Ceruso MA, Vitagliano L, Mazzarella L. Open interface and large quaternary structure movements in 3D domain swapped proteins: insights from molecular dynamics simulations of the C-terminal swapped dimer of ribonuclease A. *Biophys J*. 2005;88(3):2003-2012. doi:10.1529/biophysj.104.048611
107. Gotte G, Bertoldi M, Libonati M. Structural versatility of bovine ribonuclease A. Distinct conformers of trimeric and tetrameric aggregates of the enzyme. *Eur J*

Biochem. 1999;265(2):680-687. doi:10.1046/j.1432-1327.1999.00761.x

108. Matousek J, Gotte G, Pouckova P, et al. Antitumor activity and other biological actions of oligomers of ribonuclease A. *J Biol Chem*. 2003;278(26):23817-23822. doi:10.1074/jbc.M302711200
109. Bennett MJ, Sawaya MR, Eisenberg D. Deposition diseases and 3D domain swapping. *Structure*. 2006;14(5):811-824. doi:10.1016/j.str.2006.03.011
110. Cozza G, Moro S, Gotte G. Elucidation of the ribonuclease A aggregation process mediated by 3D domain swapping: a computational approach reveals possible new multimeric structures. *Biopolymers*. 2008;89(1):26-39. doi:10.1002/bip.20833
111. Fruchter RG, Crestfield AM. On the structure of ribonuclease dimer. Isolation and identification of monomers derived from inactive carboxymethyl dimers. *J Biol Chem*. 1965;240(10):3875-3882.
112. Libonati M. Molecular aggregates of ribonucleases. Some enzymatic properties. *Ital J Biochem*. 1969;18(6):407-417.
113. Pares X, Nogues M V, de Llorens R, Cuchillo CM. Structure and function of ribonuclease A binding subsites. *Essays Biochem*. 1991;26:89-103.
114. Nogues M V, Vilanova M, Cuchillo CM. Bovine pancreatic ribonuclease A as a model of an enzyme with multiple substrate binding sites. *Biochim Biophys Acta*. 1995;1253(1):16-24. doi:10.1016/0167-4838(95)00138-k
115. Usher DA, Erenrich ES, Eckstein F. Geometry of the first step in the action of ribonuclease-A (in-line geometry-uridine2',3'-cyclic thiophosphate- 31 P NMR). *Proc Natl Acad Sci U S A*. 1972;69(1):115-118. doi:10.1073/pnas.69.1.115
116. Lee JE, Bae E, Bingman CA, Phillips GNJ, Raines RT. Structural basis for catalysis by onconase. *J Mol Biol*. 2008;375(1):165-177. doi:10.1016/j.jmb.2007.09.089
117. Libonati M. Degradation of poly A and double-stranded RNA by aggregates of pancreatic ribonuclease. *Biochim Biophys Acta*. 1971;228(2):440-445. doi:10.1016/0005-2787(71)90049-9
118. Wu Y, Saxena SK, Ardelt W, et al. A study of the intracellular routing of cytotoxic ribonucleases. *J Biol Chem*. 1995;270(29):17476-17481. doi:10.1074/jbc.270.29.17476
119. DE LAMIRANDE G. Action of deoxyribonuclease and ribonuclease on the growth of Ehrlich ascites carcinoma in mice. *Nature*. 1961;192:52-54. doi:10.1038/192052a0
120. ROTH JS. Ribonuclease activity and cancer: a review. *Cancer Res*. 1963;23:657-

666.

121. Patutina OA, Mironova NL, Ryabchikova EI, et al. Tumoricidal Activity of RNase A and DNase I. *Acta Naturae*. 2010;2(1):88-94.
122. Klink TA, Woycechowsky KJ, Taylor KM, Raines RT. Contribution of disulfide bonds to the conformational stability and catalytic activity of ribonuclease A. *Eur J Biochem*. 2000;267(2):566-572. doi:10.1046/j.1432-1327.2000.01037.x
123. Haigis MC, Kurten EL, Raines RT. Ribonuclease inhibitor as an intracellular sentry. *Nucleic Acids Res*. 2003;31(3):1024-1032. doi:10.1093/nar/gkg163
124. Johnson RJ, McCoy JG, Bingman CA, Phillips GNJ, Raines RT. Inhibition of human pancreatic ribonuclease by the human ribonuclease inhibitor protein. *J Mol Biol*. 2007;368(2):434-449. doi:10.1016/j.jmb.2007.02.005
125. Naddeo M, Vitagliano L, Russo A, Gotte G, D'Alessio G, Sorrentino S. Interactions of the cytotoxic RNase A dimers with the cytosolic ribonuclease inhibitor. *FEBS Lett*. 2005;579(12):2663-2668. doi:10.1016/j.febslet.2005.03.087
126. Libonati M, Sorrentino S, Galli R, La Montagna R, Di Donato A. Degradation of DNA . RNA hybrids by aggregates of pancreatic ribonuclease. *Biochim Biophys Acta*. 1975;407(3):292-298. doi:10.1016/0005-2787(75)90096-9
127. Lopez-Alonso JP, Diez-Garcia F, Font J, et al. Carbodiimide EDC induces cross-links that stabilize RNase A C-dimer against dissociation: EDC adducts can affect protein net charge, conformation, and activity. *Bioconjug Chem*. 2009;20(8):1459-1473. doi:10.1021/bc9001486
128. Ardelt W, Shogen K, Darzynkiewicz Z. Onconase and amphinase, the antitumor ribonucleases from Rana pipiens oocytes. *Curr Pharm Biotechnol*. 2008;9(3):215-225.
129. Ardelt W, Shogen K, Darzynkiewicz Z. Onconase and Amphinase, the Antitumor Ribonucleases from Rana pipiens Oocytes. *Curr Pharm Biotechnol*. 2008;9(3):215-225. doi:10.2174/138920108784567245
130. Chen S, Le SY, Newton DL, Maizel JVJ, Rybak SM. A gender-specific mRNA encoding a cytotoxic ribonuclease contains a 3' UTR of unusual length and structure. *Nucleic Acids Res*. 2000;28(12):2375-2382. doi:10.1093/nar/28.12.2375
131. Mosimann SC, Ardelt W, James MN. Refined 1.7 A X-ray crystallographic structure of P-30 protein, an amphibian ribonuclease with anti-tumor activity. *J Mol Biol*. 1994;236(4):1141-1153.
132. Lee JE, Raines RT. Contribution of active-site residues to the function of onconase, a ribonuclease with antitumoral activity. *Biochemistry*.

2003;42(39):11443-11450. doi:10.1021/bi035147s

133. Ardelt W, Mikulski SM, Shogen K. Amino acid sequence of an anti-tumor protein from Rana pipiens oocytes and early embryos. Homology to pancreatic ribonucleases. *J Biol Chem*. 1991;266(1):245-251.
134. Notomista E, Catanzano F, Graziano G, Di Gaetano S, Barone G, Di Donato A. Contribution of chain termini to the conformational stability and biological activity of onconase. *Biochemistry*. 2001;40(31):9097-9103. doi:10.1021/bi010741s
135. Saxena SK, Sirdeshmukh R, Ardelt W, Mikulski SM, Shogen K, Youle RJ. Entry into cells and selective degradation of tRNAs by a cytotoxic member of the RNase A family. *J Biol Chem*. 2002;277(17):15142-15146. doi:10.1074/jbc.M108115200
136. Singh UP, Ardelt W, Saxena SK, et al. Enzymatic and structural characterisation of amphinase, a novel cytotoxic ribonuclease from Rana pipiens oocytes. *J Mol Biol*. 2007;371(1):93-111. doi:10.1016/j.jmb.2007.04.071
137. Kelemen BR, Schultz LW, Sweeney RY, Raines RT. Excavating an active site: the nucleobase specificity of ribonuclease A. *Biochemistry*. 2000;39(47):14487-14494. doi:10.1021/bi001862f
138. Suhasini AN, Sirdeshmukh R. Transfer RNA cleavages by onconase reveal unusual cleavage sites. *J Biol Chem*. 2006;281(18):12201-12209. doi:10.1074/jbc.M504488200
139. Qiao M, Zu L-D, He X-H, Shen R-L, Wang Q-C, Liu M-F. Onconase downregulates microRNA expression through targeting microRNA precursors. *Cell Res*. 2012;22(7):1199-1202. doi:10.1038/cr.2012.67
140. Rutkoski TJ, Raines RT. Evasion of ribonuclease inhibitor as a determinant of ribonuclease cytotoxicity. *Curr Pharm Biotechnol*. 2008;9(3):185-189.
141. Ardelt W, Ardelt B, Darzynkiewicz Z. Ribonucleases as potential modalities in anticancer therapy. *Eur J Pharmacol*. 2009;625(1-3):181-189. doi:10.1016/j.ejphar.2009.06.067
142. Wang X-M, Guo Z-Y. Recombinant expression, different downstream processing of the disulfide-rich anti-tumor peptide Ranpirnase and its effect on the growth of human glioma cell line SHG-44. *Biomed reports*. 2013;1(5):747-750. doi:10.3892/br.2013.138
143. Smolewski P, Witkowska M, Zwolinska M, et al. Cytotoxic activity of the amphibian ribonucleases onconase and r-amphinase on tumor cells from B cell

lymphoproliferative disorders. *Int J Oncol*. 2014;45(1):419-425. doi:10.3892/ijo.2014.2405

144. Fiorini C, Cordani M, Gotte G, Picone D, Donadelli M. Onconase induces autophagy sensitizing pancreatic cancer cells to gemcitabine and activates Akt/mTOR pathway in a ROS-dependent manner. *Biochim Biophys Acta*. 2015;1853(3):549-560. doi:10.1016/j.bbamcr.2014.12.016
145. Wu Y, Mikulski SM, Ardelt W, Rybak SM, Youle RJ. A cytotoxic ribonuclease: Study of the mechanism of onconase cytotoxicity. *J Biol Chem*. 1993;268(14):10686-10693.
146. Suhasini AN, Sirdeshmukh R. Onconase action on tRNA(Lys3), the primer for HIV-1 reverse transcription. *Biochem Biophys Res Commun*. 2007;363(2):304-309. doi:10.1016/j.bbrc.2007.08.157
147. Saxena SK, Gravell M, Wu YN, et al. Inhibition of HIV-1 production and selective degradation of viral RNA by an amphibian ribonuclease. *J Biol Chem*. 1996;271(34):20783-20788. doi:10.1074/jbc.271.34.20783
148. Vasandani VM, Burris JA, Sung C. Reversible nephrotoxicity of onconase and effect of lysine pH on renal onconase uptake. *Cancer Chemother Pharmacol*. 1999;44(2):164-169. doi:10.1007/s002800050962
149. Arnold U, Ulbrich-Hofmann R. Natural and engineered ribonucleases as potential cancer therapeutics. *Biotechnol Lett*. 2006;28(20):1615-1622. doi:10.1007/s10529-006-9145-0
150. Titani K, Takio K, Kuwada M, et al. Amino acid sequence of sialic acid binding lectin from frog (Rana catesbeiana) eggs. *Biochemistry*. 1987;26(8):2189-2194. doi:10.1021/bi00382a018
151. Iordanov MS, Ryabinina OP, Wong J, et al. Molecular determinants of apoptosis induced by the cytotoxic ribonuclease onconase: Evidence for cytotoxic mechanisms different from inhibition of protein synthesis. *Cancer Res*. 2000;60(7):1983-1994.
152. Zhao H, Ardelt B, Ardelt W, Shogen K, Darzynkiewicz Z. The cytotoxic ribonuclease onconase targets RNA interference (siRNA). *Cell Cycle*. 2008;7(20):3258-3261. doi:10.4161/cc.7.20.6855
153. Turcotte RF, Lavis LD, Raines RT. Onconase cytotoxicity relies on the distribution of its positive charge. *FEBS J*. 2009;276(14):3846-3857. doi:10.1111/j.1742-4658.2009.07098.x
154. Fagagnini A, Pica A, Fasoli S, et al. Onconase dimerization through 3D domain

swapping: structural investigations and increase in the apoptotic effect in cancer cells. *Biochem J*. 2017;474(22):3767-3781. doi:10.1042/BCJ20170541

155. Beintema JJ, Wietzes P, Weickmann JL, Glitz DG. The amino acid sequence of human pancreatic ribonuclease. *Anal Biochem*. 1984;136(1):48-64.
156. Sorrentino S. Human extracellular ribonucleases: multiplicity, molecular diversity and catalytic properties of the major RNase types. *Cell Mol Life Sci*. 1998;54(8):785-794. doi:10.1007/s000180050207
157. Moussaoui M, Benito A, Cuchillo CM, Nogue M V, Vilanova M. Human pancreatic ribonuclease presents higher endonucleolytic activity than ribonuclease A. 2008;471:191-197. doi:10.1016/j.abb.2007.12.016
158. Potenza N, Salvatore V, Migliozzi A, Martone V, Nobile V, Russo A. Hybridase activity of human ribonuclease-1 revealed by a real-time fluorometric assay. *Nucleic Acids Res*. 2006;34(10):2906-2913. doi:10.1093/nar/gkl368
159. Libonati M, Sorrentino S. Degradation of double-stranded RNA by mammalian pancreatic-type ribonucleases. *Methods Enzymol*. 2001;341:234-248.
160. Sorrentino S, Naddeo M, Russo A, D'Alessio G. Degradation of double-stranded RNA by human pancreatic ribonuclease: crucial role of noncatalytic basic amino acid residues. *Biochemistry*. 2003;42(34):10182-10190. doi:10.1021/bi030040q
161. Sorrentino S. The eight human '' canonical '' ribonucleases : Molecular diversity , catalytic properties , and special biological actions of the enzyme proteins. *FEBS Lett*. 2010;584(11):2194-2200. doi:10.1016/j.febslet.2010.04.018
162. Landre JBP, Hewett PW, Olivot J-M, et al. Human endothelial cells selectively express large amounts of pancreatic-type ribonuclease (RNase 1). *J Cell Biochem*. 2002;86(3):540-552. doi:10.1002/jcb.10234
163. Yang D, Chen Q, Rosenberg HF, et al. Human ribonuclease A superfamily members, eosinophil-derived neurotoxin and pancreatic ribonuclease, induce dendritic cell maturation and activation. *J Immunol*. 2004;173(10):6134-6142. doi:10.4049/jimmunol.173.10.6134
164. Attery A, Dey P, Tripathi P, Batra JK. A ribonuclease inhibitor resistant dimer of human pancreatic ribonuclease displays specific antitumor activity. *Int J Biol Macromol*. 2018;107:1965-1970. doi:10.1016/j.ijbiomac.2017.10.067
165. Merlino A, Avella G, Di Gaetano S, et al. Structural features for the mechanism of antitumor action of a dimeric human pancreatic ribonuclease variant. *Protein Sci*. 2009;18(1):50-57. doi:10.1002/pro.6
166. Di Gaetano S, D'alessio G, Piccoli R. Second generation antitumour human

RNase: significance of its structural and functional features for the mechanism of antitumour action. *Biochem J*. 2001;358(Pt 1):241-247. doi:10.1042/0264-6021:3580241

167. Rodriguez M, Benito A, Ribo M, Vilanova M. Characterization of the dimerization process of a domain-swapped dimeric variant of human pancreatic ribonuclease. *FEBS J*. 2006;273(6):1166-1176. doi:10.1111/j.1742-4658.2006.05141.x
168. Russo N, Antignani A, D'Alessio G. In vitro evolution of a dimeric variant of human pancreatic ribonuclease. *Biochemistry*. 2000;39(13):3585-3591. doi:10.1021/bi992367q
169. Pica A, Merlino A, Buell AK, et al. Three-dimensional domain swapping and supramolecular protein assembly: Insights from the X-ray structure of a dimeric swapped variant of human pancreatic RNase. *Acta Crystallogr Sect D Biol Crystallogr*. 2013;69(10):2116-2123. doi:10.1107/S0907444913020507
170. Leland PA, Staniszewski KE, Park C, Kelemen BR, Raines RT. The ribonucleolytic activity of angiogenin. *Biochemistry*. 2002;41(4):1343-1350. doi:10.1021/bi0117899
171. Fett JW, Strydom DJ, Lobb RR, et al. Isolation and characterization of angiogenin, an angiogenic protein from human carcinoma cells. *Biochemistry*. 1985;24(20):5480-5486. doi:10.1021/bi00341a030
172. Shapiro R, Strydom DJ, Olson KA, Vallee BL. Isolation of angiogenin from normal human plasma. *Biochemistry*. 1987;26(16):5141-5146. doi:10.1021/bi00390a037
173. Spong CY, Ghidini A, Sherer DM, Pezzullo JC, Ossandon M, Eglinton GS. Angiogenin: a marker for preterm delivery in midtrimester amniotic fluid. *Am J Obstet Gynecol*. 1997;176(2):415-418. doi:10.1016/s0002-9378(97)70508-8
174. Acharya KR, Shapiro R, Allen SC, Riordan JF, Vallee BL. Crystal structure of human angiogenin reveals the structural basis for its functional divergence from ribonuclease. *Proc Natl Acad Sci U S A*. 1994;91(8):2915-2919. doi:10.1073/pnas.91.8.2915
175. Gao X, Xu Z. Mechanisms of action of angiogenin. *Acta Biochim Biophys Sin (Shanghai)*. 2008;40(7):619-624. doi:10.1111/j.1745-7270.2008.00442.x
176. Russo N, Shapiro R, Acharya KR, Riordan JF, Vallee BL. Role of glutamine-117 in the ribonucleolytic activity of human angiogenin. *Proc Natl Acad Sci U S A*. 1994;91(8):2920-2924. doi:10.1073/pnas.91.8.2920

177. Rybak SM, Vallee BL. Base cleavage specificity of angiogenin with Saccharomyces cerevisiae and Escherichia coli 5S RNAs. *Biochemistry*. 1988;27(7):2288-2294. doi:10.1021/bi00407a007

178. Hu G f, Xu C j, Riordan JF. Human angiogenin is rapidly translocated to the nucleus of human umbilical vein endothelial cells and binds to DNA. *J Cell Biochem*. 2000;76(3):452-462.

179. Strydom DJ. The angiogenins. *Cell Mol Life Sci*. 1998;54(8):811-824. doi:10.1007/s000180050210

180. Hu GF, Riordan JF, Vallee BL. A putative angiogenin receptor in angiogenin-responsive human endothelial cells. *Proc Natl Acad Sci U S A*. 1997;94(6):2204-2209. doi:10.1073/pnas.94.6.2204

181. Liu S, Yu D, Xu ZP, Riordan JF, Hu GF. Angiogenin activates Erk1/2 in human umbilical vein endothelial cells. *Biochem Biophys Res Commun*. 2001;287(1):305-310. doi:10.1006/bbrc.2001.5568

182. Kim H-M, Kang D-K, Kim HY, Kang SS, Chang S-I. Angiogenin-induced protein kinase B/Akt activation is necessary for angiogenesis but is independent of nuclear translocation of angiogenin in HUVE cells. *Biochem Biophys Res Commun*. 2007;352(2):509-513. doi:10.1016/j.bbrc.2006.11.047

183. Sheng J, Xu Z. Three decades of research on angiogenin: a review and perspective. *Acta Biochim Biophys Sin (Shanghai)*. 2016;48(5):399-410. doi:10.1093/abbs/gmv131

184. Hu GF, Strydom DJ, Fett JW, Riordan JF, Vallee BL. Actin is a binding protein for angiogenin. *Proc Natl Acad Sci U S A*. 1993;90(4):1217-1221. doi:10.1073/pnas.90.4.1217

185. Hu G, Riordan JF, Vallee BL. Angiogenin promotes invasiveness of cultured endothelial cells by stimulation of cell-associated proteolytic activities. *Proc Natl Acad Sci U S A*. 1994;91(25):12096-12100. doi:10.1073/pnas.91.25.12096

186. Soncin F. Angiogenin supports endothelial and fibroblast cell adhesion. *Proc Natl Acad Sci U S A*. 1992;89(6):2232-2236. doi:10.1073/pnas.89.6.2232

187. Li R, Riordan JF, Hu G. Nuclear translocation of human angiogenin in cultured human umbilical artery endothelial cells is microtubule and lysosome independent. *Biochem Biophys Res Commun*. 1997;238(2):305-312. doi:10.1006/bbrc.1997.7290

188. Ferguson R, Subramanian V. The cellular uptake of angiogenin, an angiogenic and neurotrophic factor is through multiple pathways and largely dynamin

independent. *PLoS One*. 2018;13(2):e0193302. doi:10.1371/journal.pone.0193302

189. Xu Z, Monti DM, Hu G. Angiogenin activates human umbilical artery smooth muscle cells. *Biochem Biophys Res Commun*. 2001;285(4):909-914. doi:10.1006/bbrc.2001.5255
190. Moroianu J, Riordan JF. Identification of the nucleolar targeting signal of human angiogenin. *Biochem Biophys Res Commun*. 1994;203(3):1765-1772. doi:10.1006/bbrc.1994.2391
191. Lixin R, Efthymiadis A, Henderson B, Jans DA. Novel properties of the nucleolar targeting signal of human angiogenin. *Biochem Biophys Res Commun*. 2001;284(1):185-193. doi:10.1006/bbrc.2001.4953
192. Kishimoto K, Liu S, Tsuji T, Olson KA, Hu G-F. Endogenous angiogenin in endothelial cells is a general requirement for cell proliferation and angiogenesis. *Oncogene*. 2005;24(3):445-456. doi:10.1038/sj.onc.1208223
193. Li S, Hu G-F. Emerging role of angiogenin in stress response and cell survival under adverse conditions. *J Cell Physiol*. 2012;227(7):2822-2826. doi:10.1002/jcp.23051
194. Xu Z, Tsuji T, Riordan JF, Hu G. The nuclear function of angiogenin in endothelial cells is related to rRNA production. *Biochem Biophys Res Commun*. 2002;294(2):287-292. doi:10.1016/S0006-291X(02)00479-5
195. Xu Z, Tsuji T, Riordan JF, Hu G. Identification and characterization of an angiogenin-binding DNA sequence that stimulates luciferase reporter gene expression. *Biochemistry*. 2003;42(1):121-128. doi:10.1021/bi020465x
196. Yoshioka N, Wang L, Kishimoto K, Tsuji T, Hu G. A therapeutic target for prostate cancer based on angiogenin-stimulated angiogenesis and cancer cell proliferation. *Proc Natl Acad Sci U S A*. 2006;103(39):14519-14524. doi:10.1073/pnas.0606708103
197. Pilch H, Schlenger K, Steiner E, Brockerhoff P, Knapstein P, Vaupel P. Hypoxia-stimulated expression of angiogenic growth factors in cervical cancer cells and cervical cancer-derived fibroblasts. *Int J Gynecol Cancer*. 2001;11(2):137-142.
198. Hartmann A, Kunz M, Kostlin S, et al. Hypoxia-induced up-regulation of angiogenin in human malignant melanoma. *Cancer Res*. 1999;59(7):1578-1583.
199. Gagliardi S, Davin A, Bini P, et al. A Novel Nonsense Angiogenin Mutation is Associated With Alzheimer Disease. *Alzheimer Dis Assoc Disord*. 2019;33(2):163-165. doi:10.1097/WAD.0000000000000272
200. Greenway MJ, Andersen PM, Russ C, et al. ANG mutations segregate with

familial and “sporadic” amyotrophic lateral sclerosis. *Nat Genet*. 2006;38(4):411-413. doi:10.1038/ng1742

201. Wu D, Yu W, Kishikawa H, et al. Angiogenin loss-of-function mutations in amyotrophic lateral sclerosis. *Ann Neurol*. 2007;62(6):609-617. doi:10.1002/ana.21221
202. van Es MA, Schelhaas HJ, van Vught PWJ, et al. Angiogenin variants in Parkinson disease and amyotrophic lateral sclerosis. *Ann Neurol*. 2011;70(6):964-973. doi:10.1002/ana.22611
203. Crabtree B, Thiyagarajan N, Prior SH, et al. Characterization of human angiogenin variants implicated in amyotrophic lateral sclerosis. *Biochemistry*. 2007;46(42):11810-11818. doi:10.1021/bi701333h
204. Subramanian V, Crabtree B, Acharya KR. Human angiogenin is a neuroprotective factor and amyotrophic lateral sclerosis associated angiogenin variants affect neurite extension/pathfinding and survival of motor neurons. *Hum Mol Genet*. 2008;17(1):130-149. doi:10.1093/hmg/ddm290
205. Wu D, Yu W, Kishikawa H, et al. Angiogenin loss-of-function mutations in amyotrophic lateral sclerosis. *Ann Neurol*. 2007;62(6):609-617. doi:10.1002/ana.21221
206. Corrado L, Battistini S, Penco S, et al. Variations in the coding and regulatory sequences of the angiogenin (ANG) gene are not associated to ALS (amyotrophic lateral sclerosis) in the Italian population. *J Neurol Sci*. 2007;258(1-2):123-127. doi:10.1016/j.jns.2007.03.009
207. Conforti FL, Sprovieri T, Mazzei R, et al. A novel Angiogenin gene mutation in a sporadic patient with amyotrophic lateral sclerosis from southern Italy. *Neuromuscul Disord*. 2008;18(1):68-70. doi:10.1016/j.nmd.2007.07.003
208. Gellera C, Colombrita C, Ticozzi N, et al. Identification of new ANG gene mutations in a large cohort of Italian patients with amyotrophic lateral sclerosis. *Neurogenetics*. 2008;9(1):33-40. doi:10.1007/s10048-007-0111-3
209. Bradshaw WJ, Rehman S, Pham TTK, et al. Structural insights into human angiogenin variants implicated in Parkinson’s disease and Amyotrophic Lateral Sclerosis. *Sci Rep*. 2017;7(November 2016):1-10. doi:10.1038/srep41996
210. KUNITZ M. A spectrophotometric method for the measurement of ribonuclease activity. *J Biol Chem*. 1946;164(2):563-568.
211. Libonati M, Floridi A. Breakdown of double-stranded RNA by bull semen ribonuclease. *Eur J Biochem*. 1969;8(1):81-87. doi:10.1111/j.1432-

1033.1969.tb00498.x

212. Whitmore L, Wallace BA. Protein secondary structure analyses from circular dichroism spectroscopy: methods and reference databases. *Biopolymers*. 2008;89(5):392-400. doi:10.1002/bip.20853

213. Nenci A, Gotte G, Maras B, Libonati M. Different susceptibility of the two dimers of ribonuclease A to subtilisin. Implications for their structure. *Biochim Biophys Acta*. 2001;1545(1-2):255-262.

214. Ciglic MI, Jackson PJ, Raillard SA, et al. Origin of dimeric structure in the ribonuclease superfamily. *Biochemistry*. 1998;37(12):4008-4022. doi:10.1021/bi972203e

215. Gotte G, Libonati M, Laurents D V. Glycosylation and specific deamidation of ribonuclease B affect the formation of three-dimensional domain-swapped oligomers. *J Biol Chem*. 2003;278(47):46241-46251. doi:10.1074/jbc.M308470200

216. Fagagnini A, Montioli R, Caloiu A, Ribo M, Laurents D V, Gotte G. Extensive deamidation of RNase A inhibits its oligomerization through 3D domain swapping. *Biochim Biophys Acta*. 2017;1865(1):76-87. doi:10.1016/j.bbapap.2016.10.008

217. Leland PA, Staniszewski KE, Kim B, Raines RT. Endowing Human Pancreatic Ribonuclease with Toxicity for Cancer Cells *. 2001;276(46):43095-43102. doi:10.1074/jbc.M106636200

218. Bal HP, Batra JK. Human pancreatic ribonuclease--deletion of the carboxyl-terminal EDST extension enhances ribonuclease activity and thermostability. *Eur J Biochem*. 1997;245(2):465-469. doi:10.1111/j.1432-1033.1997.t01-1-00465.x

219. Dalaly BK, Eitenmiller RR, Friend BA, Shahani KM. Human milk ribonuclease. *Biochim Biophys Acta*. 1980;615(2):381-391. doi:10.1016/0005-2744(80)90505-7

220. López-alonso JP, Gotte G, Laurents D V. Kinetic analysis provides insight into the mechanism of Ribonuclease A oligomer formation. *Arch Biochem Biophys*. 2009;489(1-2):41-47. doi:10.1016/j.abb.2009.07.013

9. Annexes

During my PhD period I studied some structural determinants affecting the oligomerization tendency of some pancreatic ribonucleases. In particular I focused my attention on RNase A, the proto-type of pancreatic-type ribonucleases superfamily, on ONC and on ANG. Both ONC and ANG are very interesting protein whose oligomerization tendency needs more investigations, and it could have an impact on human health.

Furthermore, I participated at congresses with posters or presentations, such as for example the 59th SIB congress in Caserta, Proteine 2018 in Verona, or the 30$_{th}$ National Reunion of Biochemistry PhD students in Brallo di Pregola.

Publications:

1. Fagagnini A, Pica A, Fasoli S, et al. Onconase dimerization through 3D domain swapping: structural investigations and increase in the apoptotic effect in cancer cells. *Biochem J*. 2017;474(22):3767-3781. doi:10.1042/BCJ20170541

2. Raineri A, Fasoli S, Campagnari R, Gotte G, Menegazzi M. Onconase Restores Cytotoxicity in Dabrafenib-Resistant A375 Human Melanoma Cells and Affects Cell Migration, Invasion and Colony Formation Capability. *Int J Mol Sci*. 2019;20(23). doi:10.3390/ijms20235980

3. Raineri A, Prodomini S, Fasoli S, Gotte G, Menegazzi M. Influence of onconase in the therapeutic potential of PARP inhibitors in A375 malignant melanoma cells. *Biochem Pharmacol*. 2019;167:173-181. doi:10.1016/j.bcp.2019.06.006